

NASA CR-66380

CONCEPTUAL MECHANIZATION STUDIES FOR A HORIZON DEFINITION SPACECRAFT STRUCTURES AND THERMAL SUBSYSTEM

Horizon Definition Study

Distribution of this report is provided in the interest of information exchange. Responsibility for the contents resides in the author or organization that prepared it.

May 1967

N67-32007	(ACCESSION NUMBER)	(THRU)
	140	3
OK-66380	(PAGES)	(CATEGORY)
NASA CR OR TMX OR AD NUMBER		

FACILITY FORM 602

Prepared under Contract No. NAS 1-6010 by

HONEYWELL INC.

Systems & Research Division

Minneapolis, Minn.

for

NATIONAL AERONAUTICS AND SPACE ADMINISTRATION

May 1967

NASA CR-66380

CONCEPTUAL MECHANIZATION STUDIES FOR
A HORIZON DEFINITION SPACECRAFT
STRUCTURES AND THERMAL SUBSYSTEM

By: Ivan W. Russell
David C. Peterson
Richard M. Jansson
Clarence A. Jenson

ABSTRACT

The spacecraft conceptual configuration developed during the Horizon Definition Study is a spin-stabilized, hexagonal cylinder configured for launch on a two-stage Improved Delta (DSV-3N). This configuration utilizes extended solar panels for primary power and incorporates passive radiation cooling of the spacecraft body. Separate thermal environments are provided for the experimental package and the supporting subsystem components.

NASA CR-66380

CONCEPTUAL MECHANIZATION STUDIES FOR A HORIZON DEFINITION
SPACECRAFT STRUCTURES AND THERMAL SUBSYSTEM

By Ivan W. Russell
David C. Peterson
Richard M. Jansson
Clarence A. Jensen

HORIZON DEFINITION STUDY

Distribution of this report is provided in
the interest of information exchange.
Responsibility for the contents resides in
the author or organization that prepared it.

May 1967

Prepared under Contract No. NAS 1-6010 by
Honeywell Inc.
Systems and Research Division
Minneapolis, Minnesota

for

NATIONAL AERONAUTICS AND SPACE ADMINISTRATION

FOREWORD

This report documents Phase A, Part II of An Analytical and Conceptual Design Study for an Earth Coverage Infrared Horizon Definition Study performed under National Aeronautics and Space Administration Contract NAS 1-6010 for Langley Research Center.

The Horizon Definition Study was performed in two parts. Part I, which was previously documented, provided for delineation of the experimental data required to define the infrared horizon on a global basis for all temporal and spatial periods. Once defined, the capabilities of a number of flight techniques to collect the experimental data were evaluated. The Part II portion of the study provides a measurement program plan which satisfies the data requirements established in the Part I study. Design requirements and the conceptual design for feasibility of the flight payload and associated subsystems to implement the required data collection task are established and documented within this study effort.

Honeywell Inc., Systems and Research Division, performed this study program under the technical direction of Mr. L. G. Larson. The program was conducted from 28 March 1966 to 10 October 1966 (Part I) and from 10 October 1966 to 29 May 1967 (Part II).

Gratitude is extended to NASA Langley Research Center for their technical guidance, under the program technical direction of Messrs. L. S. Keafer and J. A. Dodgen with directed assistance from Messrs. W. C. Dixon, Jr., E. C. Foudriat, H. J. Curfman, Jr., and T. F. Bonner, Jr., as well as the many people within their organization.

CONTENTS

	Page
FOREWORD	iii
SUMMARY	1
INTRODUCTION	2
STUDY REQUIREMENTS AND OBJECTIVES	5
Basic Requirements	5
Spacecraft Subsystem Requirements	8
SPACECRAFT CONFIGURATION SELECTION	11
Basic Design Considerations	11
Configuration Matrix	18
Baseline Configuration Selection	24
SUBSYSTEM EVOLUTION AND DESCRIPTION	26
Experiment Package	26
Attitude Control	33
Data Handling	37
Communications	37
Electrical Power	40
Structural Subsystem	43
THERMAL CONTROL CONCEPTUAL DESIGN	43
General	43
Orbital Heat Fluxes	45
External Skin and Solar-Cell Temperatures	49
Heat Loading of Experiment Package	58
Internal Electronic Package Thermal Control	77
Thermal Control Summary	83
SPACECRAFT CONCEPTUAL DESIGN	84
Evolution	84
Final Spacecraft Concept Description	87
CONCLUSIONS	107
APPENDIXES	
A A TECHNIQUE FOR EVALUATING THE MOMENTS OF INERTIA AND PRINCIPAL AXES OF ASSEMBLY OF COMPONENTS (TEMPAC)	111
B FINAL SPACECRAFT BALANCE	119
REFERENCES	133

ILLUSTRATIONS

Figure		Page
1	Spacecraft Structural Subsystem Functional Flow Diagram	9
2	Axial to Transverse Mass Moment of Inertia Ratios for a Solid Cylinder	13
3	Effects of Length to Diameter Ratios on the Mass Moments of Inertia of a Hollow Cylinder	14
4	Shadow Fraction versus Days	16
5	Sun-Line/Orbit Normal Angle versus Days	17
6	Improved Delta Fairing	19
7	Improved Delta Acoustical Environment	20
8	Improved Delta Fairing Typical Thermal History	22
9	An Early Experiment Package Concept	31
10	Possible Starmapper Design	32
11	Experimental Package Concept - Starmapper Viewing 60° Off Axis	35
12	Attitude Control Subsystem Block Diagram	38
13	Data Handling Subsystem Functional Diagram	39
14	Vehicular Communications Subsystem - Command, Telemetry, and Ranging	41
15	Satellite Electrical Power Subsystem	42
16	Conceptual Spacecraft Thermal Control Compartments and Structural Assemblies	44
17	Space Heating Incident to Front Face of Spacecraft and Cell Side of Solar Panels	46
18	Space Heating Incident to Sidewalls, No Shadowing by Panels or Other Objects	47
19	Space Heating Incident to Rear Face of HDS Spacecraft	48
20	External Surface Temperatures - Hexagonal Spacecraft With Body-Mounted Cells on All Sunlit Faces	51
21	External Surface Temperatures - Hexagonal Spacecraft with Extended Solar Panels and No Extra Sun Shielding	52
22	External Surface Temperatures - Hexagonal Spacecraft With Extended Solar Panels and Sun Shielding in Plane of Panels	53
23	External Surface Temperatures - Hexagonal Spacecraft With Extended Solar Panels and Local Sun Shield Over Radiometer Entrance	54
24	Local Sun Shield with Directional Emitting Surfaces	56
25	Effect of Skin Conduction on Cell Temperatures	57
26	External Surface Temperature for Varied Solar Cell Coverage - Front Surface (Sunlit Except During Shadow Passage)	59
27	External Surface Temperature for Varied Solar Cell Coverage - Sidewall Surface	60
28	External Surface Temperature for Skirt Configuration	61
29	Effect of Temperature on Emittance of the OSR	66
30	Solar Absorptance of White Paint	67

Figure		Page
31	Baseplate Temperature versus Heat Input, 31° Solar Angle	68
32	Baseplate Temperature versus Heat Input, 64° Solar Angle	69
33	Orbital Temperature Variation of Baseplate	75
34	Baseplate Thermal Gradient, a "Worst Case"	76
35	Nodal Model of Electronics Platform	79
36	Temperature of Electronics Platform, Uniform Heat Dissipation	80
37	Temperature of Electronics Platform, Nonuniform Heat Dissipation	81
38	Component Temperature versus Heat Dissipation	82
39	Preliminary Hexagonal Cylinder Spacecraft Concept	85
40	Experiment Package Concept - Starmappers Viewing Forward	89
41	Experiment Package Concept - Starmappers Viewing 60° Off Axis	90
42	Conceptual Spacecraft - External Layout	91
43	Conceptual Spacecraft - Internal Layout	93
44	Spacecraft Structural Subsystem	97
45	Conceptual Spacecraft Cover	99
46	Radiometer View Port Sun Shade	101
47	Cryogenic Cooler Venting and Refrigerant Lines	102
48	Experiment Package Concept Starmappers Viewing Aft	105
49	Spacecraft/Booster Interface	108
A1	Component Orientation and Location	115
A2	Total Assembly Coordinate Systems	116
B1	Conceptual Spacecraft - External View	123
B2	Conceptual Spacecraft - Internal View	125

TABLES

Table		Page
1	Vibration Environment to be Encountered on the Two-Stage Improved Delta	21
2	Spacecraft Configuration Matrix	23
3	Comparison of Various Cross-Sectional Configurations to the Hexagonal Baseline Concept	25
4	Subsystem Evolution	27
5	Subsystem Definition, Time Period 2	28
6	Subsystem Definition, Time Period 4	29
7	Subsystem Definition Final Version, Time Period 5	30
8	Plastic Materials for Structural Insulator	63
9	Heat Loads to Experiment Package Baseplate of HDS Spacecraft - Body-Mounted Cell Configuration, No Extended Panels or Shields	70
10	Heat Loads to Experiment Package/Baseplate of HDS Spacecraft-Extended Solar Panel Configuration, Shielding in Plane of Panels	71
11	Head Loads to Experiment Package/Baseplate of HDS Spacecraft - Extended Solar Panel Configuration, No Shielding	72
12	Heat Loads to Experiment Package/Baseplate of HDS Spacecraft-Local Radiometer Sun Shield Configuration	73
13	Spacecraft Out-of-Plane Attitude Effects on the Temperature of a 195°K Baseplate, One-Orbit Average Values	77
14	Dual Radiometer Installations in an Improved Delta Spacecraft	88
A1	Component Shape and Moment of Inertia Equations	117
A2	Typical Computer Printout	118
B1	TEMPAC Component Encoding Sheet - Fixed Component	127
B2	TEMPAC Component Encoding Sheet - Movable Components	128
B3	Computer Output, Fixed Components	129
B4	Computer Output, Fixed and Movable Components	130
B5	Computer Output, Fixed and Movable Components with Added Dead Weights	131

CONCEPTUAL MECHANIZATION STUDIES FOR A HORIZON DEFINITION SPACECRAFT STRUCTURES AND THERMAL SUBSYSTEM

By Ivan W. Russell
David C. Peterson
Richard M. Jansson
Clarence A. Jensen

SUMMARY

This document describes a spacecraft structural and integrated system concept configured within the basic system requirements of the Horizon Definition Study. The proposed configuration demonstrates total system feasibility and compatibility with the selected launch vehicle (Improved Delta, DSV-3N).

The basic system requirements along with the physical and functional interface requirements of the required subsystems were used in establishing an initial baseline configuration for study. The required subsystems were identified as:

- Experiment package
- Attitude control subsystem
- Data handling subsystem
- Communications subsystem
- Electrical power subsystem
- Structural and thermal control subsystem

The baseline spacecraft concept was a hexagonal cylinder utilizing orbital spin stabilization, with the spin axis normal to the orbit plane, to provide passive experiment scanning capability. Throughout the study, the development variations made to each subsystem were integrated into the total spacecraft system, their effects analyzed, and tradeoffs conducted to verify spacecraft balance and thermal control feasibility while maintaining volume and dimensional compatibility.

The spacecraft concept recommended in this study is a spin-stabilizer hexagonal cylinder configuration, 49 inches deep and 54 inches across the corner of the hexagon. It has an estimated launch weight of 723 pounds, allowing approximately a 10 per cent margin for growth within the capability of the Improved Delta (two stage-direct injection) vehicle. It is compatible with subsystem requirements and constraints and maintains the required balance ratios for the proposed spin-stabilized concept. Separate thermal environments are provided; a -100°F (200°K) compartment for the experiment package and an approximately 75°F (279°K) section for the supporting subsystem components. This recommended concept demonstrates that a very simple, highly reliable, state-of-the-art spacecraft can fulfill the mission performance requirements as defined in the Horizon Definition Study.

INTRODUCTION

The structural and thermal control subsystem and the system integration studies documented herein are a portion of the Horizon Definition Study (HDS) conducted for NASA Langley Research Center, Contract NAS 1-6010, Part II. The Purpose of the Horizon Definition study is to develop a complete horizon radiance profile measurement program to provide data which can be used to determine the earth's atmospheric state, especially at high altitudes. These data can then be effectively used in many atmospheric sciences studies and in the design of instruments and measurement systems which use the earth's horizon as a reference.

Part I of the HDS resulted in the following significant contributions to the definition of the earth's radiance in the infrared spectrum:

- The accumulation of a significant body of meteorological data covering a major portion of the Northern Hemisphere.
- Computation of a large body of synthesized horizon radiance profiles from actual temperature profiles obtained by rocket soundings.
- Generation of a very accurate analytical model and computer program for converting the temperature profiles to infrared horizon profiles (as a function of altitude).
- An initial definition of the quantity, quality, and sampling methodology required to define the earth's infrared horizon in the CO_2 absorption band for all temporal and spatial conditions.
- An evaluation of the cost and mission success probabilities of a series of flight techniques which could be used to gather the radiance data. A rolling-wheel spacecraft was selected in a nominal 500 km polar orbit.

The Part II study effort was directed toward the development of a conceptually feasible measurement system, which includes a spacecraft to accomplish the measurement program developed in Part I. In the Part II HDS, a number of scientific and engineering disciplines were exercised simultaneously to design conceptually the required system. Accomplishments of Part II of the study are listed below:

- The scientific experimenter refined the sampling methodology used by the measurement system. This portion of the study recommends the accumulation of approximately 380 000 radiance profiles taken with a sampling rate that varies and with the spacecraft's latitudinal position.

- A conceptual design was defined for a radiometer capable of resolving the earth's radiance in the 15 micron spectrum to 0.01 watt/meter²-steradian with an upper level of response of 7.0 watt/meter²-steradian.
- A starmapper and attitude determination technique were defined capable of determining the pointing direction of the spacecraft radiometer to an accuracy of 0.25 km in tangent height at the earth's horizon. The combination of the radiometer and starmapper is defined as the mission experiment package.
- A solar cell-battery electrical power subsystem conceptual design was defined which is completely compatible with the orbital and experiment constraints. This system is capable of delivering 70 watts of continuous electrical power for one year in the sun-synchronous, 3 o'clock nodal crossing, 500 km orbit.
- A data handling subsystem conceptual design was defined which is capable of processing in digital form all scientific and status data from the spacecraft. This subsystem is completely solid state and is designed to store the 151 455 bits of digital information obtained in one orbit of the earth. This subsystem also includes command verification and execute logic.
- A communications subsystem conceptual design was defined to interface between the data handling system of the spacecraft and the STADAN. The 136 MHz band is used for primary data transmission, and the S band is used for the range and range-rate transponder.
- A spacecraft structural concept was evolved to contain, align and protect the spaceborne subsystems within their prescribed environmental constraints. The spacecraft is compatible with the Thor-Delta launch vehicle.
- An open-loop, ground-commanded attitude control subsystem conceptual design was defined utilizing primarily magnetic torquing which interacts with the earth's field as the force for correcting attitude and spin rates.
- The Thor-Delta booster, which provides low cost and adequate capability, was selected from the 1972 NASA "stable".
- Western Test Range was selected as the launch site due to polar orbit requirements. This site has adequate facilities, except for minor modifications, and is compatible with the polar orbital requirements.

This report contains documentation of those areas of study directly related to the conceptual configuration of a spacecraft within the constraints of the HDS system requirements. The objective of the study was to determine the design requirements and conceptually configure a spacecraft structural subsystem within an integrated total system which would incorporate the dynamic balance and environmental control requirements necessary to achieve the radiance profile measurement and position determination accuracies of the proposed experiment. An integrated framework which provides the experiment package and its supporting subsystems with sufficient volume, protection from the anticipated environments, and the desired thermal environmental control while still meeting the system operating requirements is herein described.

STUDY REQUIREMENTS AND OBJECTIVES

Basic system requirements are those defined by the original statement of work, Phase A Part I results, and NASA instructions.

The following list itemizes the primary and secondary requirements of the Horizon Definition Study.

BASIC REQUIREMENTS

Radiance Profile Measurements

- Spectral interval: 615 to 715 cm^{-1} (14.0 to 16.28 μ)
- Profile accuracy
 - ▶ Tangent height range: +80 km to -30 km
 - ▶ Instantaneous value of radiance measured must be assignable to a tangent height value to within ± 0.25 km.
 - ▶ Radiance characteristics and resolution:
 - Maximum peak radiance = 7.0 W/m^2 - sr.
 - Minimum peak radiance = 3.0 W/m^2 - sr.
 - Maximum slope = 0.6 W/m^2 - sr - km.
 - Minimum slope = 0.02 W/m^2 - sr - km.
 - Maximum slope change = 0.15 W/m^2 - sr - km^2 .
 - Radiance magnitude resolution = 0.01 W/m^2 - sr.
 - ▶ Horizontal resolution: 25 km
- Data requirements - Data requirements for the Horizon Definition Study (HDS) experiment, as refined during the study are as follows:

Minimum requirements. --

- ▶ One-year continuous coverage
- ▶ "Uniform" time sampling in each space cell over each time cell, i. e., no more than two samples/space cell/day.
- ▶ Thirteen time cells (28 days/cell)

▶ 408 space cells	
Latitude (60°S to 60°N)	320
Latitude (60°N to 90°N)	44
Latitude (60°S to 90°S)	44
▶ Samples per cell	
Latitude (0° to 60°)	16
Latitude (60° to 90°)	38
▶ Total samples (one year)	110 032

Recommended requirements. --

▶ One-year continuous coverage	
▶ Maximum of 10° latitude separation between successive samples	
▶ 13 time cells (28 days/cell)	
▶ 588 space cells:	
Latitude (30°S to 30°N)	128
Latitude (30°N to 60°N)	134
Latitude (60°N to 82.6°N)	96
Latitude (30°S to 60°S)	134
Latitude (60°S to 82.6°S)	96
▶ Average number of samples per cell:	
Latitude (30°S to 30°N)	45
Latitude (30°N to 60°N)	39
Latitude (60°N to 82.6°N)	67
Latitude (30°S to 60°S)	39
Latitude (60°S to 82.6°S)	67
▶ Total samples (one year)	378 508

Mission Profile

Nominal circular, polar orbit of approximately 500 km altitude.

Tracking and Data Acquisition

Limited to the existing Satellite Tracking and Data Acquisition Network (STADAN) with minimum modification.

Experiment Package

- Passive radiometric and attitude measurements with redundancy (more than one unit) in the research package for the radiometer and attitude determination device.
- Minimum scan rate >0.5 scans/min average.
- Maximum scan angle with respect to orbit plane $\leq 5^\circ$.

Spacecraft

- Rolling wheel configuration (spin axis normal to the orbit plane).
- Weight in less than 800 pound class mandatory.

State of the Art

Proven subsystems shall be employed wherever possible.

Mission Effectiveness/Reliability

Reliability shall be approached on the basis of "designing in" successful performance of the one-year, data-collection mission, i. e., the effort is to be biased strongly toward mission effectiveness. Consequently, the mission effectiveness/reliability effort should involve continuing tradeoffs in each sub-function area against the criteria of maximum effectiveness. A numerical estimate of the probable system MTBF shall be made on the final configured system.

Strong consideration should be given to the use of reserve spacecraft as a "backup" means rather than as a continuously ready standby. Specifically, the "backup" concept (as opposed to ready continuously) is of more significance on a Thor-Delta sized vehicle than on a Scout vehicle.

SPACECRAFT SUBSYSTEM REQUIREMENTS

Some of the preceding basic system requirements directly affect and constrain the conceptual configuring of an integrated spacecraft subsystem while others have very little input to configuration variations. These critical requirements and constraints, as applied to the spacecraft conceptual design and integration study effort, are translated as follows.

- Utilize a near-polar orbit at about 500 km altitude.
- Utilize proven state-of-the-art subsystems whenever possible.
- Keep spacecraft maximum weight under 800 pounds.
- Utilize passive systems wherever possible
- Provide a "stabalized platform" from which to make scientific measurements.
- Utilize spin-stabilized spacecraft with spin axis normal to the orbit plane.

These requirements were then translated into the functions that must be accomplished by the spacecraft structural subsystem. They are depicted in the functional flow diagram shown in Figure 1. There are certain requirements associated with these functional blocks that must be fulfilled by the structural subsystem or must be interfaced through it with the other spacecraft subsystems. A discussion of these functional blocks describing these requirements and interfaces is contained in the following paragraphs.

Support and Enclose Subsystems

The spacecraft structural subsystem must define the enclosed spacecraft volume within the booster interface constraints and must within this volume support and maintain the subsystems components and equipment. Inherent in this support and maintenance requirement is the positioning and arranging of these components to insure compatibility with vehicle dynamics requirements and inter- and intra-system interfaces.

Provide Subsystem Positioning, Vehicle Alignment, and Body Rigidity

The structural subsystem must provide the initial component alignment and must, in the critical experiment areas, maintain that alignment throughout the mission life within the prescribed tolerances. The mechanism contained in the structural subsystem must fulfill the deployment, erection, or unfolding requirements of any of the subsystems and must position and maintain position of these items (solar panels, sun shields, antennas, etc.) within the system performance and vehicle dynamic tolerance constraints.

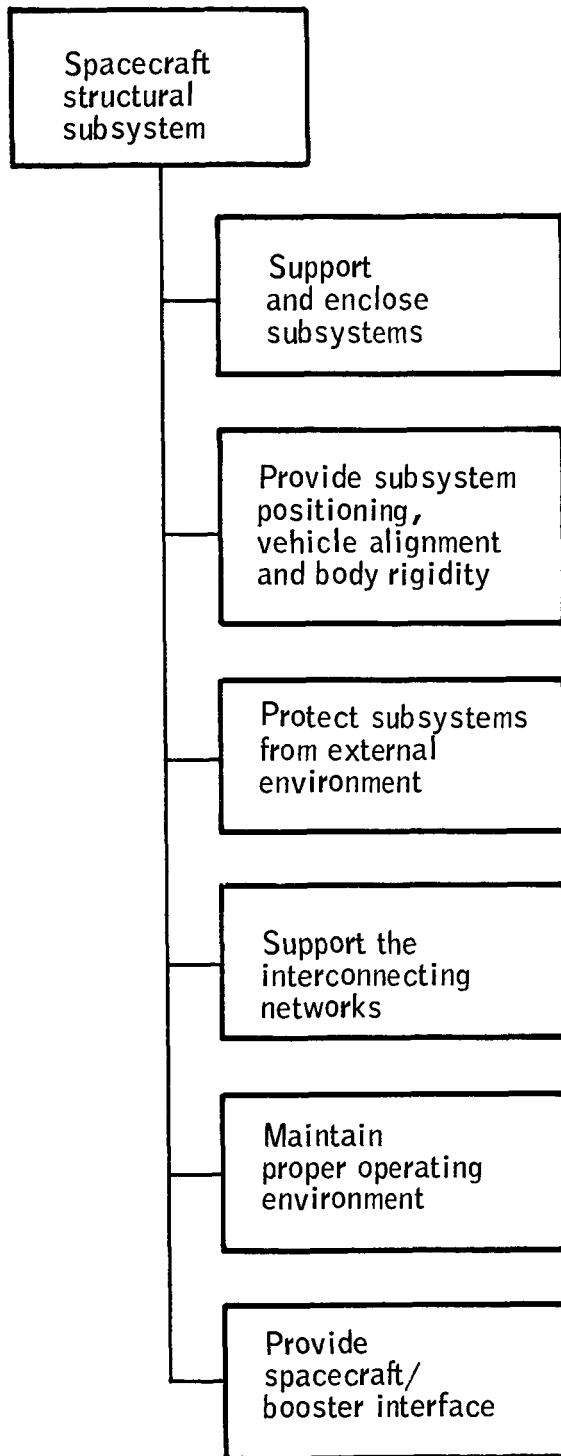


Figure 1. Spacecraft Structural Subsystem Functional Flow Diagram

Protect Subsystems From External Environments

The spacecraft structural skin must protect the internal components from the launch and orbital environments. The component requirements will determine the degree of protection necessary.

Support the Interconnecting Networks

The spacecraft structure will support and maintain the system interconnecting networks (electrical, pneumatic, etc.).

Maintain Proper Thermal Environment

The spacecraft structural subsystem must incorporate a passive thermal control system which will, through conduction and radiation, maintain the desired thermal paths and balance within the spacecraft system.

Provide Spacecraft/Booster Interface

The spacecraft structural subsystem must provide a mechanical interface with the booster, must provide a configuration compatible with the booster fairing envelope, and must be structurally compatible with the launch vehicle environments.

The conceptual configuration of a spacecraft structure is very closely related to the subsystems and the integrated total system interfacing requirements. The subsystems considered in the initial spacecraft configuration studies were:

- The experiment package consisting of the radiance measurement instrument, the attitude determination equipment, and their supporting electronics.
- The attitude control subsystem (ACS) consisting of the equipment necessary to maintain proper spacecraft orientation and stabilization.
- The data handling subsystem consisting of the equipment necessary to process and store data between transmission periods.
- The communication subsystem consisting of the equipment necessary to provide up and down communication links and to provide spacecraft location information.
- The electrical power subsystem consisting of the equipment necessary to provide and distribute electrical power for all spacecraft needs.

- The structural subsystem consisting of the hardware to support, enclose, and protect an integrated spacecraft system and to provide the mechanisms necessary to fulfill the system and subsystem deployment and positioning requirements.

A review of the system and subsystem requirements previously discussed suggests a spin-stabilized spacecraft, spinning about an axis normal to the orbit plane in a nominal 3 p. m. / 3 a. m., sun-synchronous orbit, as being most compatible with these requirements. This concept provided a baseline for the succeeding conceptual configuration studies.

SPACECRAFT CONFIGURATION SELECTION

BASIC DESIGN CONSIDERATIONS

Certain basic design considerations and constraints must be kept in mind when attempting conceptually to configure a spacecraft. Additional constraints are imposed by specific mission requirements such as, in this case, a spin-stabilized vehicle to allow passive scanning techniques. The following discussions cover the basic items that were considered in the selection of a spacecraft configuration.

Spacecraft Balance

The dynamics of a spinning body are directly controlled by the mass moments of inertia and principal axes location of the body. The mass moment of inertia is equal to a summation of the products of the mass and the square of its distance from the axis, i. e.

$$I = \sum m r^2$$

or, in the limit,

$$I = \int r^2 dm$$

Another term, frequently used, is the product of inertia; $\sum m xy$ (where x and y are the Cartesian coordinates of an element). This product of inertia is zero about principal axes and can therefore be used to locate the orientation of those axes.

In general, three mutually perpendicular principal axes, which have a maximum, minimum, and intermediate moment of inertia, can be located for a body. A spinning spacecraft should have a maximum and two approximately equal minimum moments of inertia. Thompson and Reiter (ref. 1) showed that a spinning spacecraft is stable about either the axis of maximum or minimum moment of inertia if the body is rigid. If energy is dissipated

through elastic deformation or by other means, the body is stable about the axis of maximum moment of inertia.

Estimates of the degree of dimensional design flexibility were obtained by investigating the moment of inertia ratios associated with different configurations of a homogeneous cylinder with constant total mass. Figure 2 shows the variation of the spin axis to transverse axis moment of inertia ratio with changing length to diameter ratio when it is assumed that the total cylinder mass is kept constant. The upper limit for stability about the s axis, $I_s / I_t = 1$, occurs at $l/d = 0.866$.

Several things might be done to vary the moment of inertia ratio in actual design. I_s increases faster than I_t if added mass is put as far as possible away from the s axis but still near the t and z axes. Heavier components might be kept far from the axis which is intended to be the principal axis of maximum moment of inertia. This approach tends toward a hollow cylinder concept.

Figure 3 presents the limit of length-to-diameter ratio for a homogeneous, hollow cylinder wherein a larger moment of inertia exists about the spin axis than about the transverse axis. Comparing hollow and solid cylinder results shows that the length-to-diameter ratio can be increased from 87 to 97 percent by eliminating the innermost 1/4 of the volume (1/2 the radius). This indicates that some flexibility to spacecraft design is available if needed.

The determination of the dynamic properties of a complex assembly of components within a spacecraft is a very lengthy calculation. A computer program (TEMPAC) has been written which uses a definition of the components comprising a total assembly, such as a spacecraft or missile, and calculates the total mass, the mass moments of inertia about some set of reference axes, the center of mass location, the mass moments of inertia about axes through the center of mass and coincident to the reference axes, the principal mass moments of inertia, and the orientation of the corresponding principal axes. The program has been designed so that a number of fixed components can be introduced, and the calculated values stored. Many different combinations of variable components can then be added to the stored values making the program a powerful design tool as well as a calculating tool. A discussion of the program is included in Appendix A to this report, and a demonstration of its use is given in Appendix B.

The accurate balancing of a spacecraft, which is required in a spin-stabilized orbital configuration, can be accomplished in several ways. Repositioning components inside the spacecraft is an obvious method. Adding dead weight or ballast can accomplish the balancing task, but this should be used primarily during final flight vehicle balancing. The flight vehicles will be precisely balanced prior to delivery, and this balance will be checked at the launch site prior to launch.

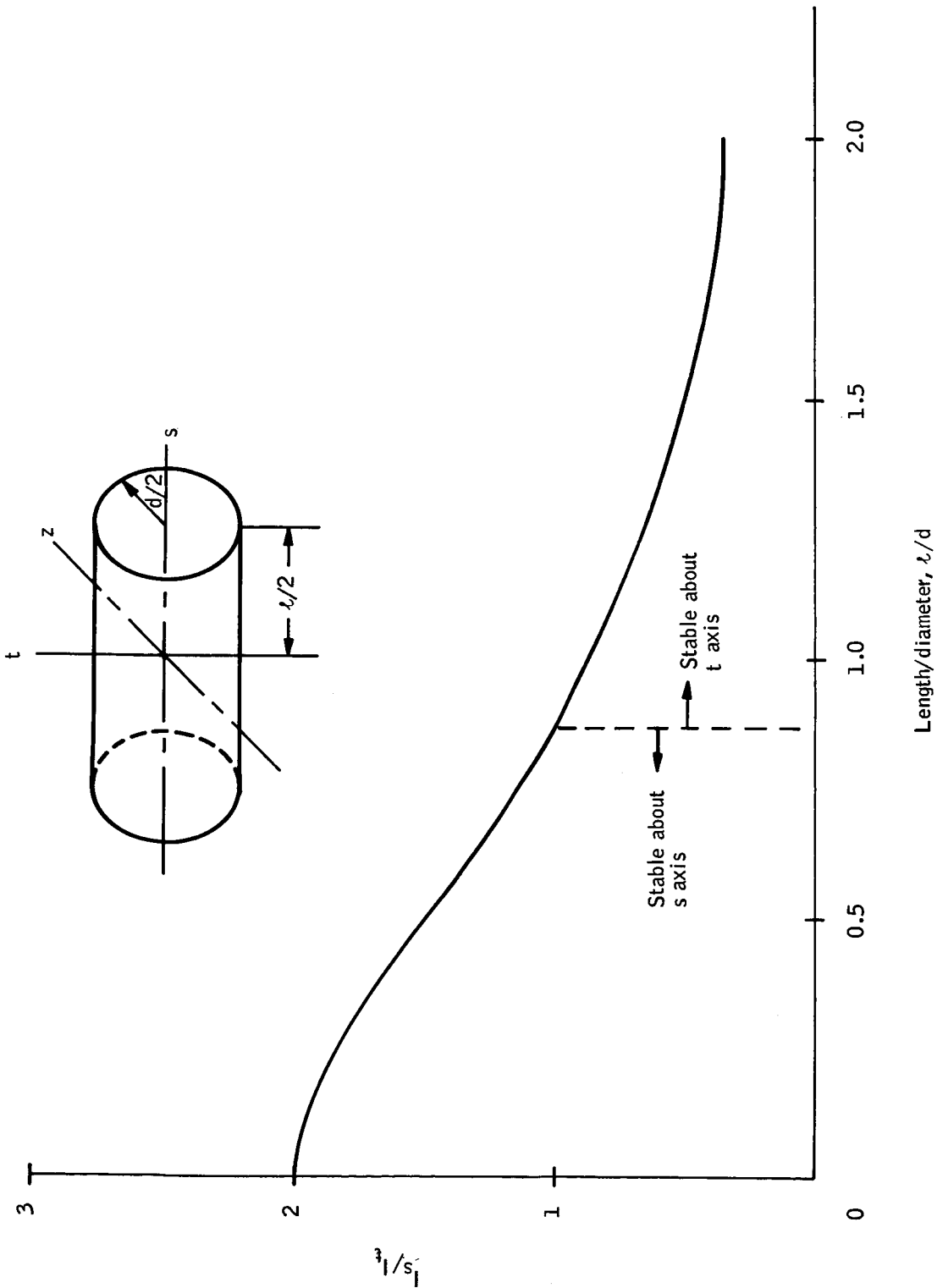


Figure 2. Axial to Transverse Mass Moment of Inertia Ratios for a Solid Cylinder

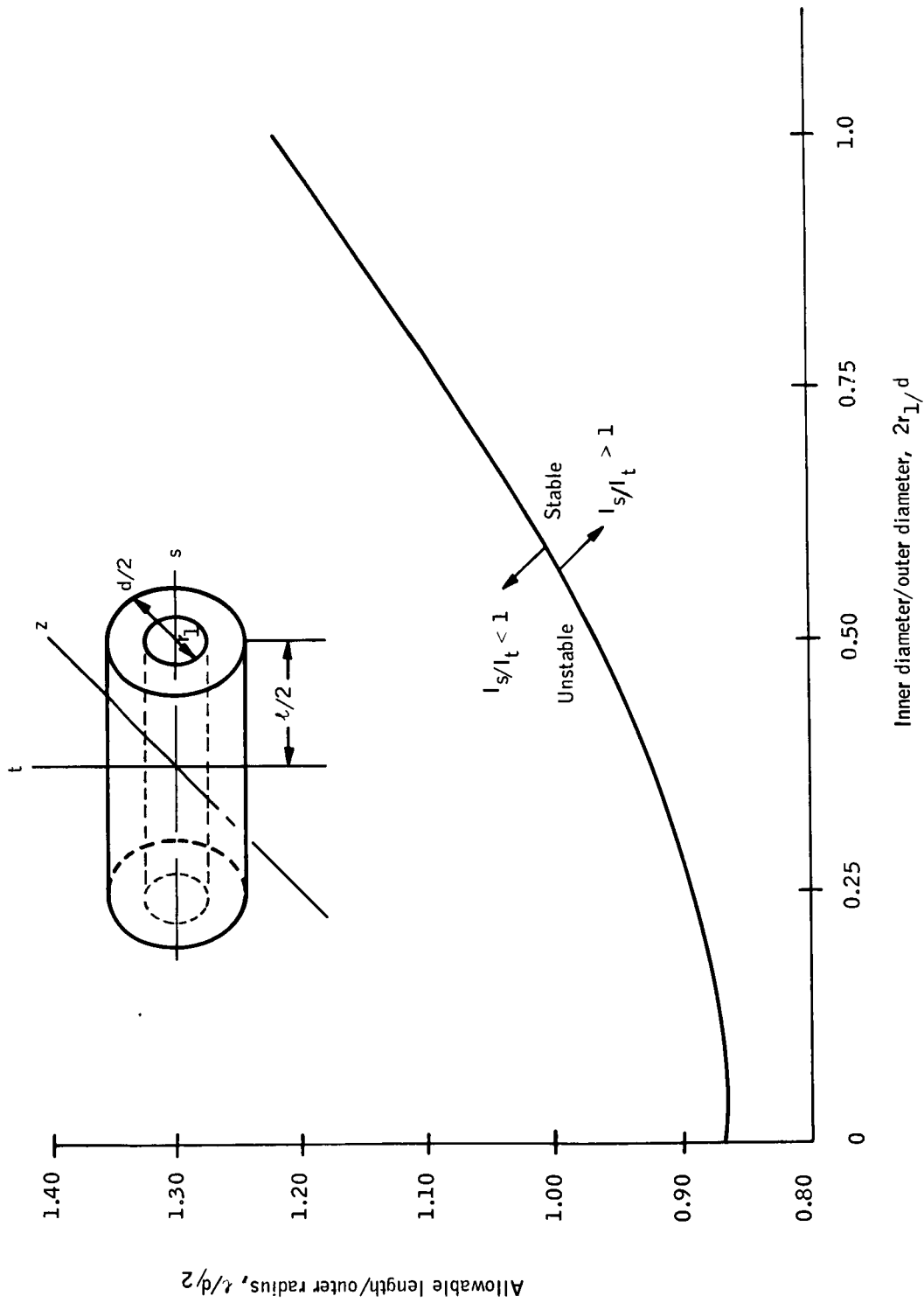


Figure 3. Effects of Length to Diameter Ratios on the Mass Moments of Inertia of a Hollow Cylinder

Thermal Control

A significant portion of this integration and conceptual design study was necessarily concerned with thermal control analysis and design which will be discussed in a later section. It is sufficient to say here that the study was guided with the understanding that there would be both internal and external heat loads. These would have to be transferred to a surface where radiation to space, the sole method of heat dissipation, could be accomplished.

The solar energy input to a spacecraft is dependent upon the orbital parameters. The anticipated 3:00 p. m., sun-synchronous orbit shadow fraction time and sun-line/orbit-normal angle for nominal and 3-sigma fast and slow precessions (based on the 2-stage Delta launch errors) are shown in Figures 4 and 5. Significant about these curves is the range of sun-line/orbit-normal angle from 31 to 64 degrees that might occur during operation.

Structural - Electrical Interfaces

Structural - electrical interfaces must be considered in the development of a feasible spacecraft concept. Factors which have to be considered are listed below.

Electromagnetic interference. -- It is necessary that the spacecraft concept provide for physical separation of electrical wire bundles and black boxes. It may be necessary to utilize structural members for physical shielding to reduce electromagnetic interference to an acceptable level.

Magnetic moment. -- The spacecraft concept must consider the requirement for location and orientation of each individual black box and the routing of interconnecting wire harnesses to reduce magnetic moments due to stray and permanent magnetic fields to an acceptable level.

Eddy currents. -- Eddy-current torques, proportional to the number of earth's magnetic flux lines intercepted, are generated when conducting materials are rotated through the earth's magnetic field. These torques must be held to a low level to avoid perturbations in the spacecraft spin rate and orientation. The spacecraft structure, the major contributor to eddy-current problems, may have to be fabricated from conduction-interrupted structural segments to minimize these torques.

Booster Interface

Early indications were that the total spacecraft weight would be beyond the Scout capabilities. Therefore, conceptual design studies were oriented toward using a two-stage, Improved Delta. That version known as the DSV-3N (long tank Thor with strap-on solids and second-stage Delta), has launch capabilities in the 800 lb class into a 300 n. mi. polar orbit from the Western Test Range.

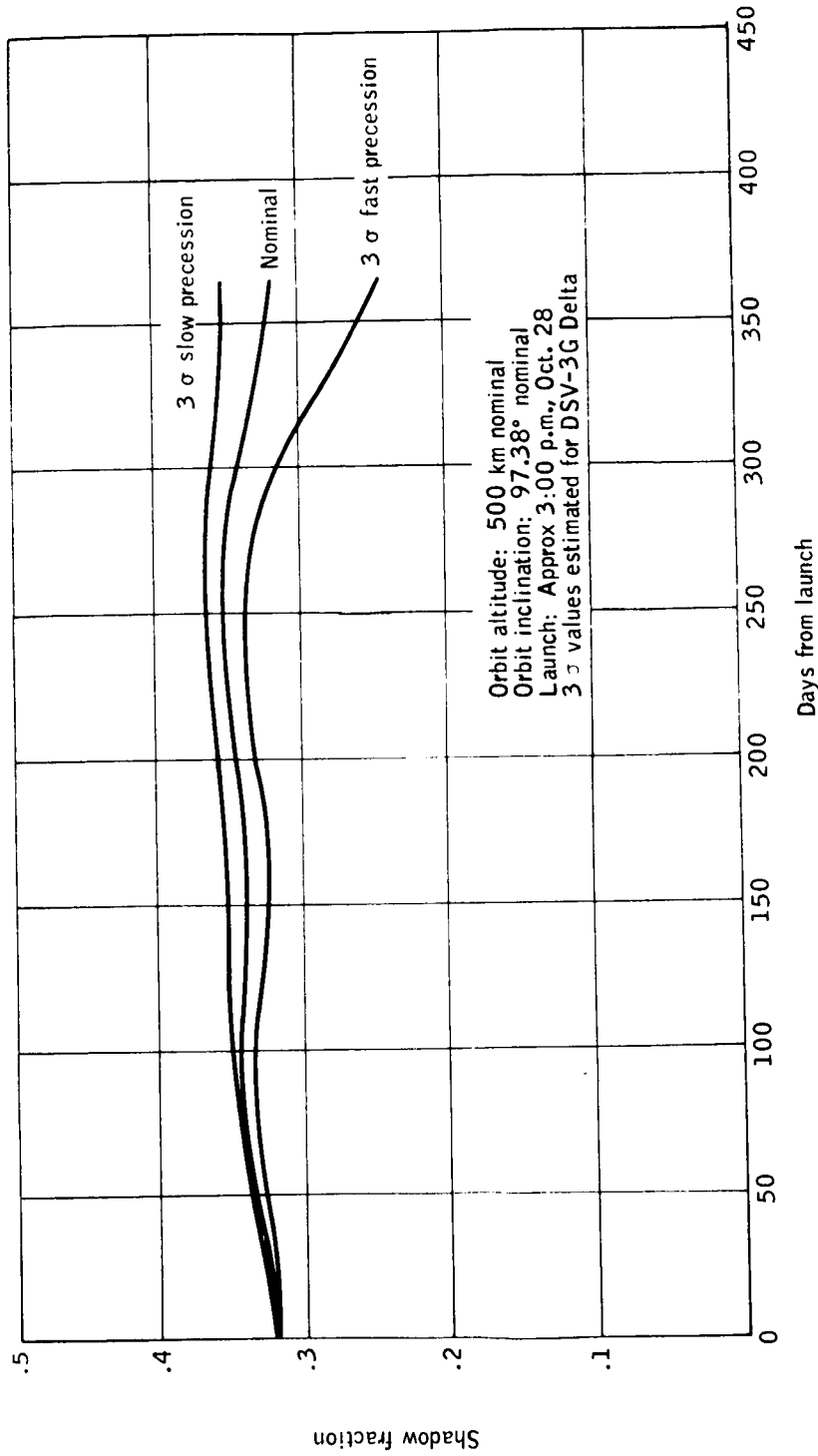


Figure 4. Shadow Fraction versus Days

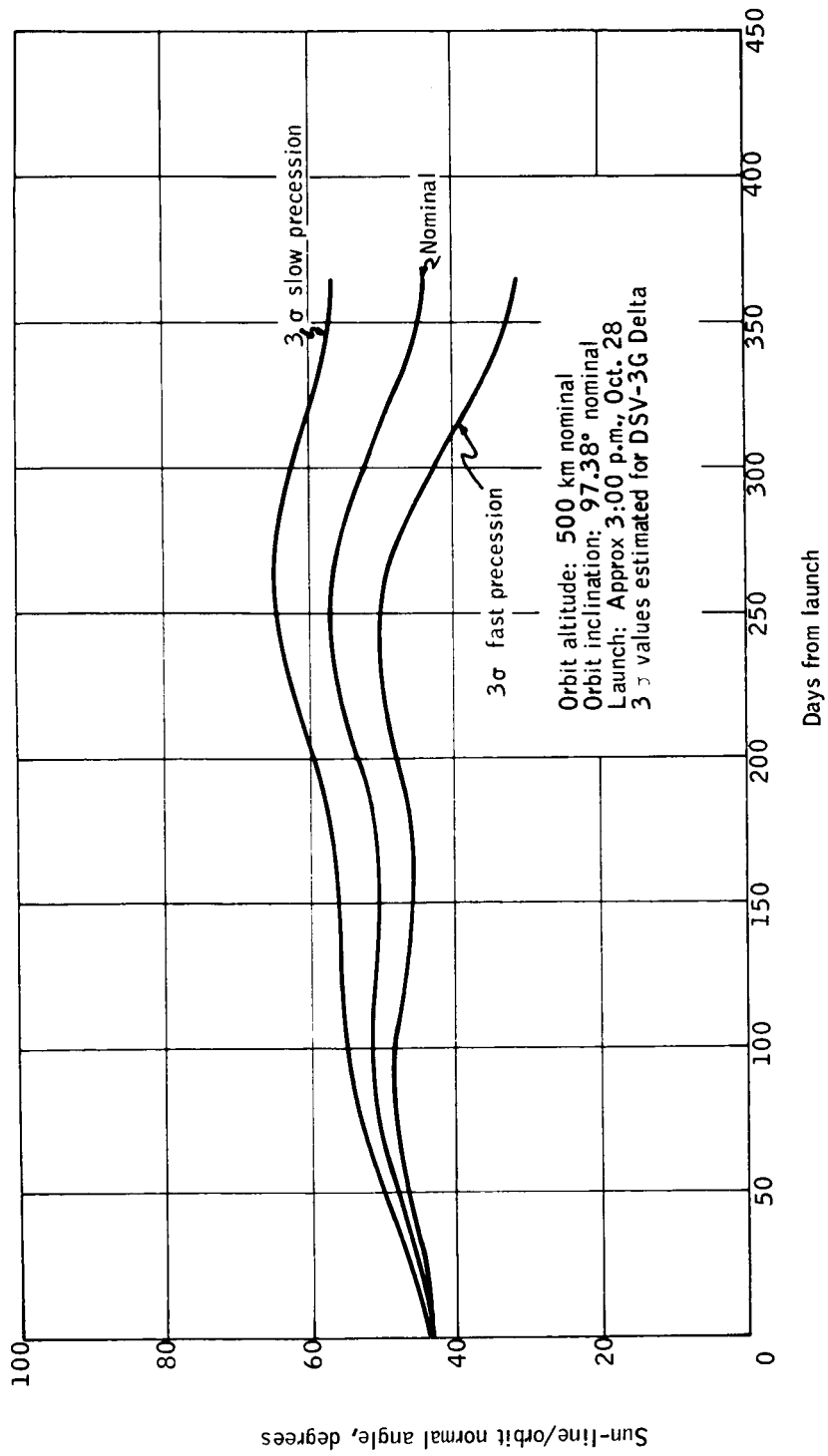


Figure 5. Sun-Line/Orbit Normal Angle versus Days

The allowable fairing volume and dimensional restrictions shown in Figure 6 indicate that the spacecraft body can be about 54 inches in diameter and still allow room for slight protrusions if needed. The very flexible design of the fairing allows wide variations in the number and location of access holes.

A major attach point which will carry the launch thrust will be needed on one face of the spacecraft. Semi-standard booster interface rings in various sizes from 9- to 37-inch diameter and lengths from several inches up to several feet are available. Additional support from the fairing can be provided as needed along the length of the spacecraft.

Environment

During its lifetime the spacecraft will be exposed to four significant environments which may affect the conceptual configuration.

- The fabrication, testing, check-out, and installation environment really is significant only because a large amount of spacecraft handling will take place. Sufficient attach points will be needed.
- The launch pad environment will not be severe; methods of protecting the spacecraft and controlling the environment are incorporated into launch operations.
- Significant launch environment factors are the vibration level as shown in Table 1, the sound pressure level shown in Figure 7, the temperature environment control that can be accomplished inside the fairing as shown in Figure 8, the rapid pressure decrease from atmospheric to essentially zero in several minutes, and a possible shock load during spacecraft/booster separation.
- The orbital operating environment includes hard vacuum, thermal cycling, radiation, and possible meteoroid interception. The conceptual configuration design in this study should also consider the contamination of optical systems, the degradation of material physical properties, and the change of thermal properties on coated radiative surfaces.

CONFIGURATION MATRIX

After a first round conceptual design study was conducted within each of the subsystem design groups, a spacecraft configuration matrix was generated to determine the best general spacecraft shape. By this time, it was possible to anticipate what might be the desirable properties that would enable a spacecraft best to satisfy the needs of each subsystem. For example, it was anticipated that the experiment package would need large areas for unobstructed viewing or that there might be need for fold-out solar panels. The matrix, which reflects these and other anticipations, is shown in Table 2.

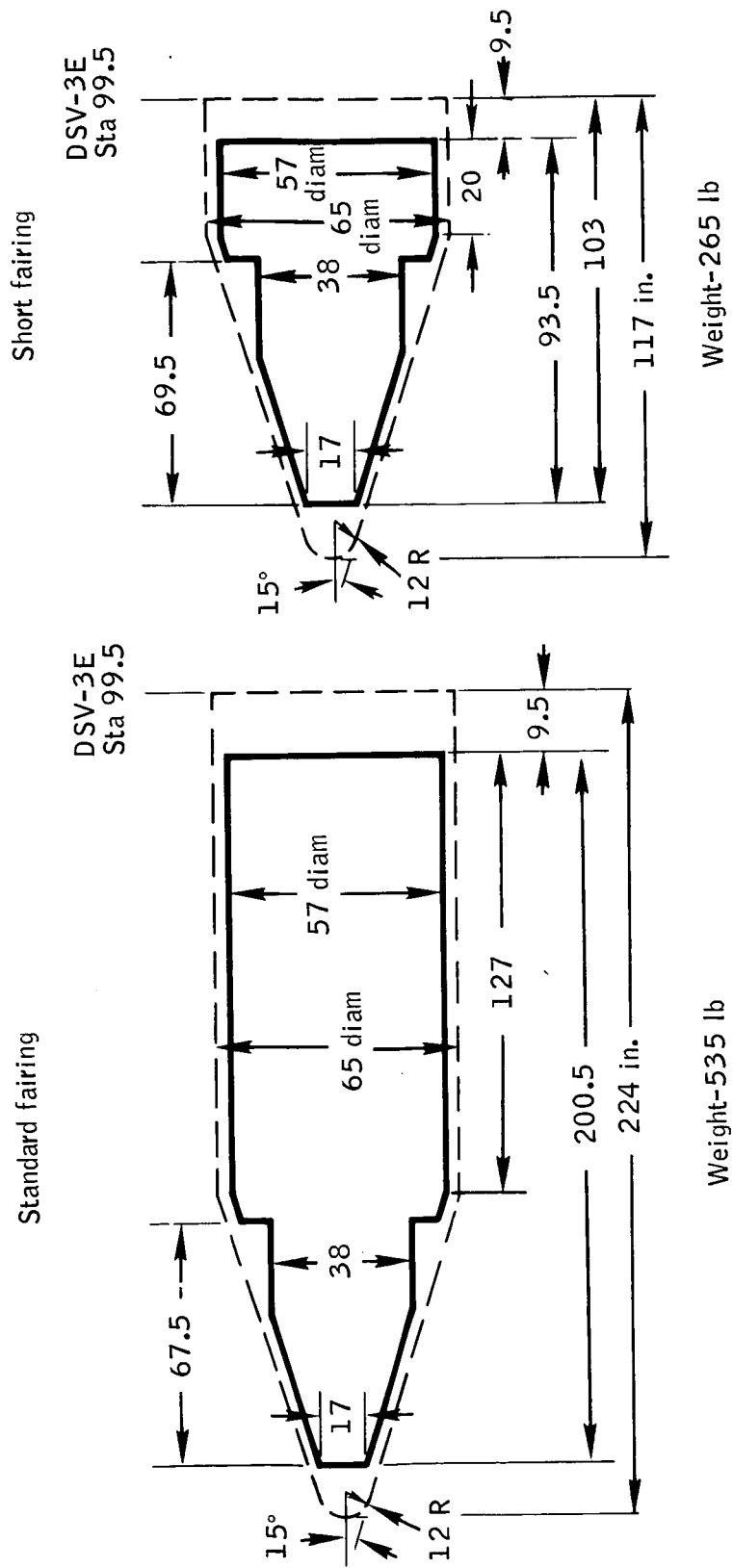


Figure 6. Improved Delta Fairing

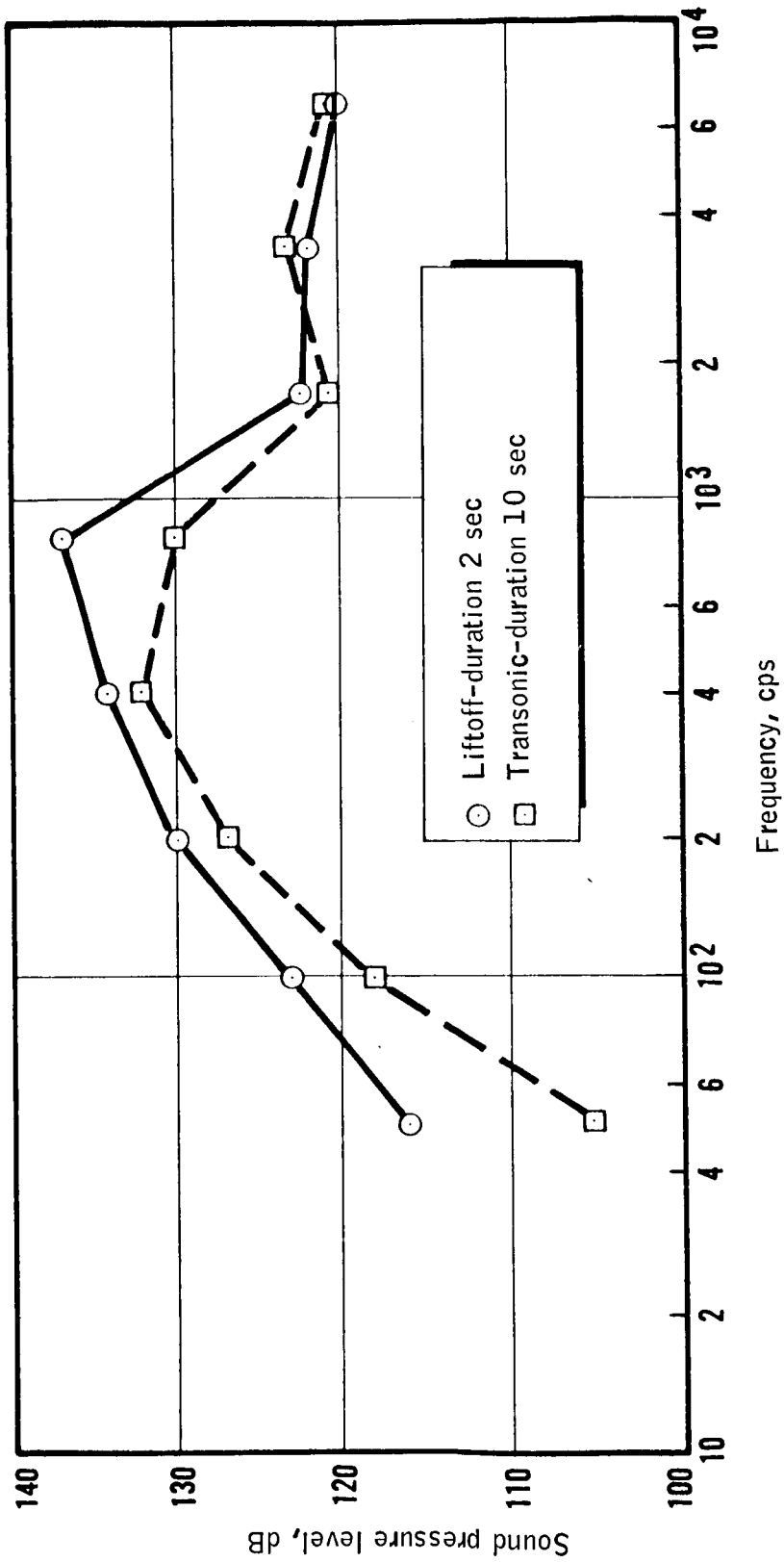


Figure 7. Improved Delta Acoustical Environment

TABLE 1. - VIBRATION ENVIRONMENT TO BE ENCOUNTERED
ON THE TWO-STAGE IMPROVED DELTA

Flight sinusoidal vibration restraints				
Axis	Frequency, cps	Level, g, 0-peak (a)	Sweep rate (b)	
Thrust (Z-Z)	10 - 16	2.0	2 octaves/minute	
	16 - 26	2.5		
	26 - 250	2.0		
	250 - 400	5.0		
	400 - 2000	10.0		
Lateral (X-X) and (Y-Y)	5 - 250	1.5	2 octaves/minute	
	250 - 400	5.0		
	400 - 2000	10.0		
^a Qualification levels = 1.5 x flight levels ^b Qualification sweep rate = 1/2 flight equivalent rates				
Flight random vibration restraints				
Axis	Frequency, cps	PSD Level, g ² /cps (a)	Acceleration, g (rms)	Duration, minutes (b)
Thrust (Z-Z)	20 - 150	0.01	12.3	1 min/axis
	150 - 425	+4 dB/octave	12.3	
Lateral (X-X)	425 - 1200	0.04	12.3	
Lateral	1200 - 2000	-2 dB/octave	12.3	
^a Qualification levels = 2.25 x flight levels ^b Qualification duration = 2 x flight duration				

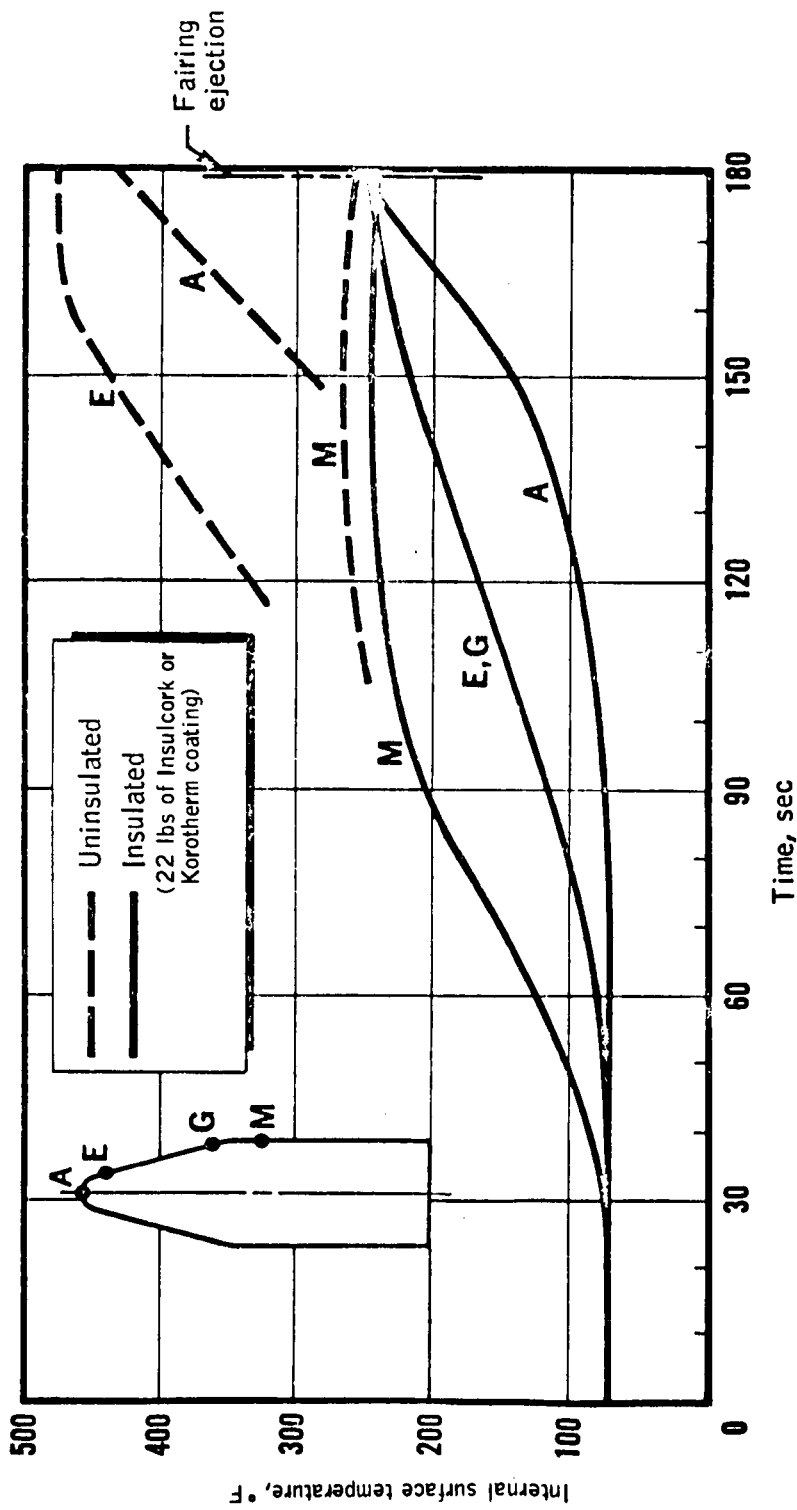


Figure 8. Improved Delta Fairing Typical Thermal History

TABLE 2. - SPACECRAFT CONFIGURATION MATRIX

Description of criteria	Cylinders									
	Arch/Flat Cylinder	Triangular	Square	Pentagonal	Hexagonal	Octagonal	Multisided	Round	Elongated Hexagonal	Sphere
1. Experiment package	0-20									
a. General compatibility		4	8	6	10	10	10	10	10	10
b. View area availability		6	10	6	10	10	10	10	8	10
c. Alignment surfaces		8	14	6	12	10	8	6	12	5
d. Accessibility		10	12	10	10	8	7	5	8	4
2. ACS	0-20									
a. Torquing coil shape		8	10	10	12	12	14	15	16	12
b. Jet mounting area		9	10	9	10	10	10	10	12	10
c. Sensor mounting area		10	10	10	10	10	10	10	10	10
3. Data handling/communications	0-10									
a. Length of leads		5	5	5	5	5	5	5	5	5
b. Whip antenna mount area and interference		4	5	5	5	5	5	5	5	4
c. Slot antenna mount area and interference		2	6	4	5	6	6	5	5	6
4. Power	0-10									
a. Body mount area										
b. Loss area		7	6	5	4	2	2	5	6	1
c. Projected area versus time		4	4	4	5	5	6	5	6	5
d. Total area		3	4	5	5	6	6	6	8	5
e. Flat area		5	5	5	5	5	5	2	5	3
f. Sun-intercept area		5	5	5	5	5	5	5	5	5
g. Angle of faces with sun		2	3	4	5	6	6	6	5	6
h. Sunometry		2	5	4	5	5	5	5	5	5
i. Fold-out feasibility		5	5	5	5	5	3	0	5	8
j. No. of fold-outs needed		7	6	5	5	4	2	0	5	0
5. Structure-physical properties	0-10									
a. Volume efficiency		4	4	4	5	6	7	8	5	2
b. Weight efficiency		5	5	5	5	5	5	5	5	5
c. Strength		3	4	4	5	6	7	8	5	8
d. Ease of fabrication		5	6	5	6	5	5	5	5	4
e. Simplicity		5	5	5	5	5	5	5	5	4
6. Component mounting	0-10									
a. Flat surfaces		4	5	5	5	5	5	4	5	4
b. Usable volume		4	5	4	5	5	5	5	5	4
c. Accessibility		5	5	5	5	5	5	5	4	5
7. Mounting area ratio	0-20									
a. Allowable ratio		6	8	8	10	11	11	12	10	5
b. Design flexibility		6	8	8	10	11	11	12	10	5
8. Thermal	0-10									
a. Flux intercepted		5	5	5	5	5	4	4	2	5
b. Radiating surface area		5	5	5	5	5	6	4	8	5
9. Booster interface	0-10									
a. Mounting area		4	5	5	5	5	5	5	5	5
b. Shroud mating		3	4	4	5	5	6	6	5	3
c. Load transfer to interface		3	4	4	5	5	5	5	4	4
10. Launch support	0-10									
a. Check-out accessibility		5	5	5	5	5	5	5	5	5
Total		177	216	194	224	223	222	216	228	180
Major items total		70	100	84	104	103	98	92	103	70

The desirable properties, shown along the left column with their weighting factor, were intended to cover both the requirements of each subsystem and the total integrated system requirements. The cylinders, with cross section as shown, and a sphere were then assigned values within the weighting factor range according to the manner in which they met the requirements. Some desirable properties were felt to be of higher importance than others and were marked and classed as "major items".

The summation of assigned values showed that the hexagonal cross-section configuration had the highest desirable property level. It should be mentioned that the study matrix showed only minor differences in desirable property level among the more conventional (square, hexagonal, octagonal, and multi-sided) spacecraft configurations.

BASELINE CONFIGURATION SELECTION

In addition to the numerical assignment analysis of the previous section, the potential spacecraft configurations were inspected from a practical viewpoint. Since the hexagonal cross-section version yielded the highest desirable property level, it was selected as the probable baseline configuration. Salient features of this configuration are

- Experiment package compatibility
- Spacecraft symmetry
- Simple construction
- Flat surfaces for mounting solar cells
- Flat surfaces for fold-out panels
- Flat internal surfaces for component mounting
- Satisfactory booster fairing interface.

Each of the other configurations has certain advantages or disadvantages relative to the baseline configuration as is shown in Table 3. Since no configuration was shown to be more practical than the hexagonal, it was chosen as the baseline for further conceptual study.

TABLE 3. - COMPARISON OF VARIOUS CROSS-SECTIONAL CONFIGURATIONS TO THE HEXAGONAL BASELINE CONCEPT

Configuration	Advantages	Disadvantages
Triangular	Fewer fold-outs	Nonsymmetrical Uneven power output from body-mounted cells Lower structural strength Lower balance flexibility Inefficient fairing volume usage
Square	Fewer fold outs	Uneven power output from body-mounted cells Lower structural strength Lower balance flexibility Inefficient fairing volume usage
Pentagonal	Fewer fold-outs	Nonsymmetrical Uneven power output from body-mounted cells Lower balance flexibility
Octagonal	Smoother power output from body-mounted cells	More fold-out panels needed
Multi-sided	Smoother power output from body-mounted cells. Higher booster fairing volume usage	Fold-outs complicated Internal accessibility restricted
Circular	Total symmetry High booster fairing volume usage	Fold-outs difficult Internal accessibility restricted Curved internal mounting surfaces
Elongated hexagonal	Could possibly have sufficient area for body-mounted cells	Experimental package interference Excess volume, drag area, solar energy intercept area, etc. Thermal control interference Balance interference
Spherical	Constant projected area to sun Total symmetry	Fold-outs difficult Thermal control interference Balance restricted

SUBSYSTEM EVOLUTION AND DESCRIPTION

Each of the six subsystems which comprise the total spacecraft system was being studied concurrently with the spacecraft conceptual configuration effort. Design groups were conducting their own tradeoff studies and arriving at a best solution to their particular problem. Each solution and the approaches that were used as the subsystem was being studied had a major effect on the conceptual configuration of the total spacecraft.

The following discussion covers the steps in each of the subsystem designs that appeared to be significant to the spacecraft conceptual design. It is not intended, nor is it necessary for this discussion, to cover fully the tradeoff studies or detailed design analyses that were conducted. Table 4 presents changes that were made at approximately one-month intervals between the original possible concept and the final version. This table presents the changes, but not the total description of the subsystem; therefore, Tables 5, 6, and 7 describe the subsystems in more detail at about the time periods indicated as 2, 4, and 5 in Table 4. The final version of the subsystems are described in Table 7 and will be discussed in more detail in a later section covering the total spacecraft conceptual design.

EXPERIMENT PACKAGE

Evolution

The experiment package, as first conceived, was described as two separate radiance measuring devices and an associated attitude determination device. Each radiometer would require a detector cooler, envisioned to be a large conical space radiator well insulated from the rest of the spacecraft. However, the space radiator approach was not compatible with the orbit selected and the level of cooling required and was abandoned in favor of a subliming cryogen cooler.

A cryogenic cooler cools because it absorbs heat from its environment as the included cryogen sublimates. The amount of cooling is in accordance with the heat of sublimation of the cryogen. This type of cooler operates very efficiently in a space environment where the ambient pressure is well below the vapor pressure level of the cryogen. A single cooler was conceived which would cool redundant radiometer detectors as shown in the possible experiment package assembly shown in Figure 9. It was found that the optics in the radiometer would also have to be cooled to reduce their radiance to an acceptable level. Since they are integrally tied to the remainder of the experiment package, it was decided to cool the entire package. A space radiation approach from the base of the spacecraft was selected for this cooling.

Starmapping during sunlit portions of the orbit proved very difficult. Very large baffles for the starmapper, as shown in Figure 10, were suggested to alleviate the earth and sun shine problem, but they were not compatible with

TABLE 4. - SUBSYSTEM EVOLUTION

Time period	0	1	2	3	4	5
Experiment package	Dual 10" radiometers Dual 5" starmappers Radiative cooler wt = 285	Dual 10" radiometers Dual 5" starmappers Cryogenic cooler wt = 240	Dual 15" radiometers Dual 6" starmappers Cryogenic cooler wt = 280	Dual 18" radiometers Dual 6" starmappers Cryogenic cooler wt = 280	Dual 18" radiometers Dual 6" starmappers Cryogenic cooler Total package cooling required wt = 286	Single 16" optics Dual 4" starmappers Dual sun sensors Cryogenic cooler Total package cooling required wt = 324
Attitude control	Horizon sensors Sun sensors Magnetometers Spin-up jets De-spin mechanism wt = 90	No change wt = 90	De-spin not needed Redundancy added Fuel supply reduced wt = 280	Cold jets replaced by solid jets wt = 53	Coils changed Sun sensors not needed wt = 49	Horizon sensors Magnetic coils Spin-up jets not needed Redundant subsystem wt = 48
Data handling	Core storage Tape storage wt = 50	Core storage selected wt = 35	Data processor Data storage wt = 60	Redundancy added wt = 59	No change wt = 59	Data processor Data storage Redundant system wt = 59
Communications	S band Range and range-rate wt = 20	No change wt = 20	VHF added wt = 26	No change wt = 26	No change wt = 26	VHF and S band Redundant subsystem wt = 26
Power	Solar cells, radioisotope, or fuel cell wt = 200	Solar cells (body mount or panels) wt = 185	Solar cells on face and fold out panels wt = 66	No change wt = 79	Body cells removed Panel size changed wt = 89	Fold-out panels Redundant battery wt = 121
Spacecraft structural	Skeleton, skin, and bulkheads wt = 120	No change wt = 120	Heat paths and miscellaneous integration material added wt = 120	No change wt = 120	Thermal approach changed Heavy baseplate Experiment package cooled wt = 147	Sun shield added Experiment package cooled wt = 145
Spacecraft system	Circular cylinder Rolling-wheel concept wt = 765 lb	Multi-sided cylinder Rolling-wheel concept wt = 680 lb	Hexagonal cylinder Rolling-wheel concept wt = 584 lb	Hexagonal cylinder Rolling-wheel concept wt = 617 lb	Hexagonal cylinder Rolling-wheel concept wt = 666 lb	Hexagonal cylinder Rolling-wheel concept wt = 723 lb

TABLE 5. - SUBSYSTEM DEFINITION, TIME PERIOD 2

Subsystem	Weight, lb	Volume, in. ³	Maximum length, in.	Surface area needed	Remarks
<u>Experiment package</u>	<u>280</u>				
(2) Radiometer(R)/ Starmappers(SM)					
Optics (R) Detector Electronics Structure Baffle Optics (SM) P. M. tube Electronics Structure	120	10 000	15x15x18	2-15" diam view areas	
Cooler Support	150 10	3 450	12x12x24	Coolant exhaust	
<u>Attitude control</u>	<u>60</u>				
Rotation jets Fuel supply Mag. coil	3 5 10	20 200		Small	250 turns each way
(2) Sensors (2 horizon and 1 sun)	20	360		6-3" diam openings	Redundancy
(2) Electronic control Damper Support	16 1 5	700			Redundancy
<u>Data Handling</u>	<u>32</u>				
Timing and control Data processor R conv. SM conv. S/C status conv.	2.5 1.5 2.0 2.0	46 20 34 28	3.7 3.0 4.0 5.7	None	Will be two boxes of electronics with interconnecting wires
Storage Buffer Main Formatter Command verifier and decoder Support	1.5 14.5 1.0 2.0 5.0	50 500 20	2.0 0.7 2.0 2.2		
<u>Communications</u>	<u>26</u>				
Antenna Command receiver, Range and range rate transponder, and Transmitter Beacon Antenna Support	2 16 1 2 5	1 200 10	24 inch 10x10x12 2x2x2 24 inch	4 stubs and 4 slots 4 stubs and 4 slots	Dark side Sun side
<u>Power</u>	<u>66</u>				
Fold/unfold mech Cell array Power conditioning Batteries Lines, etc. Support	1 20 9 21 10 5		25"x30" panels	Hinge lines 40"x32" body- mount area	
<u>Structure</u>	<u>120</u>				
Adapter ring Separation unit Skeleton Skin Heat paths Misc. wire, clips, test points, etc.	10 10 25 20 20 35			Ring on booster	
<u>Total</u>	<u>584</u>				

TABLE 6. - SUBSYSTEM DEFINITION, TIME PERIOD 4

Subsystem	Weight, lb	Volume, in ³	Maximum length, in	Surface area needed	Remarks
<u>Experiment package</u>	<u>296</u>				
(2) Radiometer (R)/ Starmappers (SM)	160				
Optics (R)			18" diam x 18" long	2-18" diam view areas	
Detector					
Electronics					
Structure					
Baffle					
Optics (SM)			6x10x10	2-6" diam view areas	
P. M. tube			Plus baffle		
Electronics					
Structure					
(2) Sun sensors	6			2-3" diam view areas	
Cooler	120		18" diam x 28" long	Coolant exhaust	
Support	10				
<u>Attitude control</u>	<u>49</u>				
Rotation jets	1	20		Small	
(2) Horizon sensors	10	130	4x4x8	4-3" diam openings	Redundancy
(2) Logic	16	480	5x6x8		Redundancy
Mag. coils					
Attitude	8	60			Circumferential coil normal to S/C face
Spin	3	30			
Residual	2	30			
Dampër	4	40			
Support	5				
<u>Data handling</u>	<u>59</u>				
Timing and control					
Data processor					
R conv					
SM conv					
S/C status conv					
Formatter	22	360	4x9x10	None	1 unit with redundancy
Command verifier and decoder					
Storage					
Buffer	32	1100	10x10x10	None	1 unit with redundancy
Main					
Support	5				
<u>Communications</u>	<u>26</u>				
Antennas	2		19.5 inch	4 stubs and 6 slots	Dark Side
Command receiver					
Range and range rate transponder	17	1200	10x10x12		
Transmitter					
Beacon	2	10	2x2x2		
Antennas	2		21.5 inch	4 stubs and 6 slots	Sun side
Support	5				
<u>Power</u>	<u>89</u>				
Fold/unfold mech	2		23 x 44" panels		
Cell array	42			Hinge lines	No body-mounted cells
Power conditioning	9		8x8x6		
Batteries	21		5x5x16		
Lines, etc.	10				
Support	5				
<u>Structure</u>	<u>147</u>				
Adapter	8				
Booster ring	8			Ring on booster	
Base plate	40			Ring on S/C	
Skeleton	20				
Skin	20				
Bulkhead	8				
Heat paths	8				
Misc. wire, clips test points, etc.	35				
Total	666				

TABLE 7. - SUBSYSTEM DEFINITION FINAL
VERSION, TIME PERIOD 5

Subsystem	Weight. lb	Volume. in ³	Maximum length, in	Surface area needed	Remarks
<u>Experimental package</u>	<u>324</u>				
(2) Radiometer (R)					
Starmappers (SM)					
Optics (R)	60		16" diam x 42" long	16" diam view areas	Single optics; remainder is redundant
Detector	4				
Electronics					
Structure	92				
Baffle	20		4" diam x 18" long plus baffle	2-7" diam view areas	Redundancy
Optics (SM)					
P. M. tube	4				
Electronics					
Structure					
(2) Sun sensors	6		2" diam x 6" long	2-3" diam view areas	
Cooler	45		17" diam x 12" long	Coolant exhaust	
Support	93				
<u>Attitude control</u>	<u>48</u>				
(2) Horizon sensors	10	130	2x4x8	4-3" diam openings	Redundancy
(2) Logic	16	480	5x6x8		Redundancy
Magnetic coils					
Attitude	10	160			Circumferential coil normal to S/C face
Spin	3	60			
(2) Damper	4	192			
Support	5				
<u>Data handling</u>	<u>59</u>				
Timing and control					
Data processor					
R conv					
SM conv					
S/C status conv	22	360	4x9x10	None	1 unit with redundancy
Formatter					
Command verifier and decoder					
Storage					
Buffer	32	1 100	10x10x10	None	1 unit with redundancy
Main					
Support	5				
<u>Communications</u>	<u>26</u>				
Antennas	2		19.5 inch	3 stubs and 6 slots	Dark side
Command receiver					
Range and range-rate transponder	17	1 200	10x10x12		Redundancy
Transmitter					
Beacon		10	2x2x2		
Antennas	2		21.5 inch	3 stubs and 6 slots	Sun side
Support	5				
<u>Power</u>	<u>121</u>				
Fold/unfold mech	2		26x44" panels		No body-mounted cells
Cell array	48			Hinge lines	
Power conditioning	14		8x8x6		
(2) Batteries	42		5x5x16		Redundancy
Lines, etc.	10				
Support	5				
<u>Structure</u>	<u>145</u>				
Base plate	50				Thermal radiator
Skeleton	12				
Skin	12				
Shield	10				Folds out
Cover plate	8				Sun reflector
Bulkhead	8				
Heat paths	10				
Misc. wire, clips, test points, etc.	35				
<u>Total</u>	<u>723</u>				

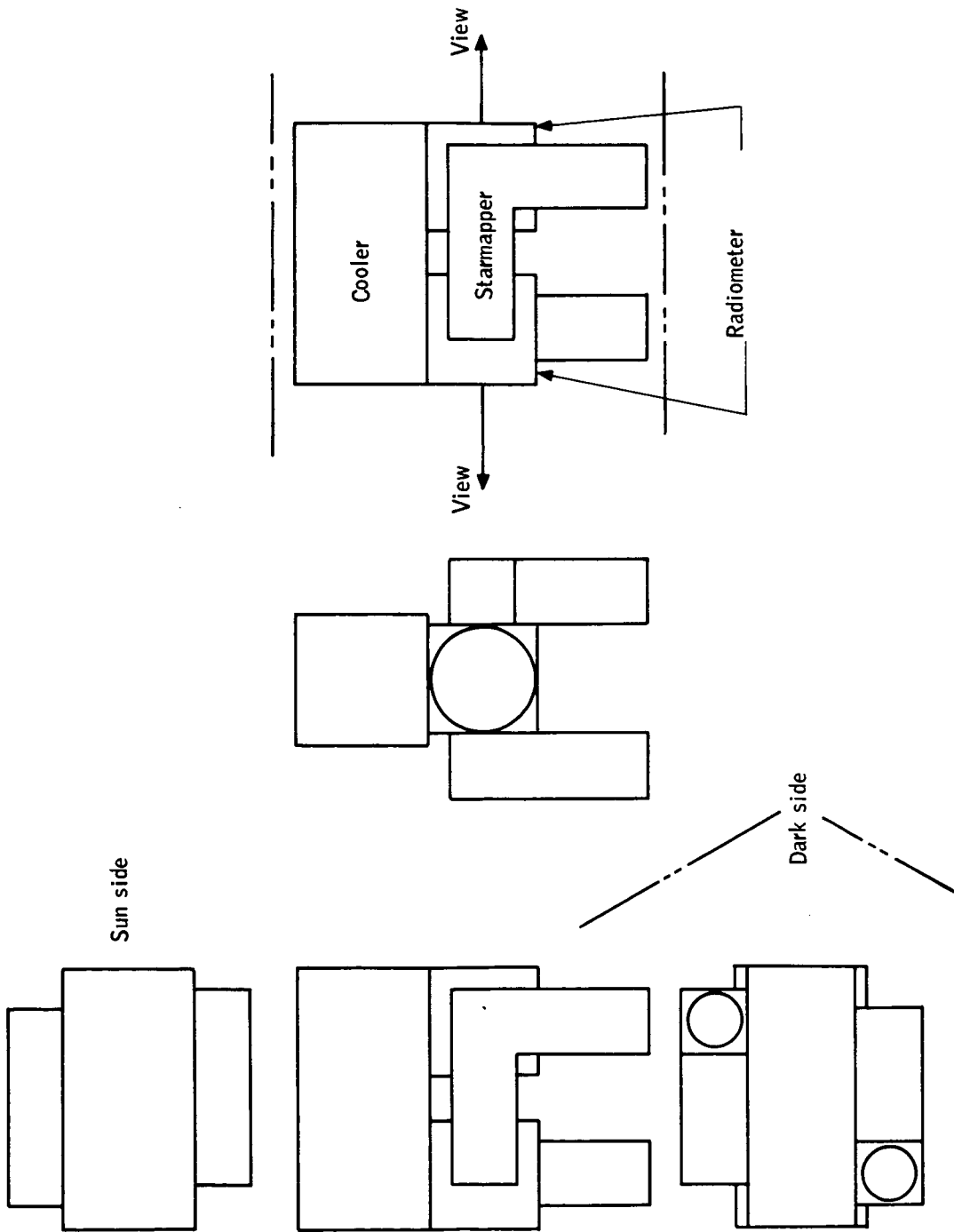


Figure 9. An Early Experiment Package Concept

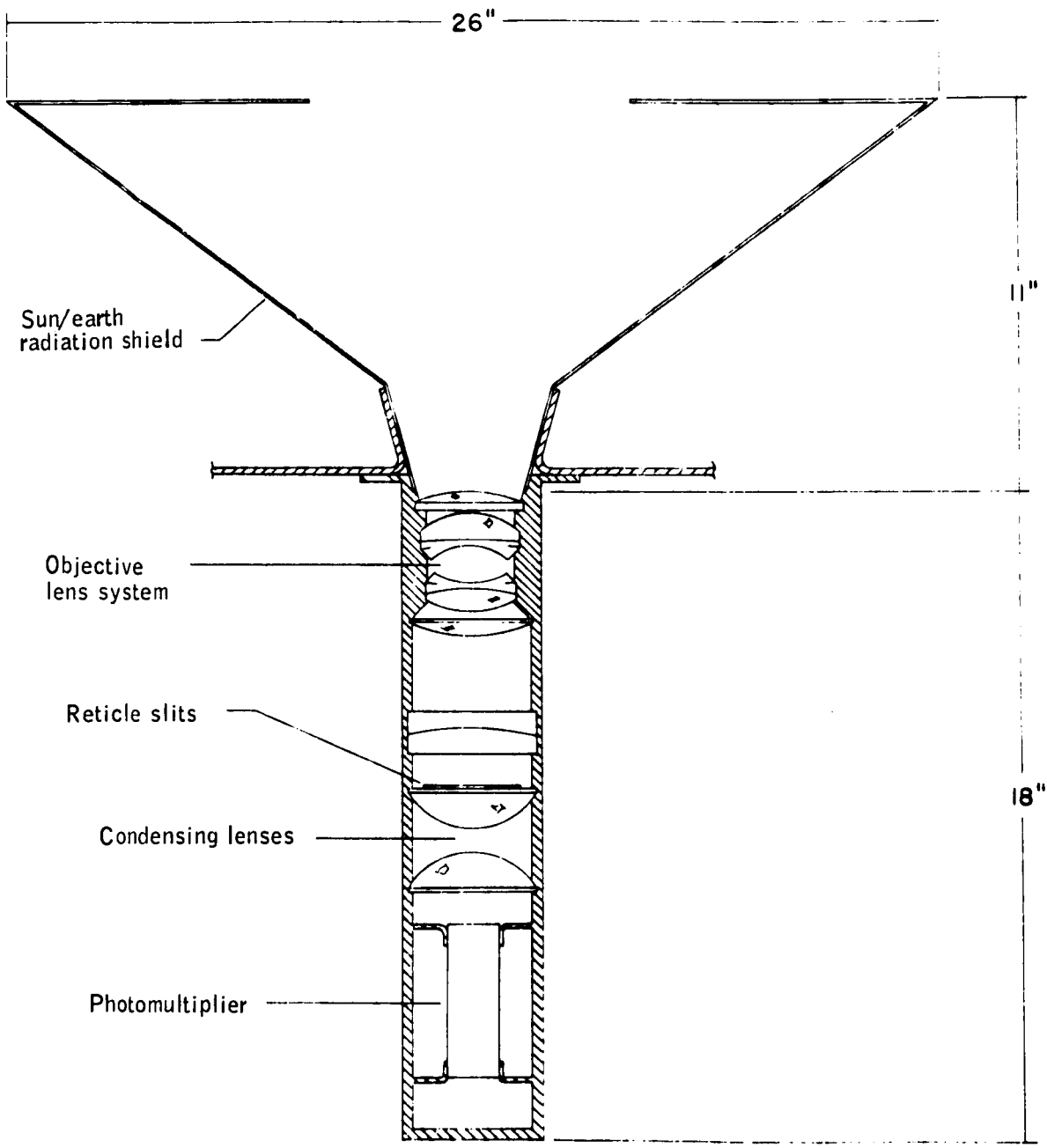


Figure 10. Possible Starmapper Design

the spacecraft and booster fairing envelope constraints. Sun sensors were substituted for orientation measurements during sunlit portions of the orbit, and the starmappers were intended for dark side operation only.

It was suggested that the radiometer could not "see" any direct sunlight during orbital operation because the IR radiance affected the readings, and the heating disturbed the thermal balance. Since the orbital plane was selected to be nominally at 45 degrees to the sun line, but could increase to 64 degrees because of injection errors, it was necessary to provide a sun shield around the radiometer view port. Although the sun shield is not directly a part of the experiment package, it is required for the satisfactory operation of the radiometer.

Final Concept Description

The final configuration of the highly sophisticated experiment package is shown in its spacecraft mounting orientation in Figure 11. The single, 16-inch diameter, radiometer optical system, which will view out the rim of the rolling spacecraft, incorporates a redundant signal channel consisting of a chopper, detector, detector bias supply, preamplifier, and amplifier. The dual set of starmappers, with about four-inch optics and seven-inch diameter "megaphone" baffles, will also look out the spacecraft rim and will make star readings when the spacecraft is in the dark. The two-inch diameter sun sensors complete the components within the experiment package. A small box of supporting electronics is needed for the radiometer as well as the starmappers.

Special precautions must be taken to enclose the entire package shown in Figure 11 within a cooled and well-controlled environment so that unwanted radiation is kept to a minimum and thermal distortions will not affect the precise alignment that is necessary. Also, no radiating body or obstruction can be positioned within the field of view of the optical systems.

ATTITUDE CONTROL

Evolution

The baseline, spin-stabilized-spacecraft concept requires control of the spin rate and orientation of the spacecraft axis relative to the orbit plane. The original concept of the attitude control subsystem (ACS) was to determine spacecraft orientation by fixing on the earth's horizon and the sun and correct that orientation as needed by energizing magnetic torquing coils at proper orientation with the earth's magnetic field. Initial spin-up or de-spin requirements would be met with jets or a yo-yo type of de-spin mechanism.

As the study progressed, the 2-stage Delta selection eliminated the possible requirement for a de-spin mechanism, and solid jets were found to be much more applicable than the cold gas. Redundant electronics support and horizon sensors were added to assure satisfactory operation. It was determined that the horizon sensors would provide adequate orientation information without the sun sensors. The need for spin-up jets was eliminated when it was determined that the spacecraft could be properly oriented and rotated before being separated from the booster.

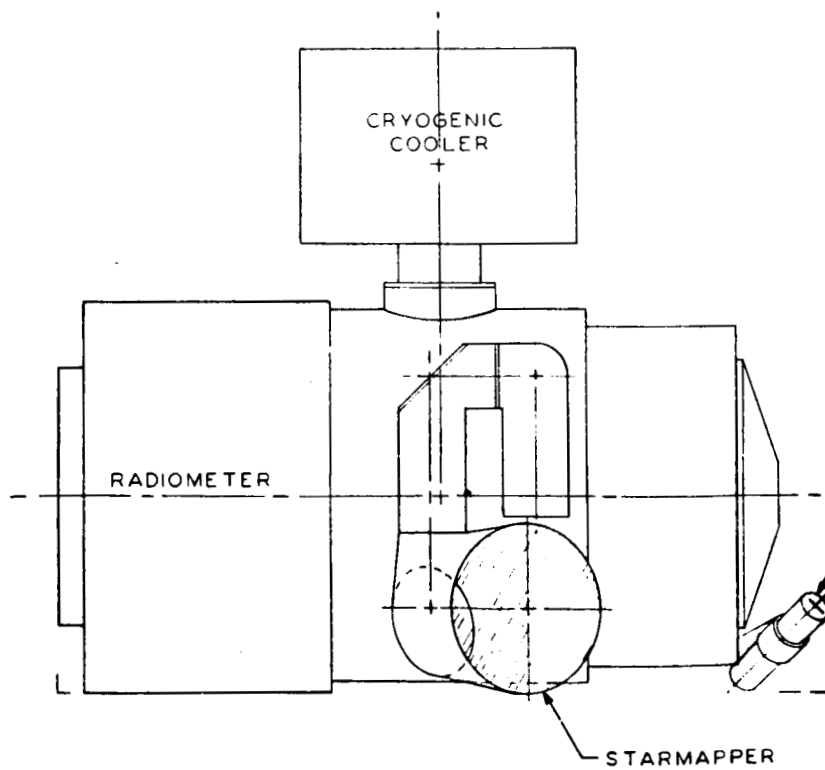
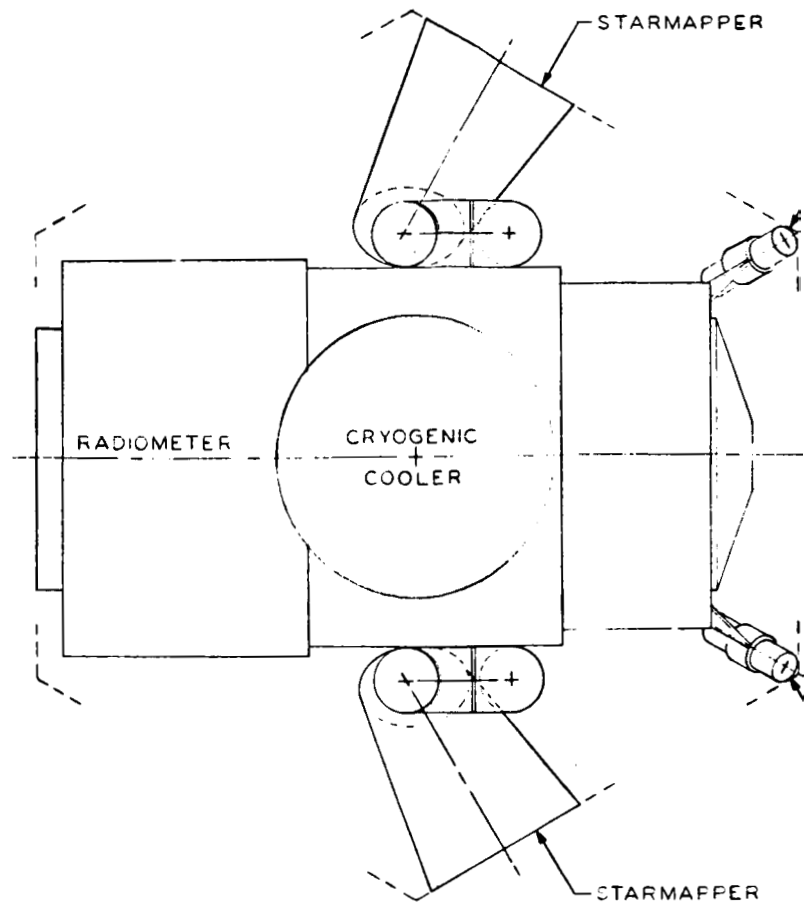
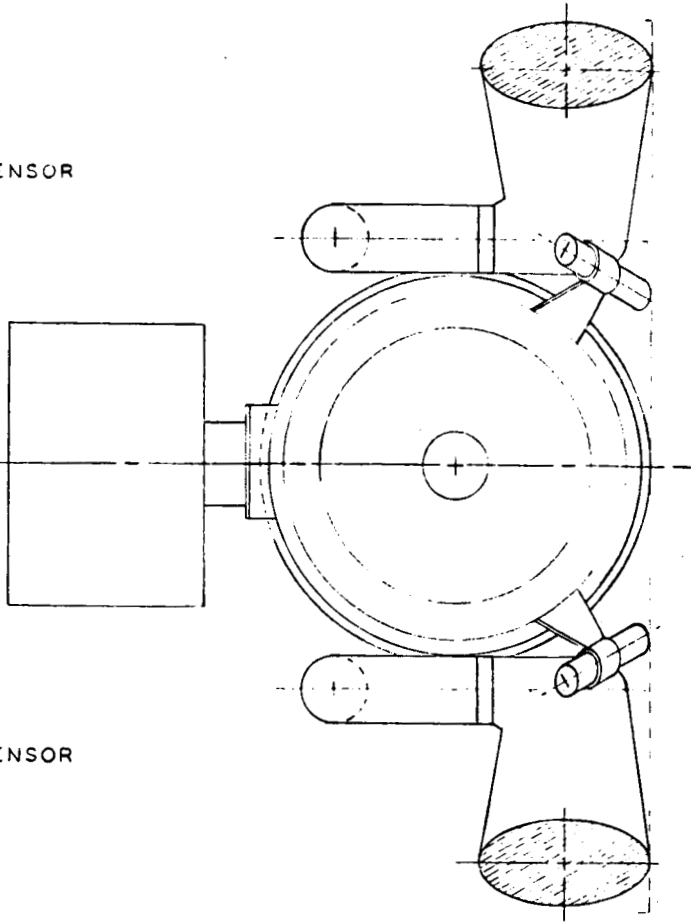


Figure 11. Experiment Package
60° Off Axis

SUN SENSOR

SUN SENSOR

SUN SENSOR



Final Concept Description

The finally described ACS is shown in block diagram form in Figure 12. It consists of redundant horizon sensors viewing out from the rim of the rolling wheel and electronic logic to control pulses of current to the magnetic coils. One coil, around the periphery of the rim, controls the attitude in the orbit plane; another, perpendicular to the first, controls spin rate. No special location relative to the center of mass is required since only a pure torque is exerted by the coil; i. e., there is no mass translation. An energy dissipating damper reduces the coning action of the spacecraft whenever it occurs.

The special spacecraft integration requirements for the final version of the ACS have been reduced to assuring that the horizon sensors look approximately 68 degrees behind the plane of the spin coil and that the torquing coils intercept as large an area of the earth's magnetic field as is reasonable.

DATA HANDLING

Evolution

The data handling subsystem was described very early as two boxes of electronic equipment; the data processing equipment (which could in turn be split into several packages) and the data storage. Redundancy was added in some areas during the study resulting in an increase in size and weight of the boxes.

Final Concept Description

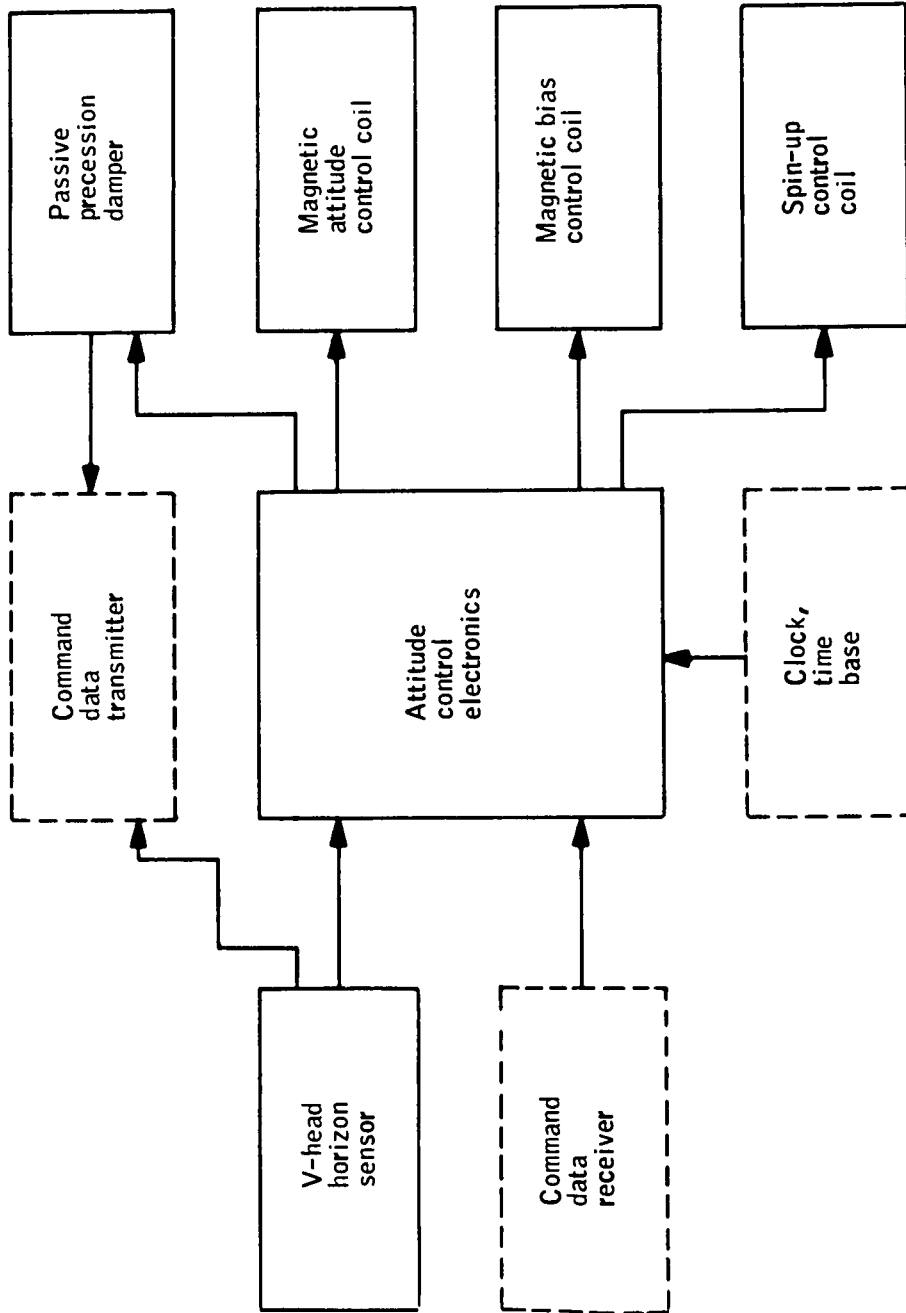
As indicated in the preceding section, the data handling subsystem consists of two boxes of electronics. They should be positioned close together, so electronic noise and other inaccuracies of data will not be present, and should have a thermal environment of $70 \pm 30^\circ\text{F}$. More detail of the final version is shown in the functional diagram of Figure 13.

COMMUNICATIONS

Evolution

The initial concept of the communications subsystem used the S-band, range and range-rate system of the NASA STADAN. As such, it consisted of 1700 MHz slot receiving antennas; a box of electronics for receiving, processing, and transmitting; and 2200 MHz slot transmitting antennas. A Minitrack beacon and 136 MHz stub antennas were also included as an acquisition aid.

During the study, it was determined that telemetry should be in the vhf range, since worldwide S-band coverage is very limited. Receiving of commands is at 148 MHz via three stub antennas, and transmission is at 136 MHz via a different set of three stub antennas. A redundant transponder was added late in the study to meet reliability requirements.



Solid lines - ACS components
 Dashed lines - periphery components

Figure 12. Attitude Control Subsystem Block Diagram

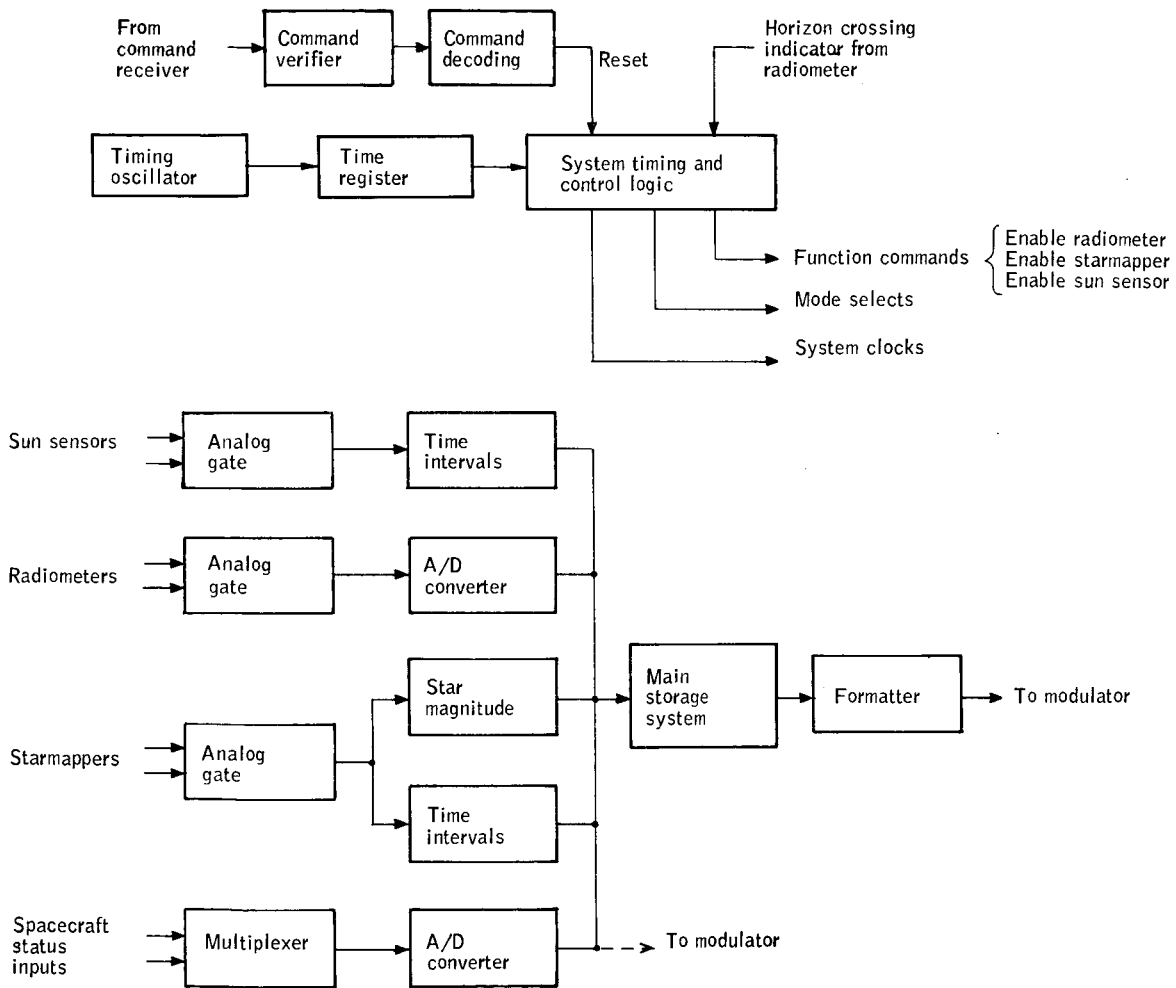


Figure 13. Data Handling Subsystem Functional Diagram

Final Concept Description

The suggested communications subsystem concept for this mission utilizes both S band and vhf, the S band for accurate tracking and vhf for mechanization and handling of accumulated data. Double sets of both slot and stub antennas (receiving and transmitting) are needed in combination with a box of electronics. The electronics could be broken into several separate units.

The stub antennas require orientation on a face normal to the spin axis to produce satisfactory earth coverage. The slots must be positioned on the extremes of the periphery so there is no blocking of the radiated signal. Figure 14 presents more details of this subsystem.

ELECTRICAL POWER

Evolution

Three possible types of power subsystems were considered for this application - fuel cells, radioisotope thermoelectric generators (RTG), and solar cells. Fuel cells were shown to be very heavy; the RTG produced serious handling problems, was very expensive, and appeared to be pressing the state of the art. Solar cells in a combination body mount/fold-out panel configuration was the first power generation concept. Power conditioning equipment and storage batteries along with the distribution lines completed the subsystem. The body-mounted cells were soon eliminated in favor of putting all cells on fold-out panels. Again, reliability requirements necessitated redundancy in the battery and part of the power conditioner.

Final Concept Description

Approximately 48 square feet of solar cells mounted on fold-out solar panels are needed to generate the power necessary to assure operation of the total spacecraft. Power conditioning equipment prepares the output of the solar array for direct use by the other subsystems or for battery storage to be used during sunlit portions of the orbit.

Special thermal considerations are necessary to maintain the narrow range of battery operating temperature while dissipating the large amounts of heat energy generated through operating inefficiencies in the batteries and power distribution equipment. It is also desirable to maintain the solar array at a low equilibrium temperature. The conceptual design details of this subsystem are presented in Figure 15.

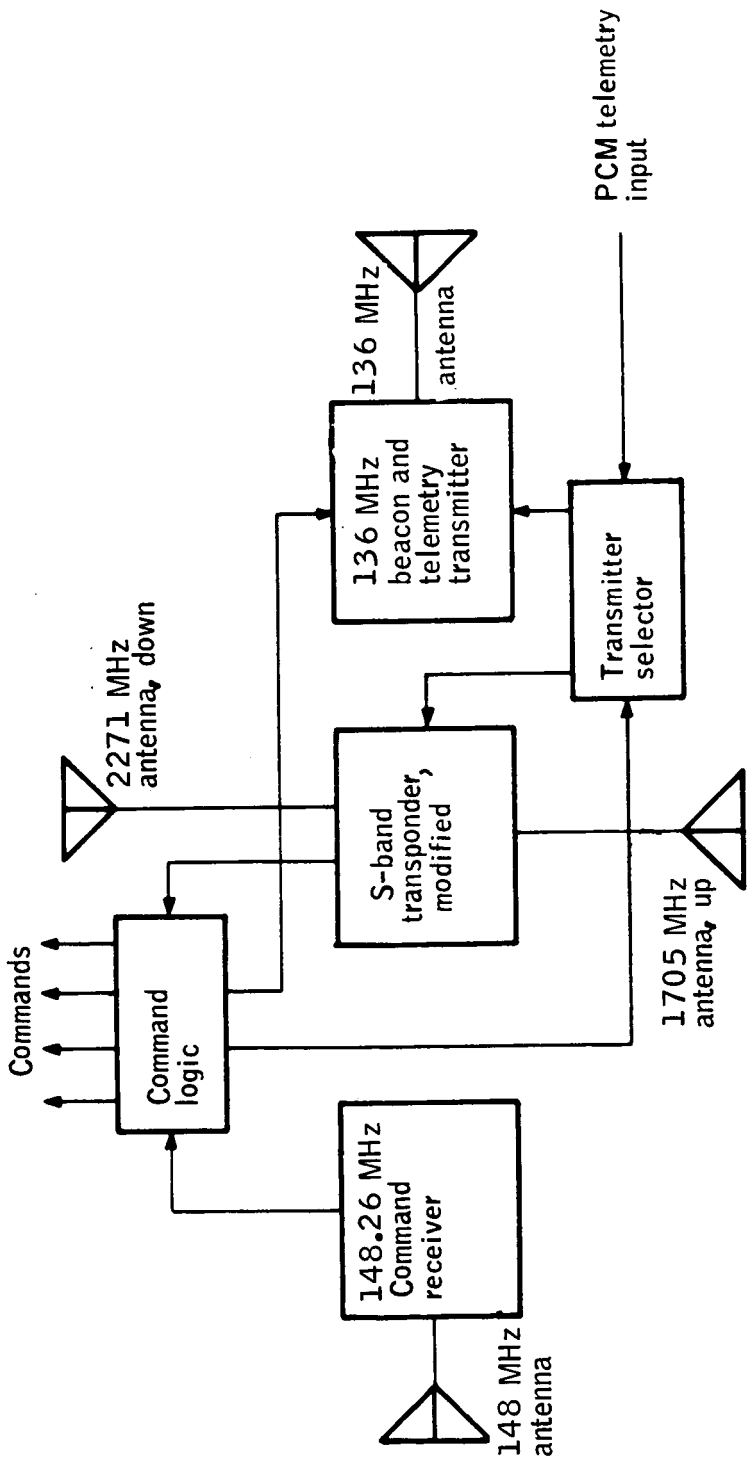


Figure 14. Vehicular Communications Subsystem - Command, Telemetry, and Ranging

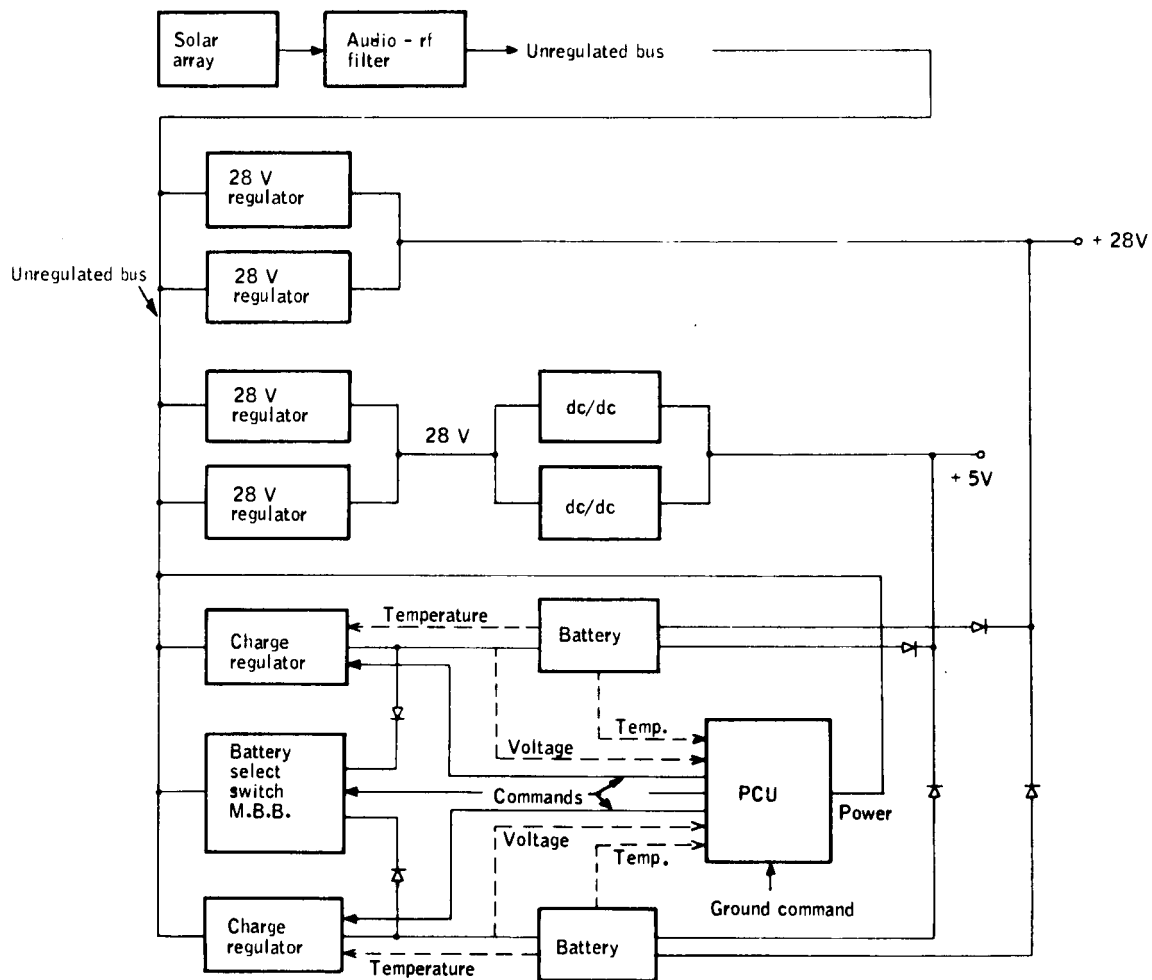


Figure 15. Satellite Electrical Power Subsystem

STRUCTURAL SUBSYSTEM

Evolution

The first structural subsystem concept was, very simply, a cylindrical skeleton with skin and bulkheads as needed to provide rigidity and component mounting frames. After early concepts of the subsystems were described, a hexagonal cylinder with enclosing bulkheads at each end and another in the center for component mounting was considered. It was envisioned that thermal control of the components would be through the sidewalls. Booster thrust loads would be carried from the end bulkhead to the center component-mounting bulkhead through supporting struts.

Final Concept Description

The requirement that the entire experiment package be radiatively cooled changed the concept to that roughly depicted in Figure 16. Superinsulation encloses the cooler, radiometer, sun sensors, and starmappers except for the megaphone baffles. The heavy, cast baseplate serves as a thermal radiator for the experiment package and as a thrust-carrying member. Sidewalls and longerons, which are thermally insulated from the baseplate, carry some of the thrust during boost and serve as a thermal radiator for internal thermal control of the units mounted on the bulkhead. The upper cover and fold-out solar panels are thermally insulated from the rest of the spacecraft. Considerably more detail of the spacecraft subsystem concept will be presented in a subsequent section covering spacecraft conceptual design.

THERMAL CONTROL CONCEPTUAL DESIGN

GENERAL

The thermal analyses were undertaken to help provide a rational basis for choosing among alternative spacecraft configurations and to lend assurance that the thermal design of the spacecraft was within the state of the art. In order to realize this objective, the assumptions that were required in the analyses were as realistic as possible, yet conservative.

Major problem study areas were

- Solar cell temperatures
- Experiment package cooling
- Electronic package thermal control.

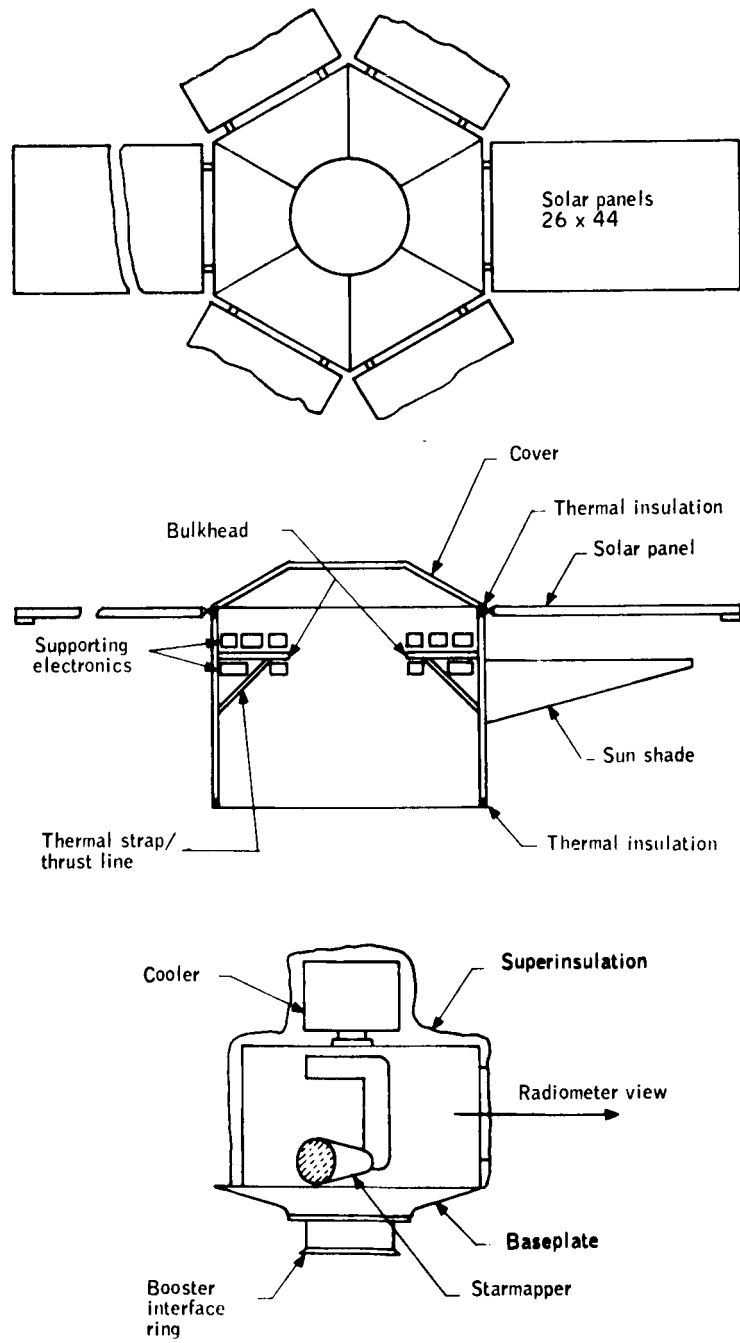


Figure 16. Conceptual Spacecraft Thermal Control Compartments and Structural Assemblies

Each area was studied in its quasi-steady state conditions, i. e., operating conditions in and out of the earth's shadow. No extensive analyses covering the launch and initial erection period were required since the booster was determined to have the capability to orient the spacecraft properly and quickly. Furthermore, no damage should occur to the spacecraft under any random orientation with the sun while the proper orbital orientation is being achieved, even if several days are needed. It has also been estimated that the experiment package will not begin to accumulate data for about seven days after orbit injection.

The study approach undertaken was to show the feasibility of proper thermal design, and not to conduct detailed analyses. For example, the feasibility of controlling each internal electronic package temperature within its allowable range is demonstrated. The actual temperature of each package can be kept within this range by using proper detailed thermal design and known and proven techniques.

ORBITAL HEAT FLUXES

The thermal environment of the spacecraft while in earth orbit was simulated. The environment consists of heat input from three sources outside the spacecraft: direct solar heating, indirect earth-reflected solar heating or albedo, and infrared radiation emitted by the earth. The amount of heat from each source is a function of spacecraft attitude and orbital position and is different for each surface of the spacecraft. A computer program (ref. 2) was used to compute the incident heating simultaneously for each surface.

Figures 17, 18, and 19 show incident heating on each face of the spacecraft for a 500 km circular orbit inclined with the orbit normal at 31°, 45°, and 64° to the sun vector. Direct solar heating is always zero on the rear face. Albedo heating varies from a maximum at a subsolar point to zero during shadow passage because the earth is a diffuse reflector of solar radiation. Earth emission is constant because the orbit is circular, and a constant temperature earth is assumed.

Orbital heat fluxes where the spin axis is not exactly perpendicular to the orbit plane were also computed. Spin-axis to orbit-normal angles of 2.5, 5, and 10 degrees were considered. These fluxes were used to demonstrate the effect of attitude errors.

In all cases, the total incident heating is greatest on the front (sunlit) face of the spacecraft, less on the side walls (spinning averages the direct solar heating), and least on the rear face and back of the solar panels. Shadowing of the sidewalls by extended solar panels reduces the incident heating shown in Figure 18 but also results in radiant interchange between the back of the panels and the sidewalls.

These effects, along with the effect of the skin thermal inertia, internal equipment dissipation, different thermal control coatings, and conduction

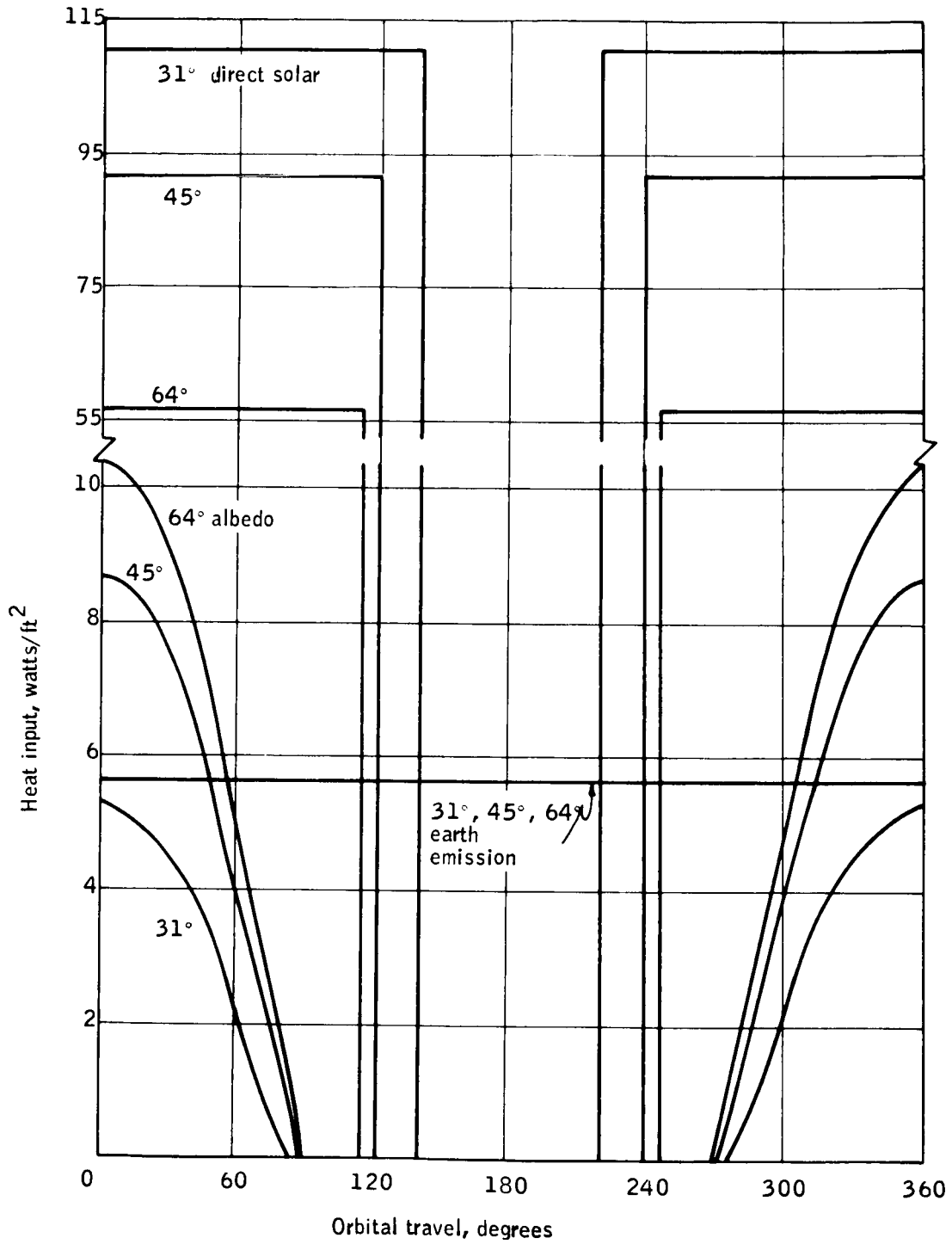


Figure 17. Space Heating Incident to Front Face of Spacecraft and Cell Side of Solar Panels

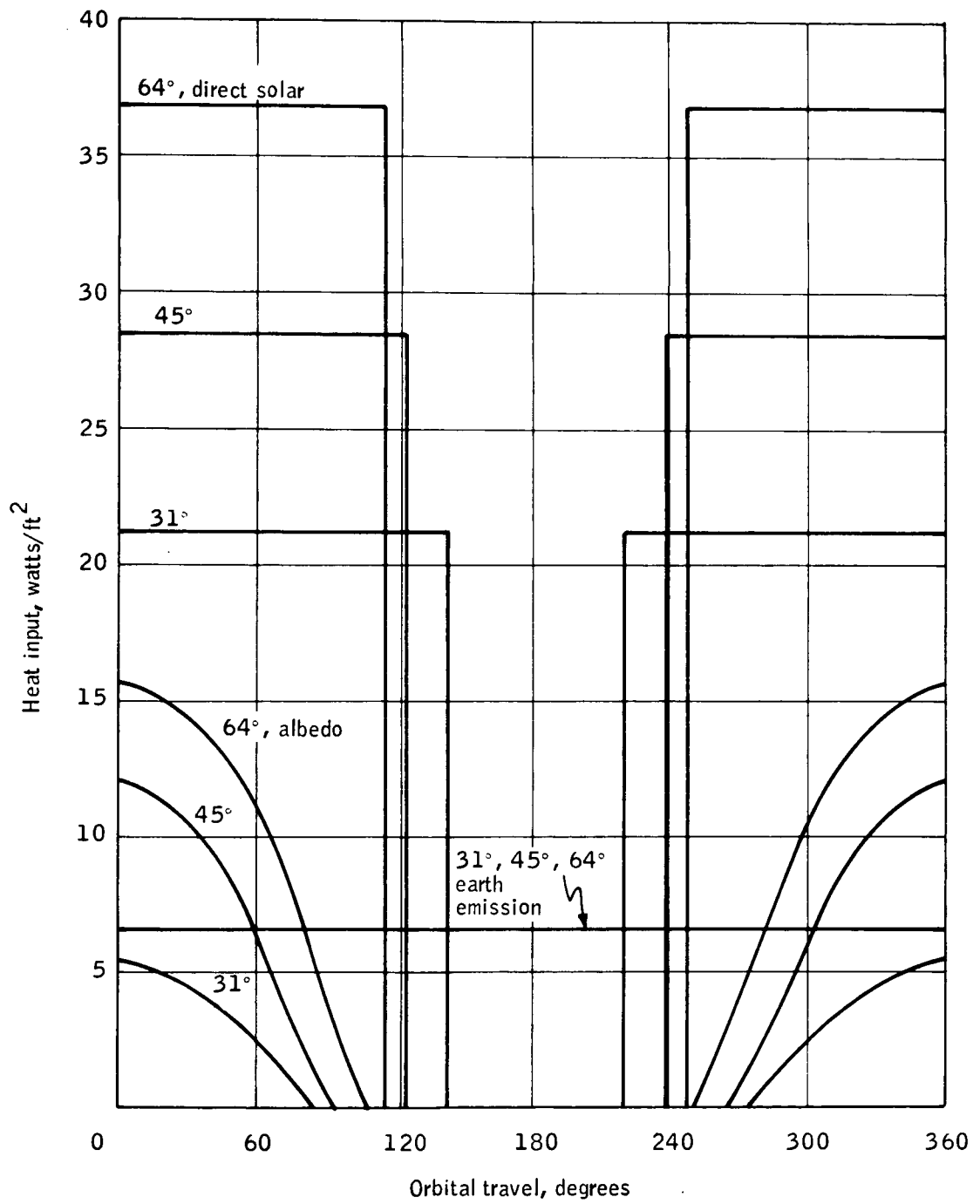


Figure 18. Space Heating Incident to Sidewalls, No Shadowing by Panels or Other Objects

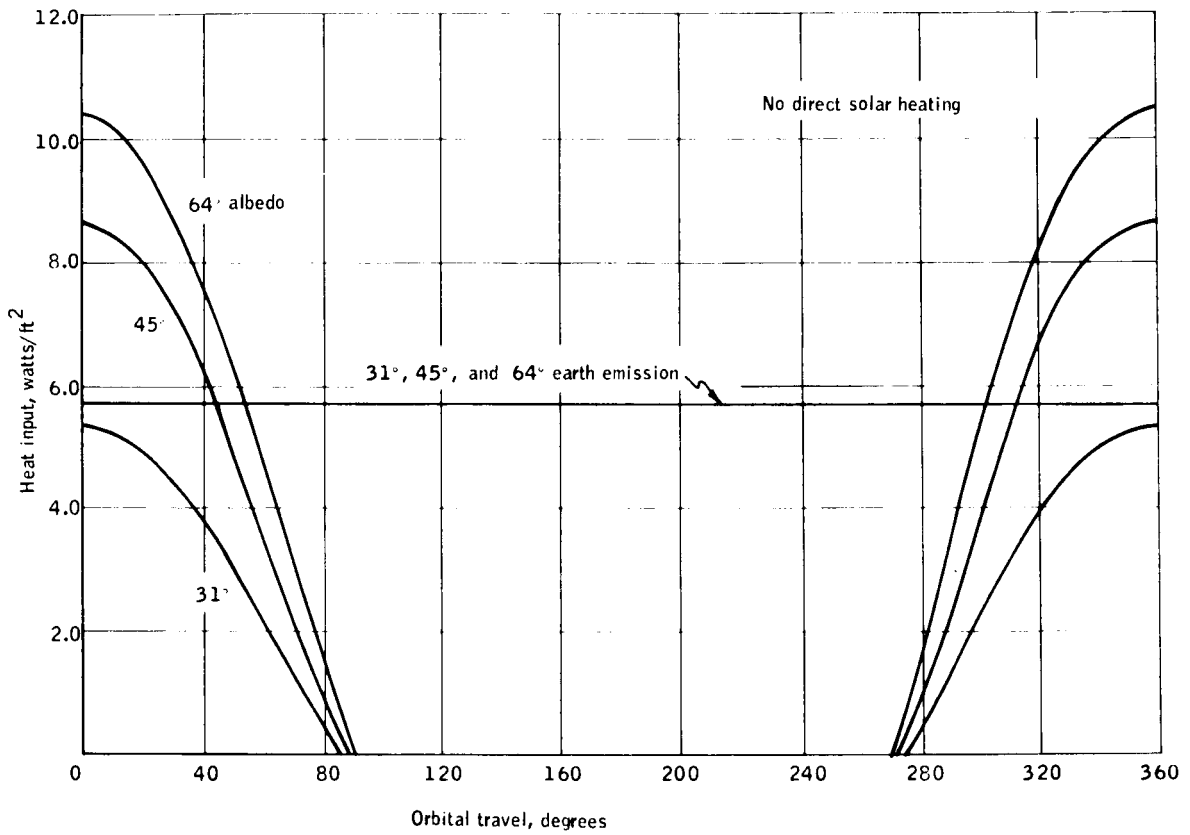


Figure 19. Space Heating Incident to Rear Face of HDS Spacecraft

through the spacecraft external structure were incorporated in a computer program (ref. 3) that predicted spacecraft temperatures as a function of time.

EXTERNAL SKIN AND SOLAR-CELL TEMPERATURES

The external skin and solar cell temperatures of the spacecraft in the 31, 45, and 64 degree sun angle orbits were computed for several spacecraft configurations. The configurations assumed were

- Hexagonal spacecraft with body-mounted cells on all sunlit faces.
- Hexagonal spacecraft with extended solar panels.
- Hexagonal spacecraft with extended solar panels and an umbrella type of sunshield between and beyond the panels (in the same plane).
- Hexagonal spacecraft with extended solar panels and a local sun shield erected around the radiometer entrance aperture.

In order to permit meaningful comparisons between these configurations, identical assumptions were made on some of the thermal characteristics involved. These significant assumptions were

- Any external surface not covered by solar cells was covered by a thermal control coating having a low α_s/ϵ (where $\alpha_s \equiv$ solar absorptance and $\epsilon \equiv$ infrared emittance) ratio, i.e., available white paints or Lockheed's Optical Solar Reflector (OSR) surface.
- The thermal inertia of the skin was based on a 0.03-inch thickness of uniformly distributed aluminum.
- The thermal inertia of extended solar panels was based on 1/2-inch aluminum honeycomb panels with 0.015-inch facings having a core density of 5 lb/ft³.
- Solar panels, front face, sidewalls, and rear face were all conductively insulated from each other. Radiation interchange between external surfaces viewing each other was accounted for. There was no internal radiation interchange between surfaces.
- 100 watts of internally generated heat was distributed with 70 watts to the sidewalls and 30 watts to the rear face.
- The spacecraft spin axis was oriented normal to the orbit plane. The effect of an off-normal spin axis was also analyzed.

- A 500 km, circular, polar orbit was used; the heat fluxes described in Orbital Heat Fluxes were for this orbit.

All of these assumptions are reasonable enough to permit a valid comparison between the alternative configurations.

The results of the analyses are shown in Figures 20 through 23. The temperatures shown are for times after the initial launch transient has died out. That is, the temperatures are quasi-transient (functions of time but periodic). Each surface was characterized as a uniform temperature nodal point. This approximation was shown in subsequent analyses to be valid enough for the purposes of the studies and will be discussed later.

Figure 20 shows the surface temperatures for the hexagonal spacecraft with body-mounted cells on the sunlit face and sidewalls. For this calculation, and in all succeeding calculations, the solar absorptance of the cells was 0.79 and the infrared emittance of the cells was 0.82. The rear face was assumed coated with white paint having a solar absorptance of 0.25 and an infrared emittance of 0.90.

It can be seen that the sunlit face temperature rises to a level between 140°F and 230°F; this level increases with a decrease in the solar angle, and then falls to subzero temperatures during shadow passage. The sidewall temperature rises to a level between 40°F and 102°F, this level increases with an increase in solar angle and also falls to subzero temperatures during shadow passage. The rear face temperature remains at a low level between -103°F and -122°F, varying only because of the varying incident albedo heating.

Figure 21 shows surface temperatures for the hexagonal spacecraft with extended solar panels and no extra sun shielding. The shadowed face of the panels, the sunlit front face, the sidewalls, and the rear face were all assumed coated with the solar-reflecting white paint. Solar cell arrays were assumed to cover the sunlit face of each panel. Because the extended panels shadow the sidewalls to some extent, the incident direct solar heating of the sidewalls is reduced from the situation with no extended panels. Because the sidewalls and the back of the solar panels view each other, radiation interchange occurs between these surfaces. Radiation is emitted by both the front and back of the panels. The temperature of the solar panels rises to a level between 56°F and 124°F during the daylit portion of the orbit and then falls to subzero temperatures during the shadow portion. The maximum temperature of the sidewalls for a solar angle of 45 degrees is approximately -26°F, a great reduction from the situation of Figure 20. This is due to the shadowing effect of the panels and the low α_s of the white paint. The maximum temperature of the front face varies between 30°F and 56°F depending on the solar angle, also a considerable reduction in temperature from the body-mounted cell situation.

Figure 22 shows surface temperatures for the hexagonal spacecraft with extended solar panels and sun shielding between and beyond the panels. This shielding lies in the same plane as the panels and is sufficient in size to

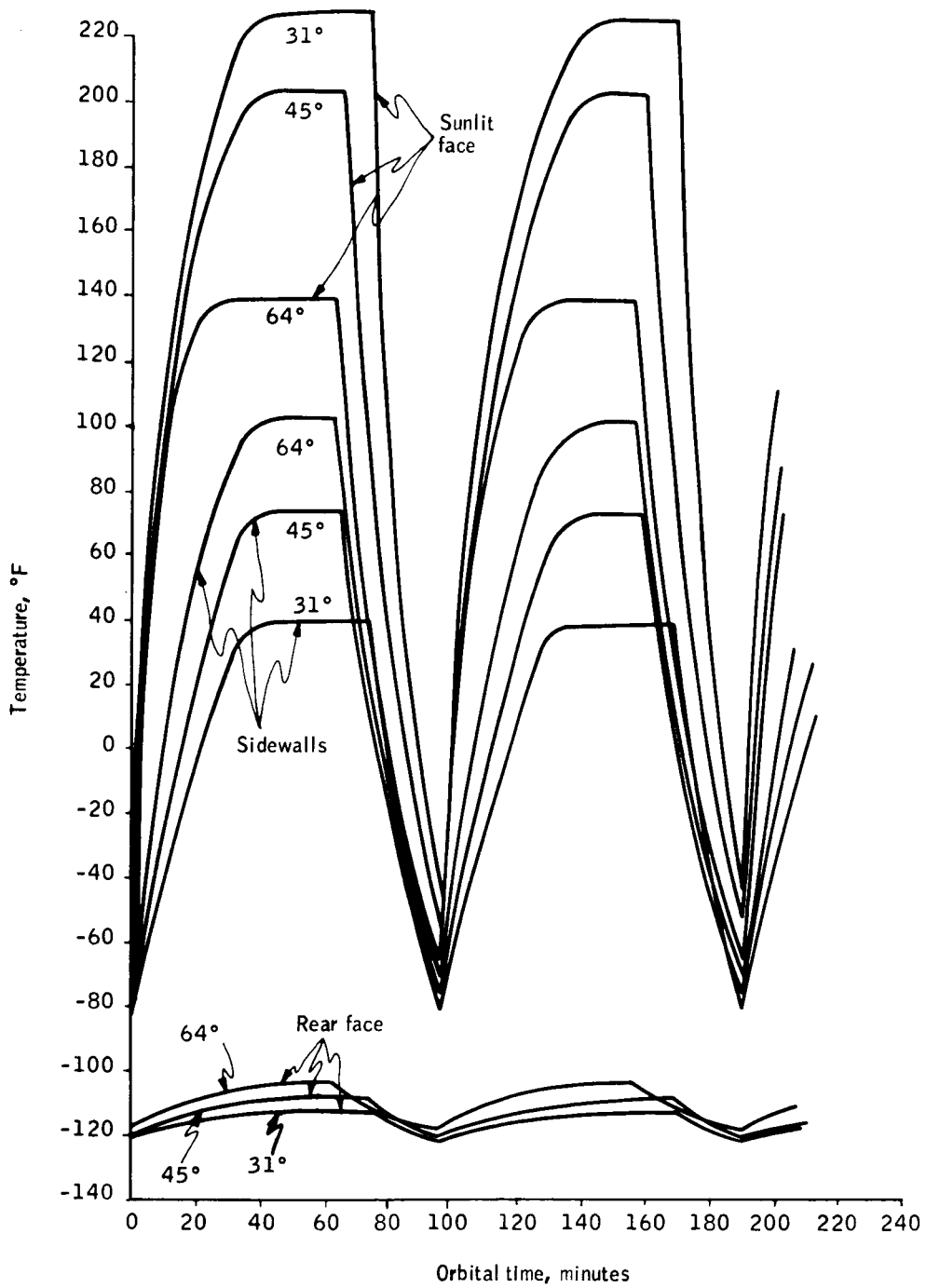


Figure 20. External Surface Temperatures - Hexagonal Spacecraft With Body - Mounted Cells on All Sunlit Faces

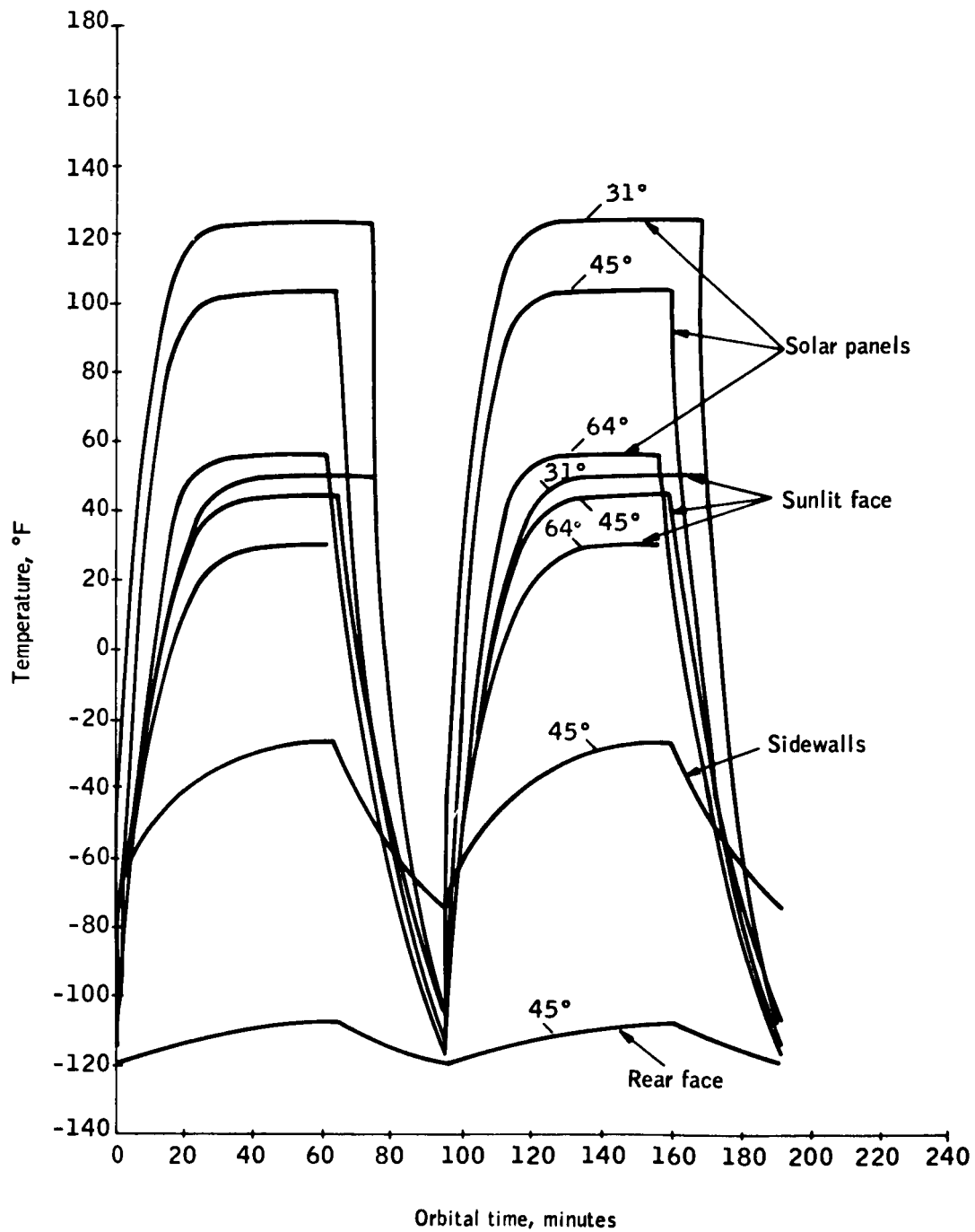


Figure 21. External Surface Temperatures - Hexagonal Spacecraft with Extended Solar Panels and No Extra Sun Shielding

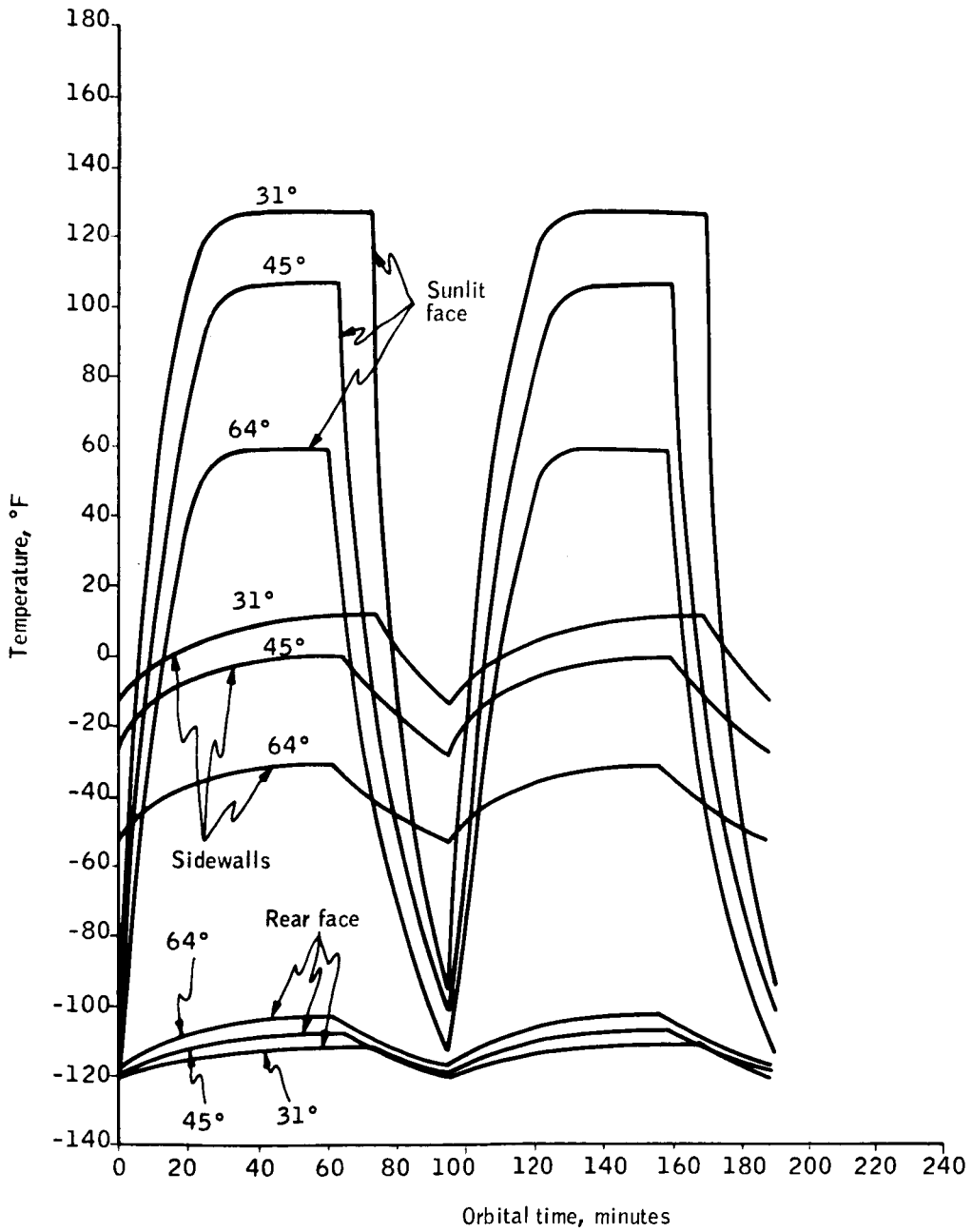


Figure 22. External Surface Temperatures - Hexagonal Spacecraft With Extended Solar Panels and Sun Shielding in Plane of Panels

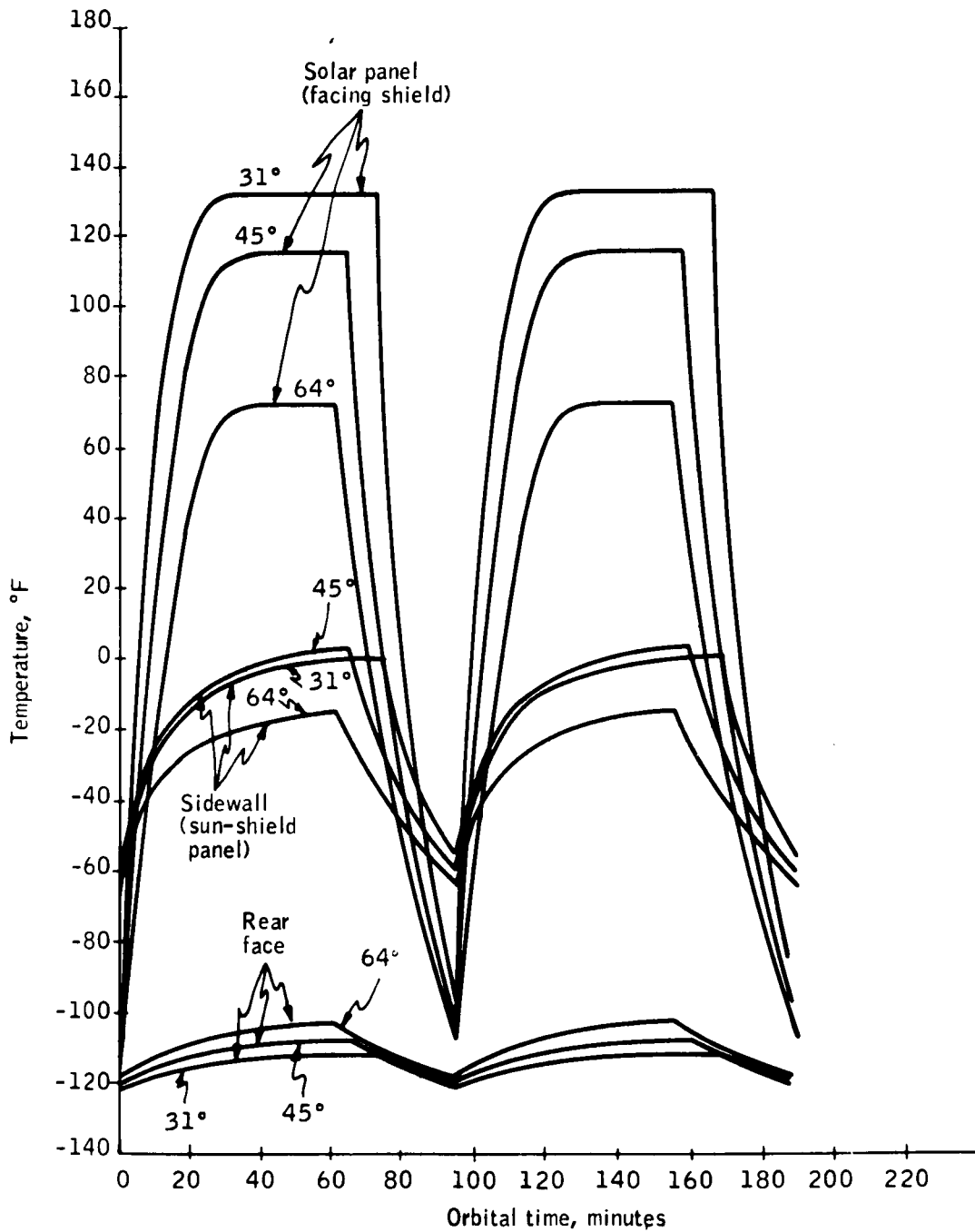


Figure 23. External Surface Temperatures - Hexagonal Spacecraft With Extended Solar Panels and Local Sun Shield Over Radiometer Entrance

preclude direct solar illumination of any portion of the sidewalls. White paint is applied to the sidewalls and rear face. The solar panel temperature rises to 59°F to 127°F, depending on the solar angle. This is not significantly different from the configuration with extended panels and no shielding. The sidewalls have maximum temperatures in the range of -31°F to +12°F. The sidewalls temperature is more stable throughout an orbit, compared with the configuration with no extra shielding, varying at the most 28°F in an orbit.

Figure 23 shows surface temperatures for the hexagonal spacecraft with extended solar panels and a local, lightweight sun shield erected over the radiometer entrance aperture. Opposing faces of the sun shield are thermally isolated by multifoil radiation insulation. Direct solar illumination is incident on portions of the sidewalls and sun shield. The solar panel that is located above the local sun shield is slightly warmer (up to 16°F) than the panels that do not view the sun shield. This is due to radiation interchange between the sun shield and panel. The maximum sidewall temperature lies between -15°F and +4°F. It is thus also affected by the presence of the shield. The shield should be coated with a reflecting coating on the sunlit side and a highly emitting coating on the shadowed side. The multifoil insulation layers between shield sides will essentially eliminate radiation and conduction modes of heat transfer between sides of the shield.

A directional emitting surface on the cold side of the local sunshade and on the shaded spacecraft body as shown in Figure 24 has potential advantages and should be investigated to optimize the sunshade design. This surface would place highly emitting strips (white paint or OSR) facing away from the radiometer entrance and low emitting strips (vapor-deposited silver) facing toward the radiometer, thus resulting in both a cold shade temperature (-144 to -108°F) and a decreased emission to the radiometer. Emission of the shaded spacecraft sidewall toward the shade would likewise be reduced. Thus, radiation interchange between body and shade would be minimized. No detrimental effect on the radiometer baffling design is envisioned, since the baffling must be capable of attenuating stray radiation from up to 68 degrees from the radiometer axis in any case.

A directional-emitting surface design for the cold side of the local sun shade could be optimized with regard to its function-minimizing heat loading on the experiment package and stray radiation to the radiometer. This design optimization could be achieved in three steps.

1. Search for candidate coatings exhibiting space stability, desirable radiation properties (emittance extremes, low solar absorptance), and compatibility with the sun shade.
2. Analyses to select the optimum geometry-groove depth, angle, and spacing. This would require some advancement in radiation interchange analysis, since mixed diffuse/specular problem has been neglected in the past.
3. Monitor the model surface chosen from steps 1 and 2 with a directional reflectometer or emissometer to measure the directional distribution of radiation.

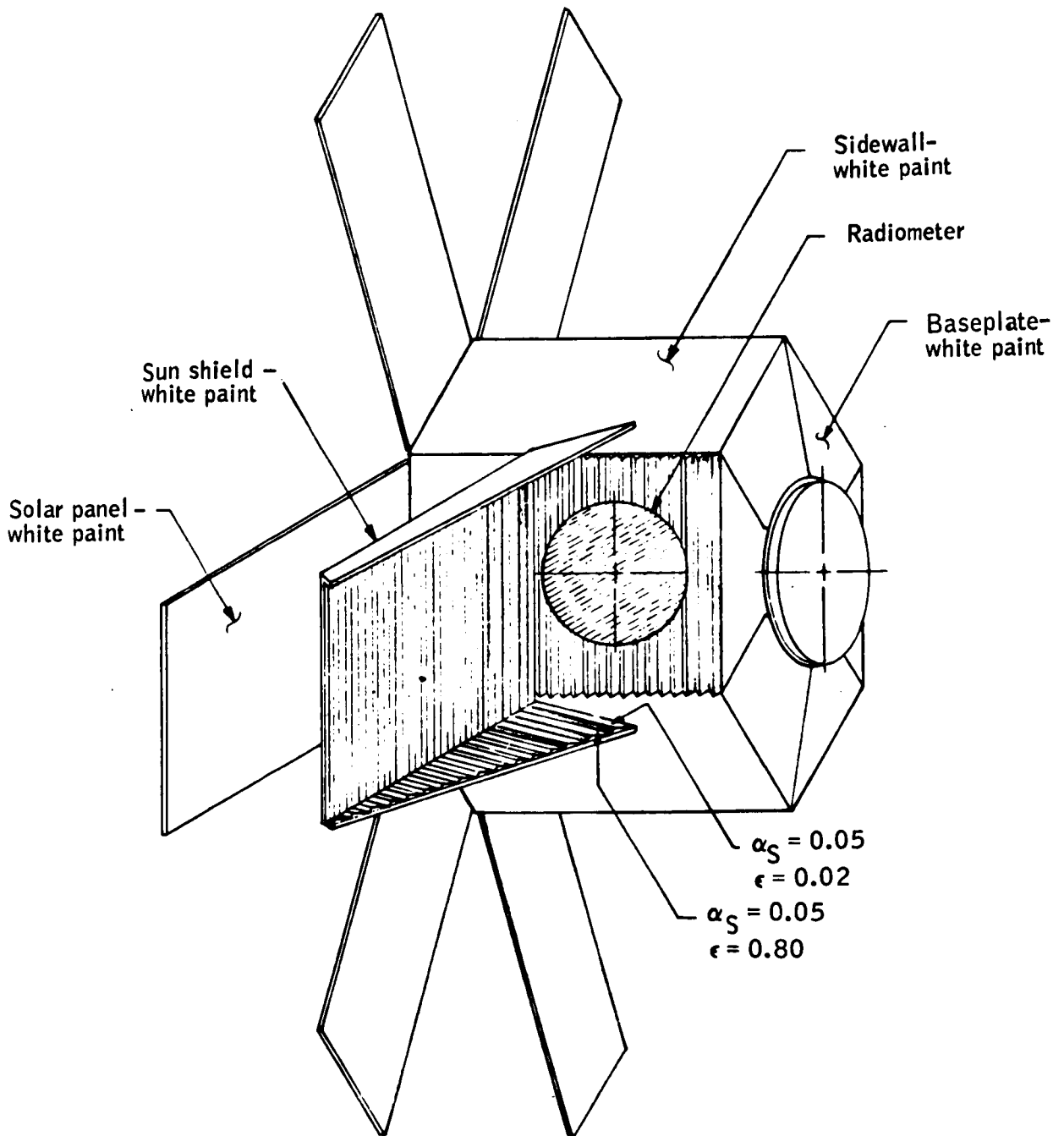


Figure 24. Local Sun Shield with Directional Emitting Surfaces

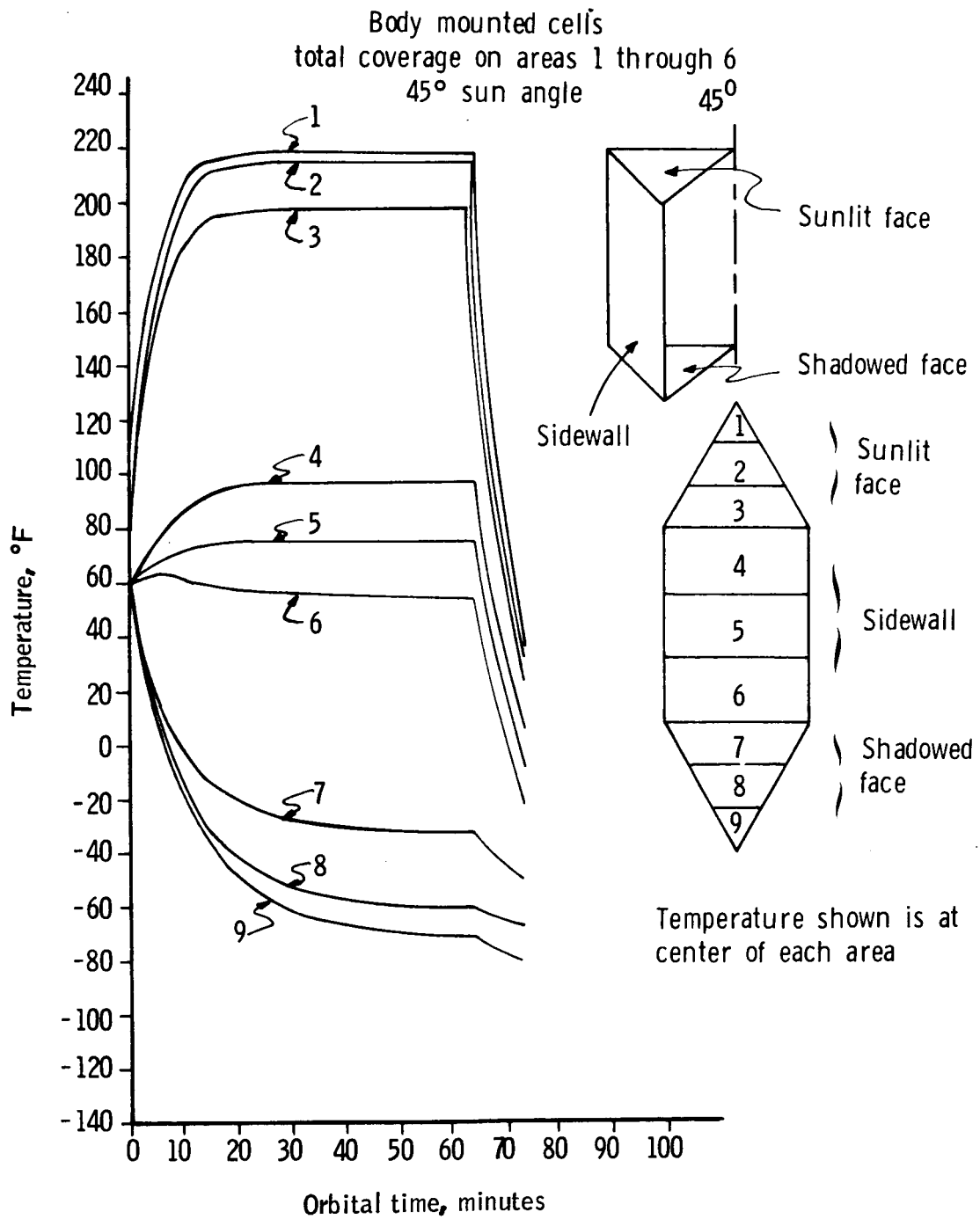


Figure 25. Effect of Skin Conduction on Cell Temperatures

All the curves shown in Figures 20 through 23 were found by neglecting lateral skin conduction. In order to assess the importance of this factor, a study was made of the body-mounted cell configuration, incorporating conduction along the 0.003-inch aluminum skin. The skin was divided up into nine areas as shown in Figure 25. The effect of skin conduction can be seen by comparing temperatures at the center of each of these areas, as shown in Figure 25, with the temperatures of Figure 20. The assumption of no-skin conduction is good since the average temperature of each surface is well estimated.

In addition to the preceding results, the effect on cell temperature of varying solar-cell coverage on various areas of the spacecraft was studied. The maximum equilibrium cell temperature was calculated as a function of solar-cell coverage, assuming that the remainder of the surface was covered by white paint. The aim of this was to guide in maximizing power generation by the cells, since solar-cell efficiency decreases with increasing temperature and an increase in output may be possible by keeping the cells cooler. Figure 26 displays the effect of varying coverage on the sunlit face, and Figure 27 shows the effect on the sidewalls. Figure 28 gives the effect of extending the sidewall surface back like a skirt. In this case, additional cooling will occur by radiation from the back of the extended surface. Using these results and the functional relationship between cell temperature and power generation, no advantage (total power generation increase) could be derived by using partial cell and partial white paint coverage.

Another study determined the temperature gradient induced through the extended solar-cell panels, assuming a 1/2-inch aluminum honeycomb panel substrate. Facings of 0.015 inch, core density of 5 lb/ft³, and 0.003-inch silicone adhesive for the cells was assumed. Temperature differences, front to back, of only 12°F were found; therefore, the approximation of a uniform panel temperature is also quite good for purposes of preliminary analysis.

In summary, the hexagonal spacecraft concept with no sun shielding other than the folded-out solar panels would exhibit temperatures on the external surfaces approximately as shown below for the nominal 3 p. m. / 3 a. m. orbit.

Solar panels	100°F
Sunlit face	50°F
Sidewalls	-30°F
Baseplate	-110°F

HEAT LOADING OF EXPERIMENT PACKAGE

The preceding section shows that the rear face of the spacecraft can be kept at temperatures below -100°F (200°K) if it is thermally isolated from the rest of the spacecraft and does not have too much internal heat dissipated into it (30 watts was assumed for these studies). The rear face which acts as a highly reliable, passive cooler then becomes an attractive place to tie in the experimental package (radiometer, detector cooler, starmappers, and sun sensors) which must be kept at such low temperatures. Figure 16 shows the principle involved in cooling the experiment package.

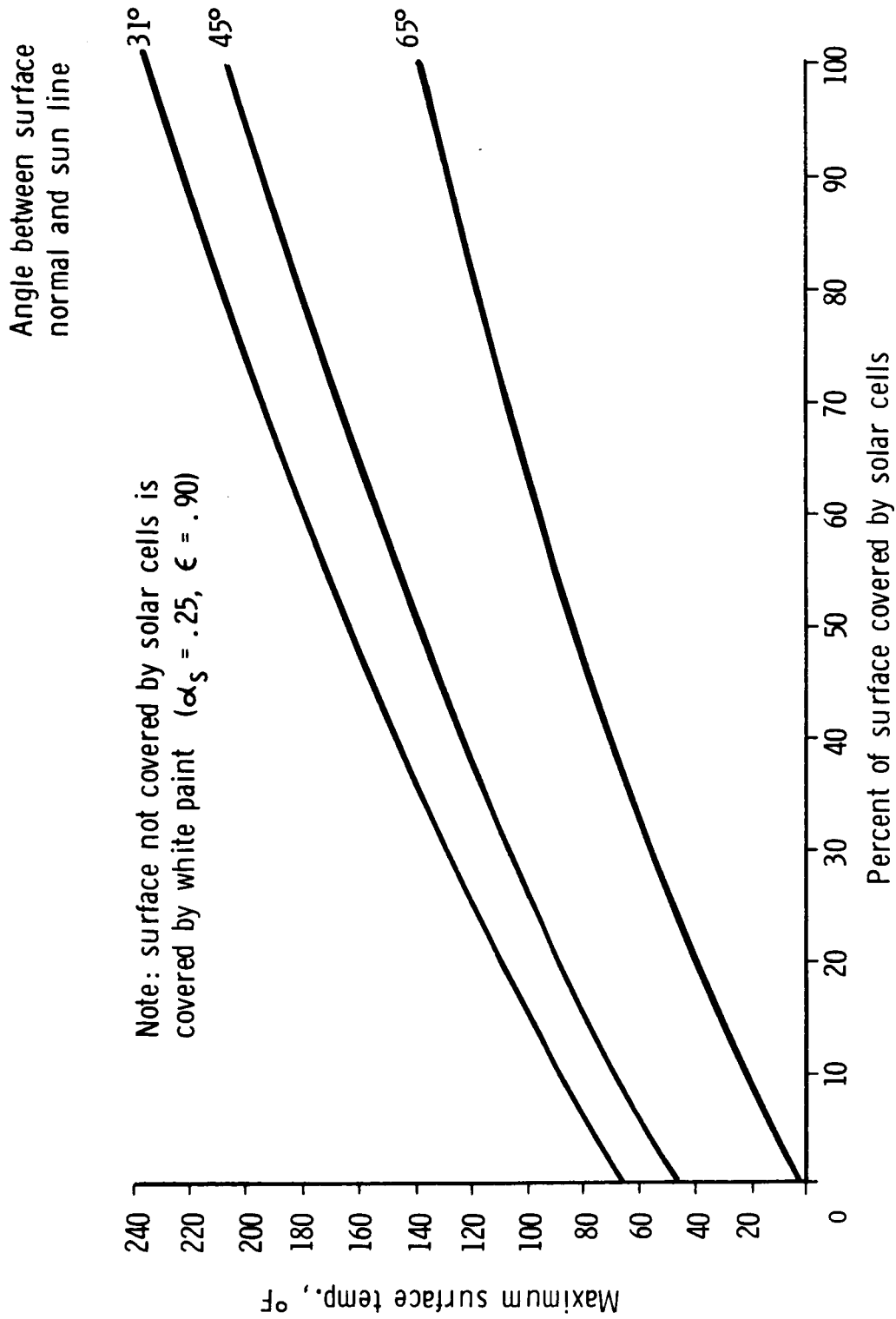


Figure 26. External Surface Temperature for Varied Solar Cell Coverage - Front Surface (Sunlit Except During Shadow Passage)

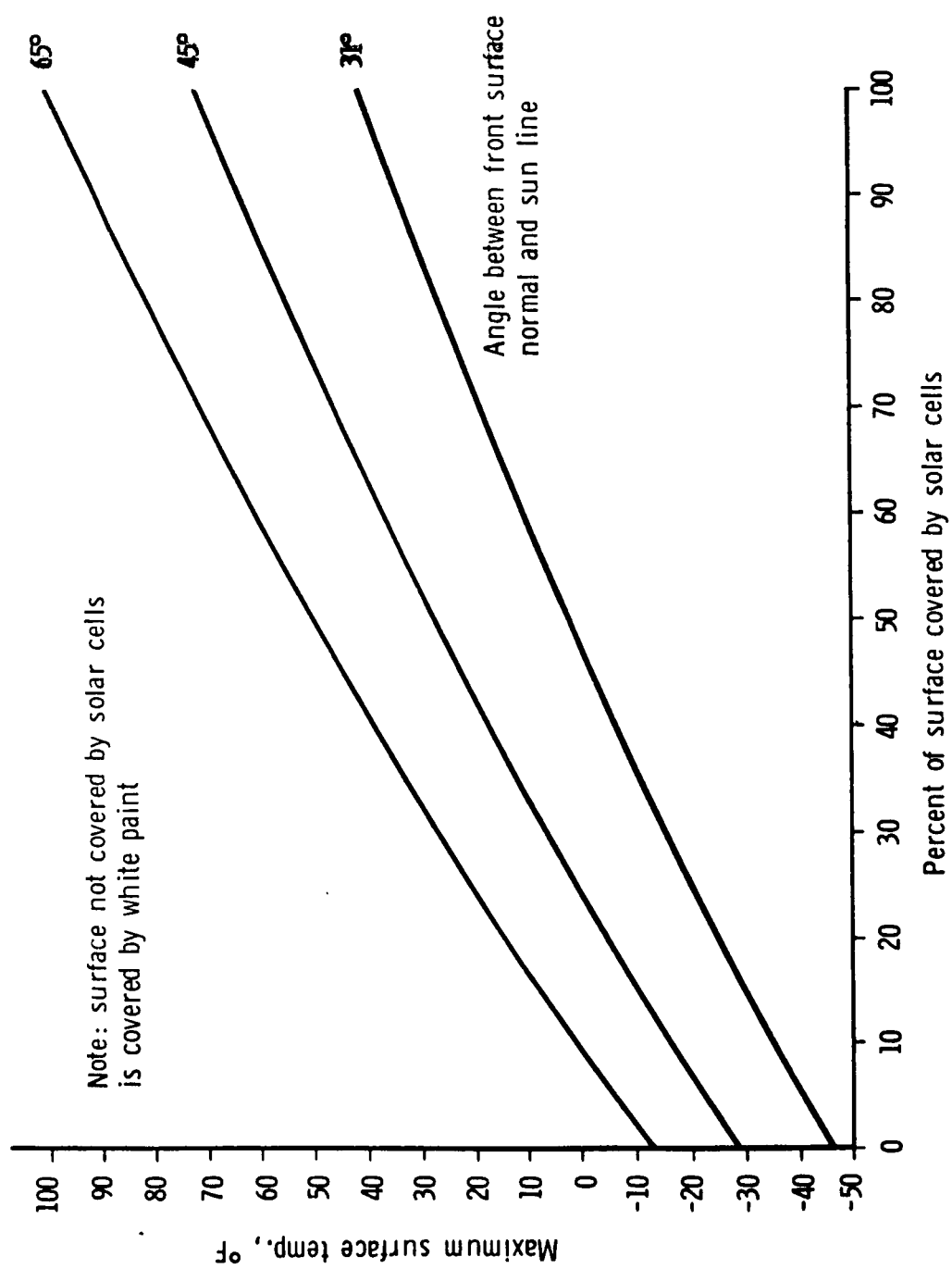


Figure 27. External Surface Temperature for Varied Solar Cell Coverage - Sidewall Surface

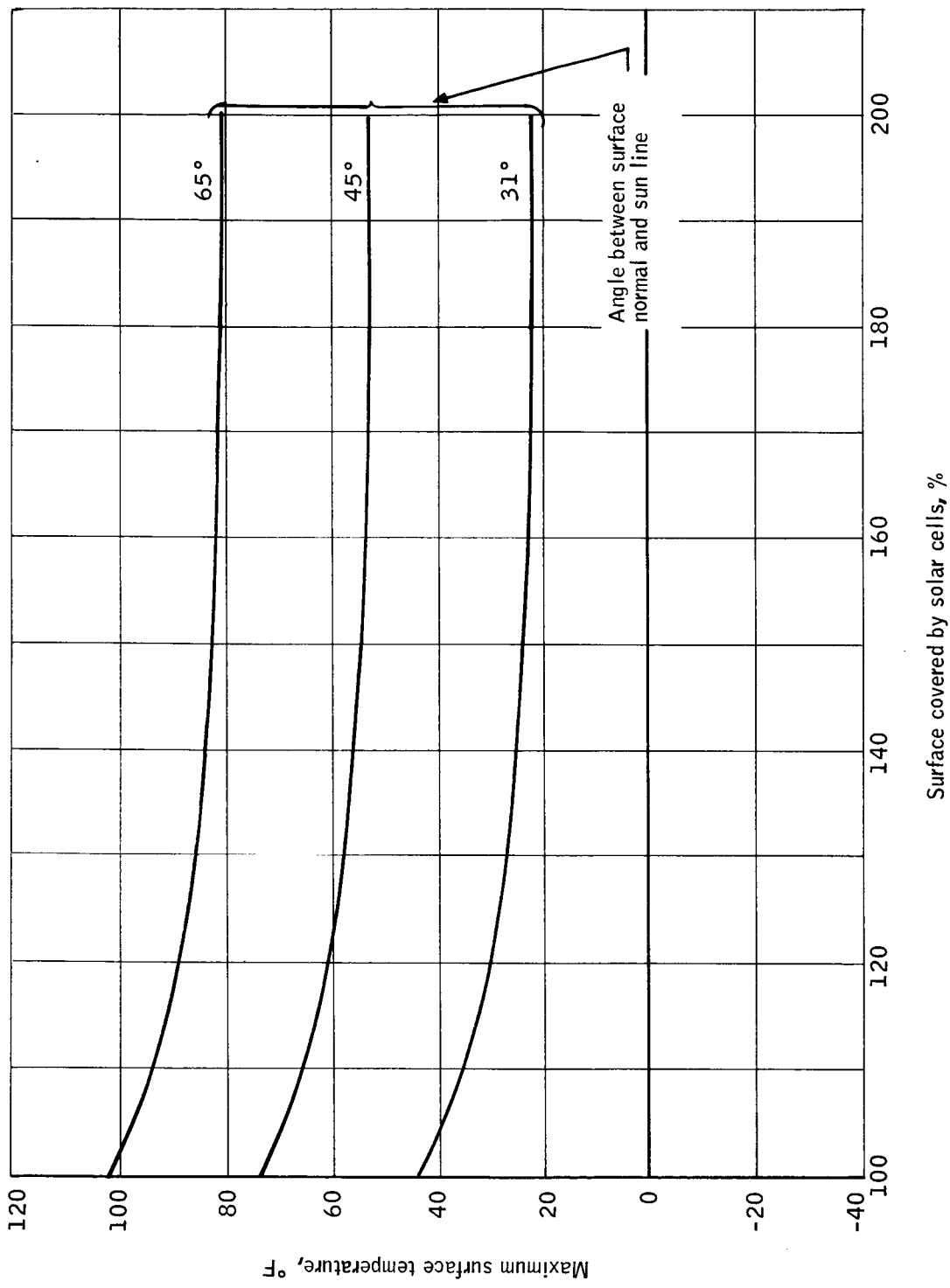


Figure 28. External Surface Temperature for Skirt Configuration

Heat loading of the rear face is caused by heat inputs from eight sources. These heat inputs are functions of spacecraft configuration, orbit, attitude, and detailed internal design. Comments on each input follow.

Conduction From The Spacecraft Sidewalls

An insulating material that provides a structural bond between the spacecraft baseplate and the sidewalls will also minimize heat leak from the sidewalls to the experiment package. Such a structural insulator must be thermally designed to provide the greatest possible resistance to heat flow. A fastening scheme must be used that does not contribute substantially to the conduction. The insulating material must have the desirable properties of low thermal conductivity, high compressive strength, high impact strength, and good dimensional stability. The materials listed in Table 8 are all candidates for the job. Channeling or segmenting the insulator are possible ways to increase the thermal resistance. For purposes of estimation, a thermal resistance of $20^{\circ}\text{F}/\text{W}$ was used.

Radiation From Internal Equipment and Structure To The Experiment Package

The electronic packages, mounting structure, sidewalls, and front face will all radiate heat to the experiment package. A multifoil insulation blanket will form an effective barrier to this heat transfer. The design and installation of this blanket will require extreme care, as any thermal shorts will eliminate the advantage of the blanket. For an estimate, $1/2$ inch of Linde S-4 superinsulation was assumed to blanket the 27 ft^2 of surface exposed in the interior. This insulation must not be compressed; measurements show a forty-fold increase in conductance when compressed in a high vacuum.

Internal Dissipation

This heat load is small since the associated electronics are mounted outside the cooled region. A total dissipation load of 2.5 watts was estimated.

Conduction Down Wiring

This heat load can be kept small if the wiring (between the cold experiment package and the warm electronics) is wrapped with superinsulation to prevent it from acting as radiating fins. If this is done, the heat transfer will only depend on the wire length, wire quantity, and wire gage.

Direct Solar Radiation to Radiometer and Starmapper Cavities

Since an IR transmitting window on the optical entrance is not feasible, it was assumed that baffling was used. An optically black cavity was assumed because it is not possible to design a reflecting baffle with sufficient attenuation for this requirement.

TABLE 8. - PLASTIC MATERIALS FOR STRUCTURAL INSULATOR

Material	Thermal conductivity, btu/hr-ft-°F	Compressive strength, psi x 10 ³
Med and extra high impact polystyrene	.024 - .090	No value
Rubber phenolic, asbestos	.04	10 - 20
Heat and chemical resistant polystyrene	.046 - .090	12 - 17
Rubber phenolic, chopped fabric	.05	10 - 15
General purpose polystyrene	.058 - .090	11.5 - 16
Phenolic, chopped fabric or cord	.07 - .10	11 - 12
Rigid PVC	.089 - .097	12 - 16
Glass fiber silicone	.097 - .170	15 - 30
Phenolic wood flour	.097 - .3	22 - 36
Polyester spray up mat	.10 - .13	15 - 25
Phenolic paper, flock or pulp	.10 - .16	24 - 35
Rigid styrene polyester	.10 - .12	12 - 37
Lexan	.11	12.5
Polyester preform	.11 - .15	18 - 30
Glass-filled Lexan	.13	18.5
Cellulose nitrate	.133	22 - 35
Glass fabric phenolic	.15	47.5

Panel and/or Sun-Shield Radiation to Radiometer and Starmapper Cavities

Any objects protruding into the hemisphere defined by the entrance apertures of the radiometer or starmappers will emit IR radiation to the cavities by virtue of their temperatures. This heat loading depends on the temperature of the objects, the emittance of the coating on the objects, and the view factor between the objects and the entrance apertures. Calculations were based on an IR absorbing baffle for the radiometer. The starmapper baffles were assumed to be thermally tied to the spacecraft sidewalls.

Earth Emission to Radiometer and Starmapper Cavities

This IR heat input was calculated for an IR absorbing baffle on the radiometer. Blockage of the input by extended panels and sun shields was accounted for.

Earth Albedo To The Radiometer And Starmapper Cavities

The effect of earth albedo on the radiometer heat loading was taken to be similar to the direct solar heating, that is, 100 percent of the incident energy was absorbed. Starmapper optics were assumed to absorb 100 percent of the incident earth albedo. Starmapper baffling horns are thermally tied to the spacecraft sidewalls.

The temperature of the rear face and experiment package is determined by

- Total heat loading from the rest of the vehicle into the rear face and experiment package; i. e., the sum of all eight inputs listed above.
- Heat absorbed by the rear face from the space environment.
- Heat lost from the rear face to the space environment.

The first determining factor is minimized by proper thermal design of the interface between the experiment package and the remainder of the spacecraft. The second factor can be minimized by using a thermal control coating on the rear face that has a low solar and albedo absorptance α_s . Maximization of the third factor can be accomplished by using a coating on the rear face that has a high emittance in the infrared ϵ . Thus, a low α_s/ϵ ratio coating is highly desirable.

Certain types of white paint have a low α_s/ϵ ratio and have been extensively used, although they suffer some degradation from ultraviolet irradiation. Lockheed has recently developed a surface with an even lower α_s/ϵ ratio that supposedly has more resistance to degradation. This surface, called the Optical Solar Reflector (OSR) surface, consists of vapor-deposited silver on Corning 7940 fused silica and must be cemented to a substrate in small pieces. The procedure for doing this is well developed.

In order to compare these two coatings for the HDS application, it is not sufficient simply to look at the range of α_s/ϵ ratios for each coating. This comparison would be valid only if the source of heat came directly from the space environment. When there is internal heat loading (across the experiment package/spacecraft interface), the emittance value itself becomes important. The radiation property extremes for white paint and OSR used to calculate the rear face temperature are shown below.

	<u>White paint</u>	<u>OSR</u>
Solar absorptance, α_s	0.15 to 0.40	0.045 to 0.055
Infrared emittance, ϵ	0.85 to 0.95	0.79 to 0.81

The two extremes (31 and 64 degrees) of space heating incident to the rear face were used. Orbit-averaged heat loads for these two extremes were used. The values were found from the plot of heating versus orbital position shown in Figure 19. Using orbit-averaged heat loads for the computations is reasonable since the large thermal mass of the assembly will largely average out orbital variations in temperature.

Figure 29 shows measured variation of the emittance of the OSR with temperature. Figure 30 illustrates measured variation of solar absorptance of white paint with ultraviolet exposure time.

Figures 31 and 32 present the results of the comparison which are summarized below. The broad band of temperatures for each coating shows the effect of coating degradation in the space environment. The temperature of the rear face and the experiment package at any time must lie within the band shown.

- The Optical Solar Reflector surface will cool the rear face to a temperature as much as 15°F below the temperature that is reached with a white-paint surface. As the heat load across the spacecraft/experiment package interface increases, the advantage of the OSR diminishes until eventually the white painted surface becomes better.
- The white-paint coating is not as stable in the space environment and so will gradually degrade, causing an increase in the experiment package temperature (approximately a 13°F increase for the white-paint surface versus a 2 or 3°F increase for the OSR).
- The advantage of the OSR surface over the white paint increases slightly with increasing solar angle, because of the increased albedo incident to the rear face.

To compare spacecraft configurations relative to their effect on the heat loading, calculations were made of the heat input for each configuration. Tables 9 through 12 show the results. The total heat loading in each table

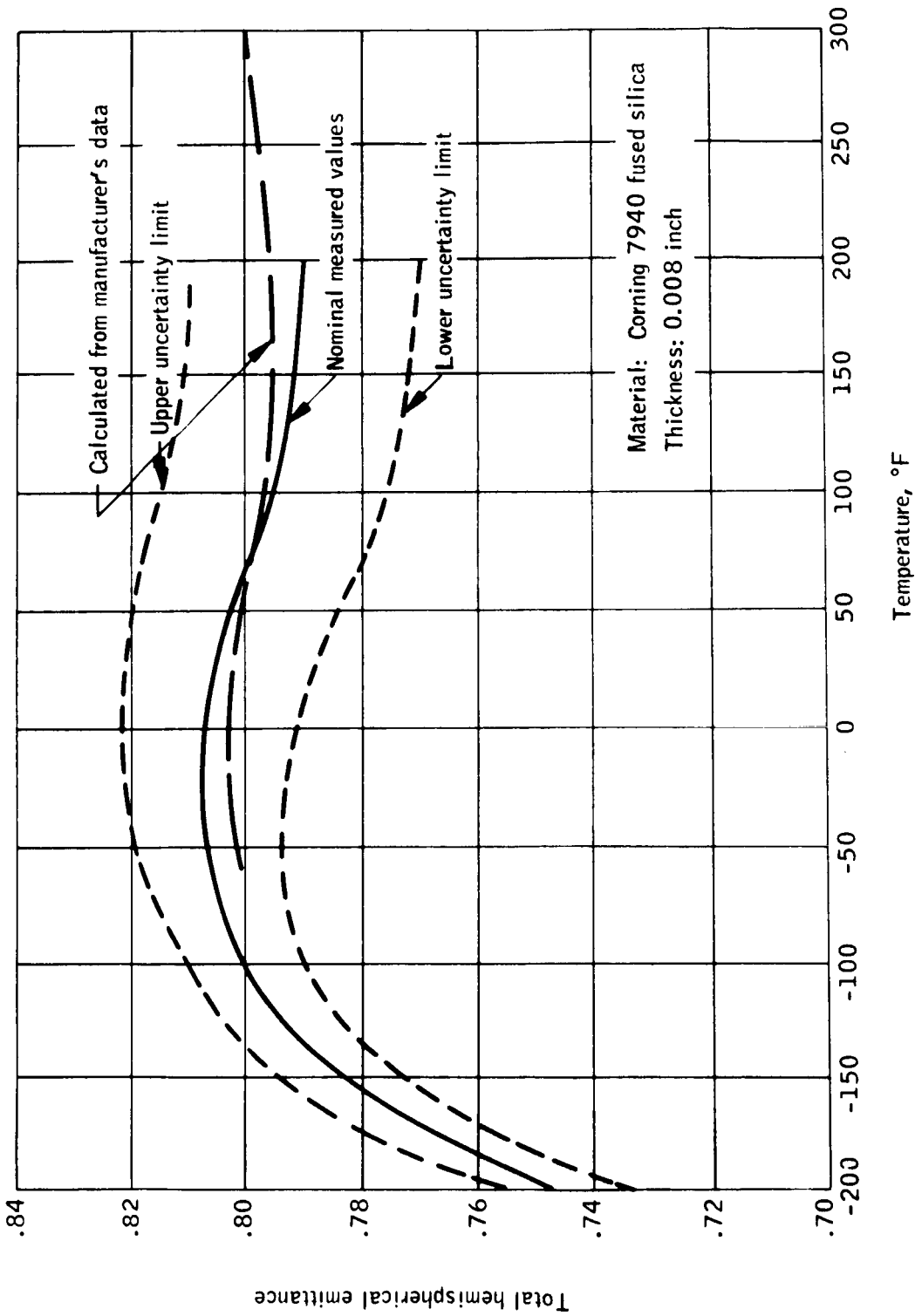
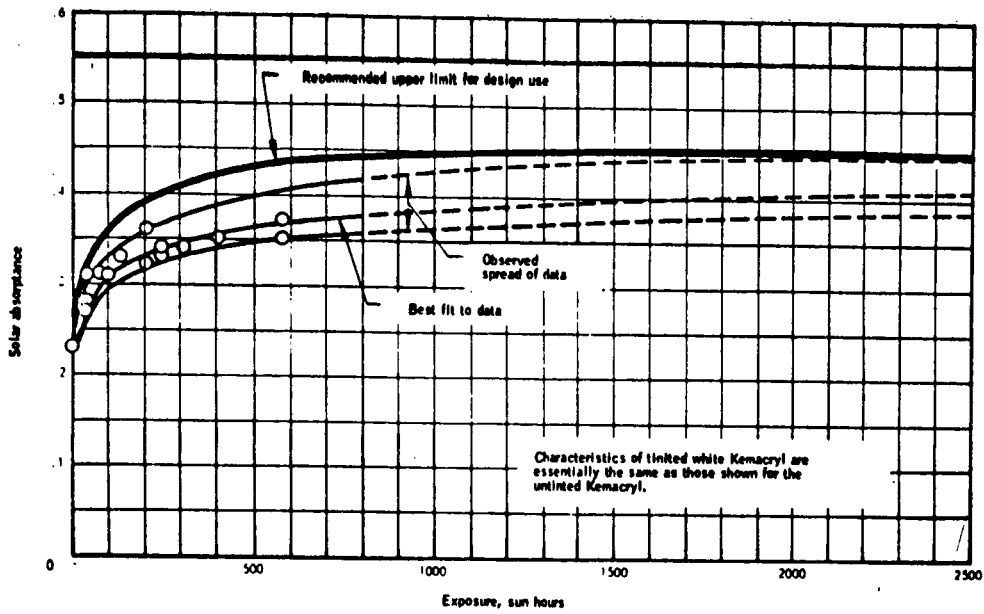
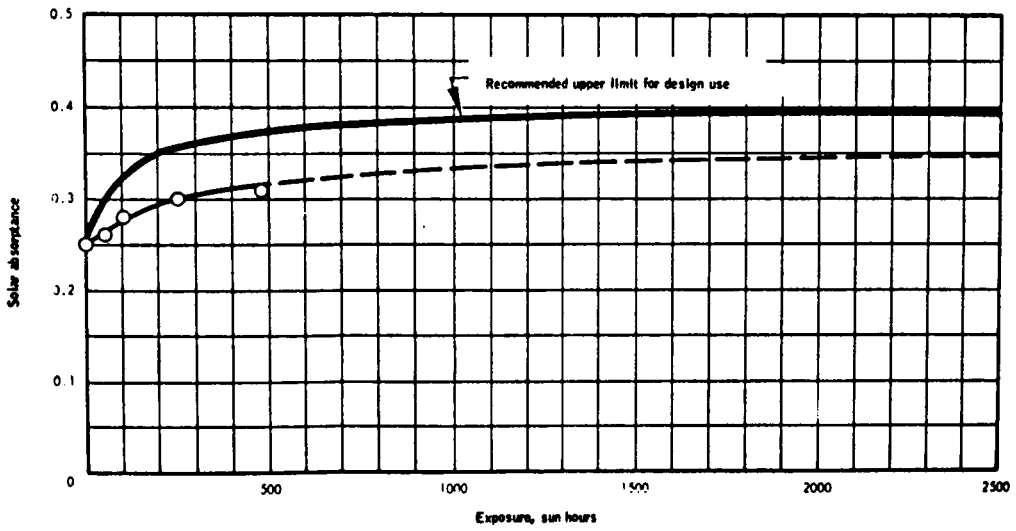


Figure 29. Effect of Temperature on Emittance of the OSR



Effect of Near- Ultraviolet Radiation in Vacuum on Solar Absorptance of United White Demacryl Lacquer



Effect of Near-Ultraviolet Radiation in Vacuum on the Solar Absorptance of Fuller Gloss White Silicone Paint on 6061 Aluminum

Figure 30. Solar Absorptance of White Paint

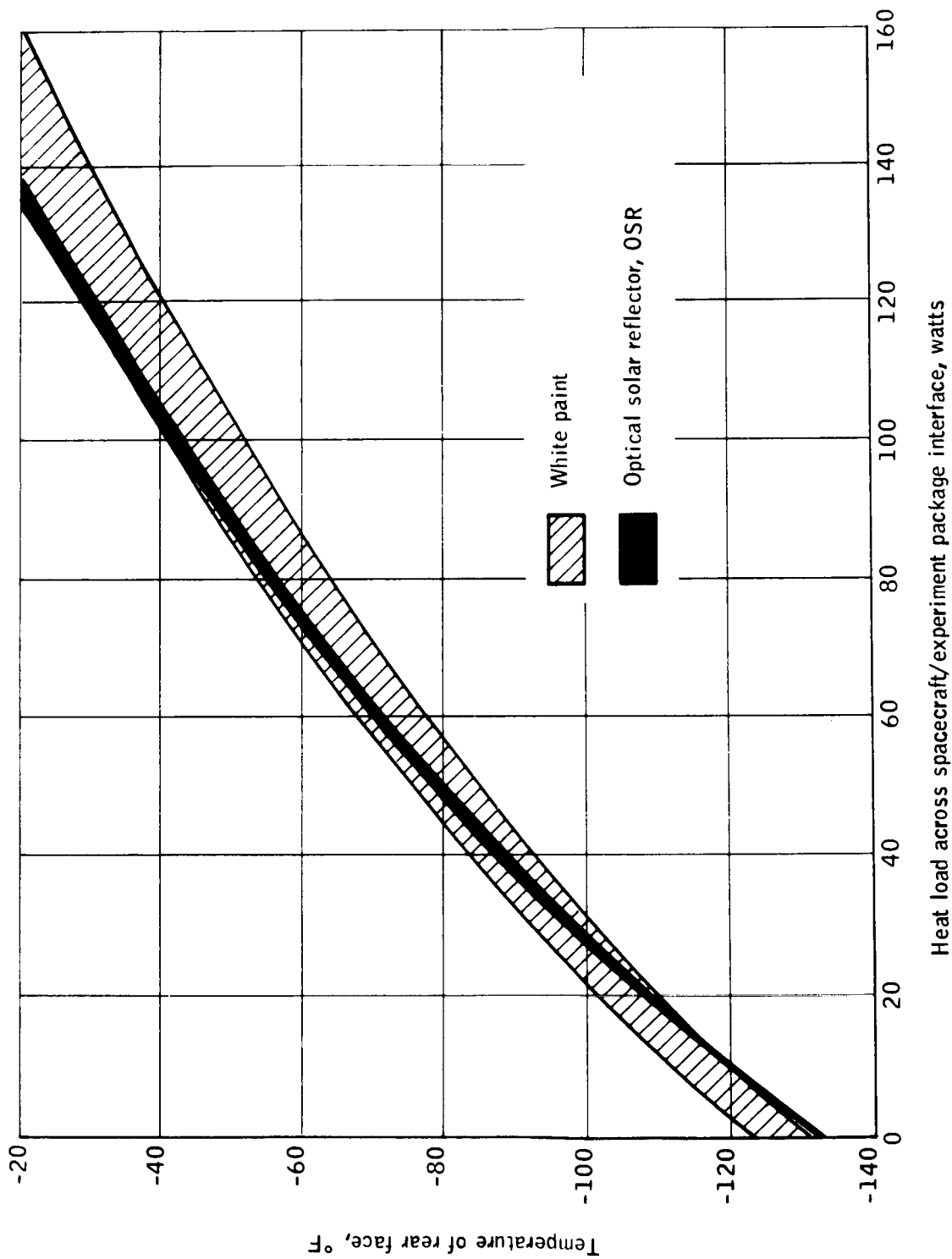


Figure 31. Baseplate Temperature versus Heat Input, 31° Solar Angle

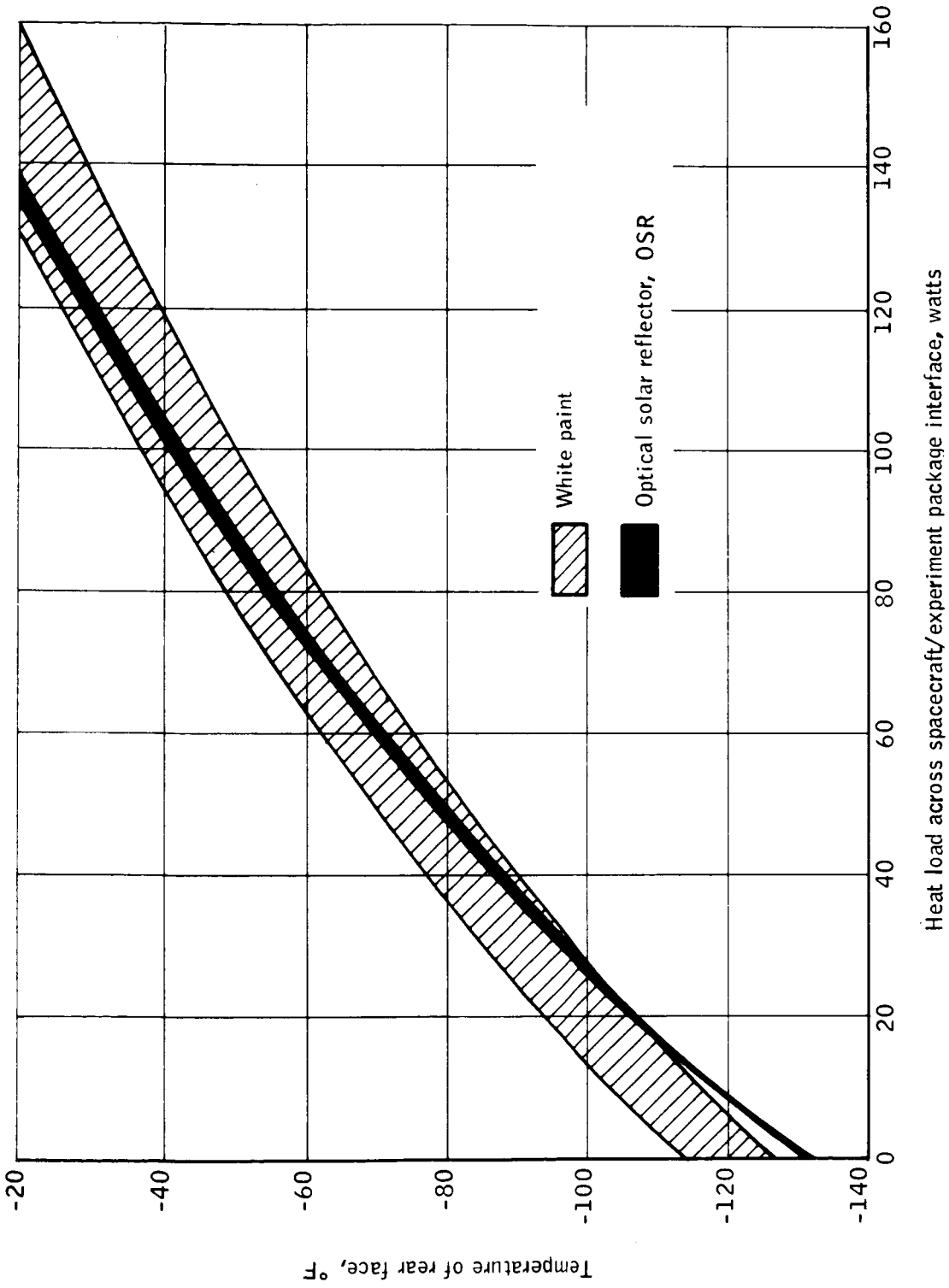


Figure 32. Baseplate Temperature versus Heat Input, 64° Solar Angle

TABLE 9. - HEAT LOADS TO EXPERIMENT PACKAGE
 BASEPLATE OF HDS SPACECRAFT - BODY -
 MOUNTED CELL CONFIGURATION, NO
 EXTENDED PANELS OR SHIELDS

Source of heat	Sun-line/orbit normal angle			Comments
	31°	45°	64°	
1. Conduction from sidewalls	5.5 W	6.5 W	7.5 W	
2. Across multifoil insulation blanket	0.9 W	0.9 W	0.9 W	
3. Internal electric dissipation	2.5 W	2.5 W	2.5 W	
4. Conduction down wiring	1.0 W	1.0 W	1.0 W	
5. Direct solar to optical cavities	23.0 W	27.0 W	33.0 W	100% of incident energy is absorbed (solar absorbing baffle)
6. Panel/sun-shield emission to optical cavities	0 W	0 W	0 W	Entrance apertures have unobstructed views
7. Earth IR to radiometer and starmapper cavities	10.5 W	10.5 W	10.5 W	100% of incident energy is absorbed (IR absorbing baffle)
8. Earth albedo to radiometer and starmapper cavities	2.5 W	4.6 W	4.9 W	100% of incident energy is absorbed
9. Sun sensor	1.0 W	1.2 W	1.5 W	100% absorption
Total heat load	46.9 W	54.2 W	61.8 W	
Temperature, °F/°K	-88/207	-78/212	-72/216	

TABLE 10. - HEAT LOADS TO EXPERIMENT PACKAGE/BASEPLATE OF HDS SPACECRAFT-EXTENDED SOLAR PANEL CONFIGURATION, SHIELDING IN PLANE OF PANELS

Source of heat	Sun-line/orbit normal angle			Comments
	31°	45°	64°	
1. Conduction from sidewalls	5.5 W	5.0 W	3.5 W	
2. Across multifoil insulation blanket	0.9 W	0.9 W	0.9 W	
3. Internal electric dissipation	2.5 W	2.5 W	2.5 W	
4. Conduction down wiring	1.0 W	1.0 W	1.0 W	
5. Direct solar to optical cavities	0 W	0 W	0 W	Sun shield eliminates direct solar heating
6. Panel/sun-shield emission to optical cavities	10.2 W	9.0 W	6.2 W	100% of incident energy is absorbed (IR absorbing baffle)
7. Earth IR to radiometer and starmapper cavities	9.0 W	9.0 W	9.0 W	100% of incident energy is absorbed (IR absorbing baffle)
8. Earth albedo to radiometer and starmapper cavities	2.5 W	4.6 W	4.9 W	100% of incident energy is absorbed
9. Sun sensor	1.0 W	1.2 W	1.5 W	100% absorption
Total heat load	32.6 W	33.2 W	29.5 W	
Temperature, °F/°K	-98/201	-96/202	-98/201	

TABLE 11. - HEAD LOADS TO EXPERIMENT PACKAGE/BASEPLATE OF HDS SPACECRAFT - EXTENDED SOLAR PANEL CONFIGURATION, NO SHIELDING

Source of heat	Sun-line/orbit normal angle			Comments
	31°	45°	64°	
1. Conduction from sidewalls	3.0 W	3.5 W	4.5 W	
2. Across multifoil insulation blanket	0.9 W	0.9 W	0.9 W	
3. Internal electric dissipation	2.5 W	2.5 W	2.5 W	
4. Conduction down wiring	1.0 W	1.0 W	1.0 W	
5. Direct solar to optical cavities	9.0 W	15.5 W	33.0 W	100% of incident energy is absorbed
6. Panel emission to optical cavities	5.1 W	4.5 W	3.1 W	100% of incident energy is absorbed (IR absorbing baffle)
7. Earth IR to radiometer and starmapper cavities	9.0 W	9.0 W	9.0 W	100% of incident energy is absorbed (IR absorbing baffle)
8. Earth albedo to radiometer and starmapper cavities	2.5 W	4.6 W	4.9 W	100% of incident energy is absorbed
9. Sun sensor	1.0 W	1.2 W	1.5 W	100% absorption
Total head load	34.0 W	42.7 W	60.4 W	
Temperature, °F/°K	-93/204	-88/207	-74/214	

TABLE 12. - HEAT LOADS TO EXPERIMENT PACKAGE/BASEPLATE OF HDS SPACECRAFT-LOCAL RADIOMETER SUN SHIELD CONFIGURATION

Sun line/orbit normal angle

Source of heat	31°	45°	64°	Comments
1. Conduction from sidewalls	5.0 W	5.0 W	4.5 W	
2. Across multifoil insulation blanket	0.9 W	0.9 W	0.9 W	
3. Internal electric dissipation	2.5 W	2.5 W	2.5 W	
4. Conduction down wiring	1.0 W	1.0 W	1.0 W	
5. Direct solar to optical cavity	0 W	0 W	0 W	Sun shield eliminates direct solar heating
6. Sun shield emission to optical cavities	2.0 W	2.0 W	2.0 W	Panel emission is blocked by sun shield. Cold surface of shield is at -100°F. Plane surface on shield. Stepping will reduce input.
7. Earth IR to radiometer and starmapper cavities	9.0 W	9.0 W	9.0 W	100% of incident radiation is absorbed
8. Earth albedo to radiometer and starmapper cavities	2.5 W	4.6 W	4.9 W	100% of incident radiation is absorbed
9. Sun sensor	1.0 W	1.2 W	1.5 W	100% absorption
Total heat load	23.9 W	26.2 W	26.3 W	
Temperature, °F/°K	-105/197	-103/198	-102/199	

can be translated into an experiment package/rear-face temperature by referring to Figures 31 and 32. The local sun-shield configuration results in the lowest total heat loading of the experiment package and thus will result in the lowest experiment package temperature (-105 to -108°F or 197 to 195°K).

It has been estimated that using a 350 lb experiment package in a spacecraft with a local sun shield and starting with a temperature of 80°F upon insertion into orbit, 20 orbits or about 32 hours will be needed for the experiment package temperature to drop to -100°F (200°K).

Previous analytical effort has shown that a six-pound baseplate will experience orbital temperature variations of up to 16°F due to variations in absorbed albedo in an orbit. A 60-pound baseplate will act as an integrator of the absorbed albedo and will reduce the temperature variations to 1.6°F in an orbit. These variations are shown as solid curves in Figure 33. Further attenuation of the temperature variation will result from the large heat capacity of the experiment package, tending toward the dashed line which assumes a 350 lb package.

Since heat loads into the baseplate from the experiment package cannot be distributed uniformly, temperature gradients will be induced on the baseplate.

An attempt was made to estimate the magnitude of the gradients by conducting an extremely worst-case analysis. In this analysis 26 watts of heat from the interior of the spacecraft was dumped into the center 18 inches of the baseplate. The remainder of the back side of the baseplate was assumed to be insulated. A 1/8-inch thick aluminum baseplate was used as a model and was assumed coated with a white-paint thermal control coating ($\alpha = 0.25$, $\epsilon = 0.90$). A nodal break up of the baseplate was used with conduction between nodes and radiation to space. The nodal network was solved with a matrix inversion computer program (ref. 4). The temperature distribution shown in Figure 34 resulted. A temperature difference of 15°F is seen to exist between the center and edge of the baseplate.

This analysis is pessimistic for several reasons and is not intended to represent realistic temperatures in the baseplate. A significant portion of the 26 watts ($\approx 20\%$) will be dumped near the outer edge of the baseplate from the sidewalls. Thermal straps between the experiment package and baseplate may be used to distribute the heat, and stiffening ribs on the inside of the baseplate will improve the lateral conduction of heat. A realistic estimate of the maximum temperature difference expected after the detailed design was carried out would be about 5°F .

Even though this baseplate concept was generated with the intention of furnishing minimum temperature as well as compatibility with the experiment package, further optimization studies might yield a more effective approach. Examples of study areas might be directional emission/absorption surfaces, different baseplate geometry, extension of shading skirts, etc.

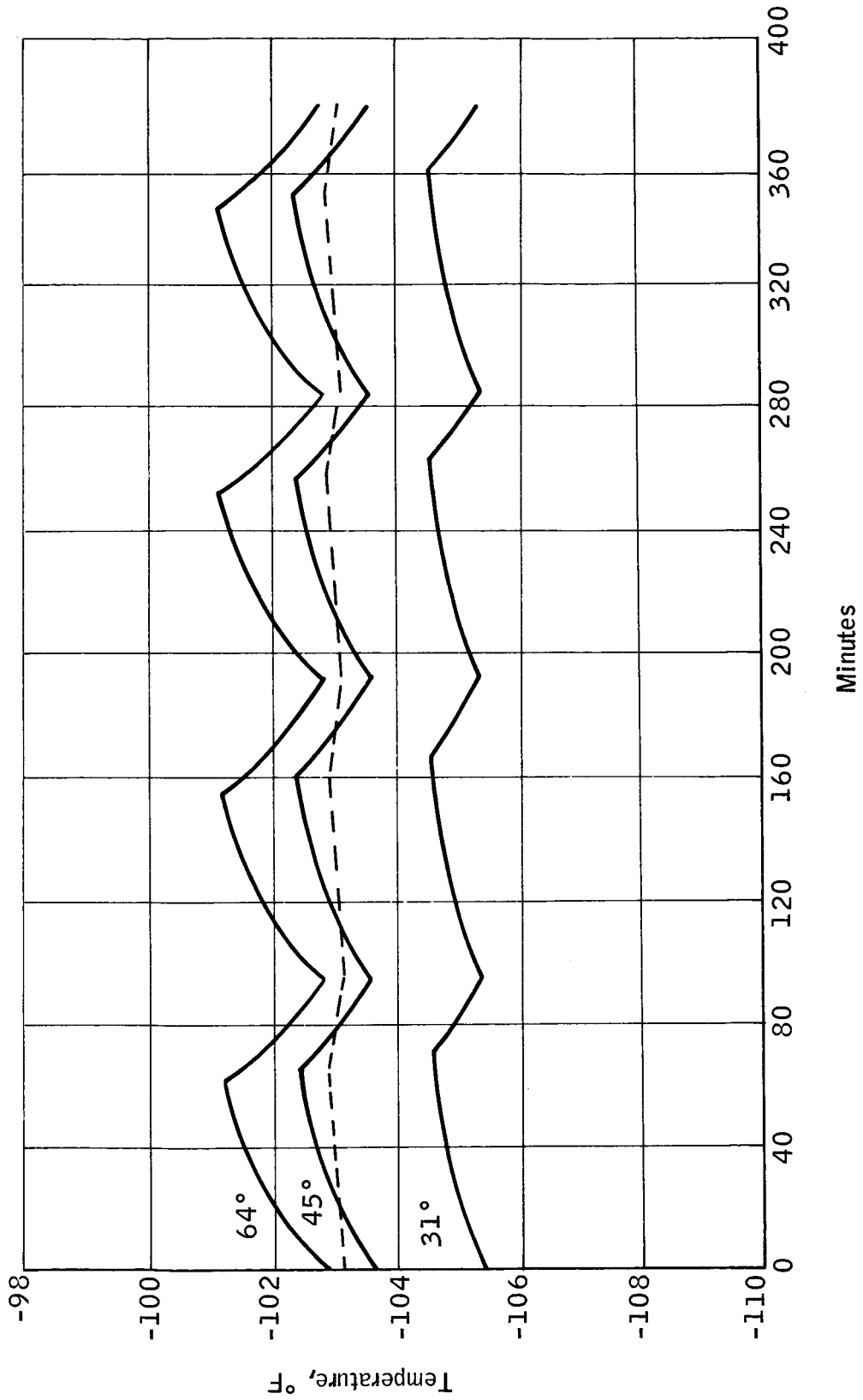


Figure 33. Orbital Temperature Variation of Baseplate

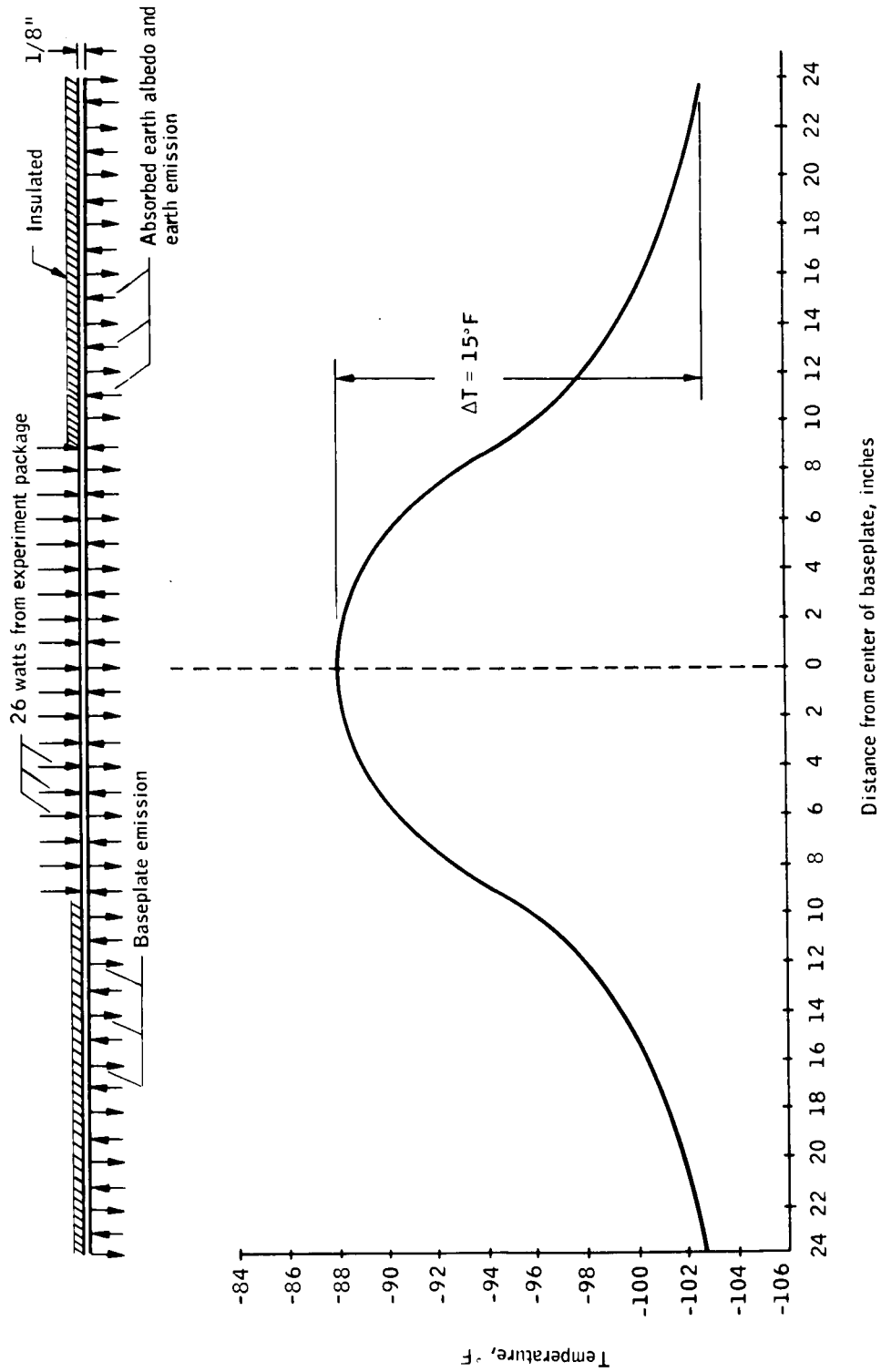


Figure 34. Baseplate Thermal Gradient, a "Worst Case"

If the spin axis is not exactly normal to the orbital plane, slightly different heating of the experiment package/baseplate will result. A recomputation of the earth heating absorbed by a flat spacecraft baseplate was made for attitude angles (referenced to the earth nearest subsolar point in the orbit) of 5 degrees and 2.5 degrees away from the earth, and 2.5, 5, and 10 degrees toward the earth. The orbit average increased baseplate heating ΔQ_E and the resultant baseplate temperature rises ΔT_{195} are shown in Table 13. At 195°K the flat baseplate has a characteristic thermal resistance to space of 2.40°K/watt, and, while the resistance is nonlinear, the linear approximation will hold for small temperature changes.

TABLE 13. - SPACECRAFT OUT-OF-PLANE ATTITUDE EFFECTS ON THE TEMPERATURE OF A 195° K BASEPLATE, ONE-ORBIT AVERAGE VALUES

Attitude, degrees	31° orbit		45° orbit		64° orbit	
	ΔQ_E , watts	ΔT_{195} , °K	ΔQ_E , watts	ΔT_{195} , °K	ΔQ_E , watts	ΔT_{195} , °K
-5	0.521	1.25	0.478	1.15	0.432	1.04
-2.5	0.260	0.62	0.219	0.53	0.218	0.52
0	0	0	0	0	0	0
+2.5	0.375	0.90	0.402	0.96	0.422	1.01
+5	0.823	1.98	0.803	1.93	0.860	2.06
+10	1.489	3.57	1.605	3.85	1.729	4.15

Tables 9 - 12 really summarize the experiment package thermal control approach. Careful design is needed to minimize the heat inputs to the experiment package compartment while maximizing the radiation from the baseplate. It appears that a temperature of about -100°F or colder will be achievable in this compartment and that only small orbital variations will occur.

INTERNAL ELECTRONIC PACKAGE THERMAL CONTROL

To control the temperatures of each of the electronic packages, these pieces of equipment will be mounted on a platform located outside the experiment package and supported at the spacecraft sidewalls. The supports will provide thermal conduction paths between the platform and sidewalls. Each package

temperature will be determined by the amount of insulation between the package and the platform, the type of thermal control coating on the package, the closeness of packing to adjacent packages, and the platform temperature at the point where the package is mounted. This last factor, platform temperature distribution, depends on the material of the platform, the number and types of bracing required, and the manner of distributing the internal heat.

To assess one possible electronics platform design, a nodal analysis was conducted on an aluminum honeycomb platform with 0.015-inch facings. This platform is shown in Figure 35. The platform is sectioned into 36 nodal areas. Each nodal area is conductively coupled to adjacent nodal areas. The outer edge of the platform is connected to the sidewall skin. Nodes 1, 7, 13, 19, 25, and 31 are also conductively coupled to the sidewall skin with one-inch o. d., 1/8-inch-wall aluminum tubes. One set of computer runs (ref. 4) was made with 30, 90 and 120 watts of heat dissipation distributed uniformly (by area) on the platform. The predicted temperature distribution is shown in Figure 36. The temperature is seen to rise to 60°F above the average sidewall temperature for 120 watts distributed uniformly. A second set of computer runs considered nonuniform distribution of heat. As shown in Figure 37, 45 watts went to node 4, 15 watts went to node 15, and the remaining 60 watts were distributed uniformly. The temperature of node 4 (under the battery) is seen to be 88°F above the average sidewall skin temperature.

Several observations were made from these results. First, a fairly uniform platform temperature should be achievable, at least except for the four or five inches near the wall. Second, average sidewall temperature should be kept at subzero levels if room temperature electronics is desirable. Packages having low dissipations can then be kept warm by insulating them from the platform and by coatings.

To show the latitude in detail thermal design for the packages that will be possible, calculations were made that resulted in two sets of curves. These curves display the package surface temperature extremes that are established with various package mounting conditions and surface coatings. Each package could be thermally isolated from the platform, in intimate thermal contact with the platform, or have any degree of thermal insulation between these extremes. Each package could also have easily applied surface coatings ranging in emittance values from about 0.10 to a black emitting coating of 1.0. A continuous range exists due to the possibility of stripping with different coatings. The possibility of providing additional conduction paths (straps) to the sidewalls also exists.

Figure 38 illustrates the range in package temperatures for an average sidewall skin temperature of 0°F (isothermal sidewall) and an average platform temperature of 40°F (isothermal platform). If the package is thermally insulated from the platform, the only heat loss mechanism possible is radiation from the package surface to surrounding surfaces. The equilibrium package temperature for this condition is shown as solid lines plotted against surface flux density (W/in^2) with coating emittance as an independent parameter. A close packing of equipment was assumed, with an emission view factor of 0.50.

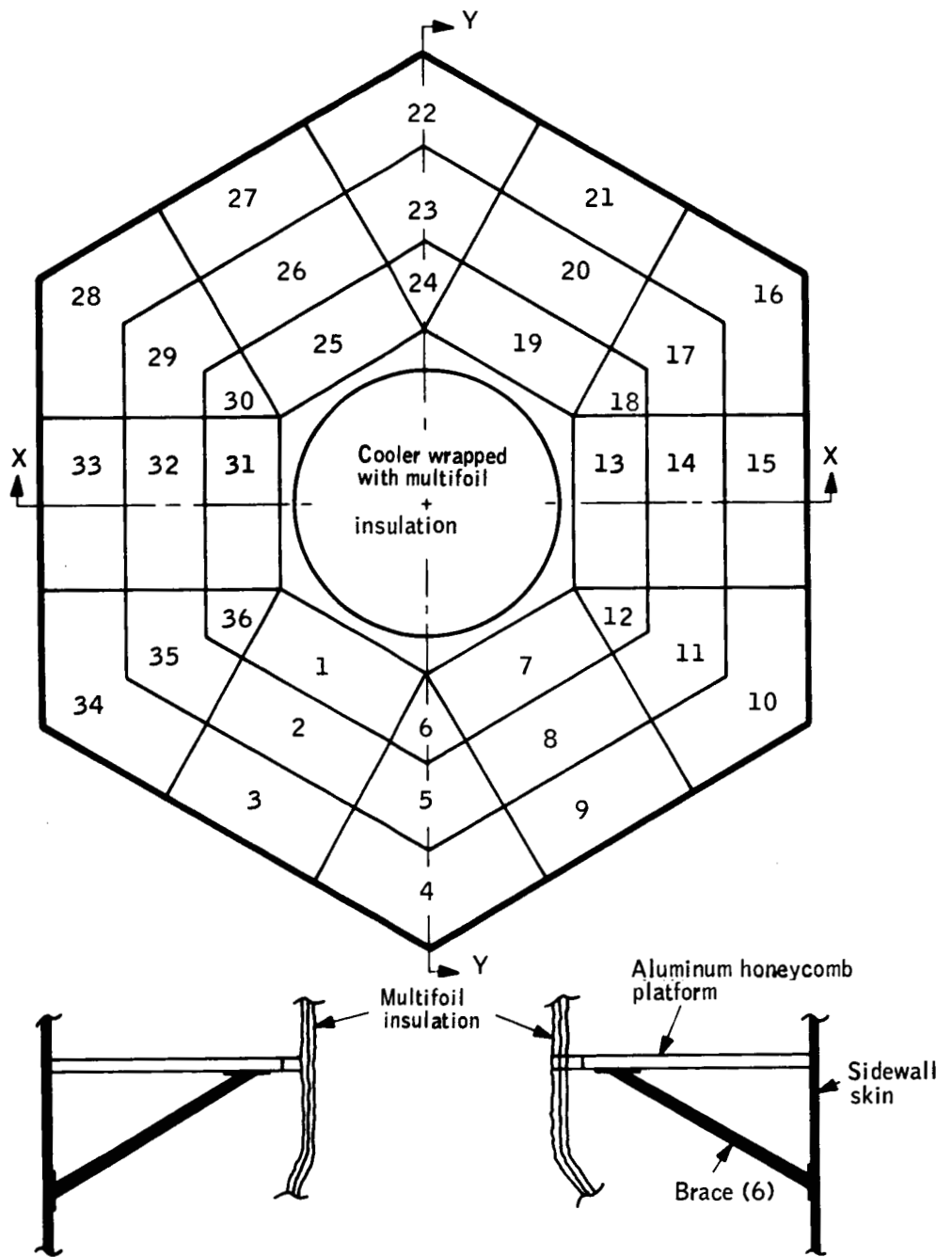


Figure 35. Nodal Model of Electronics Platform

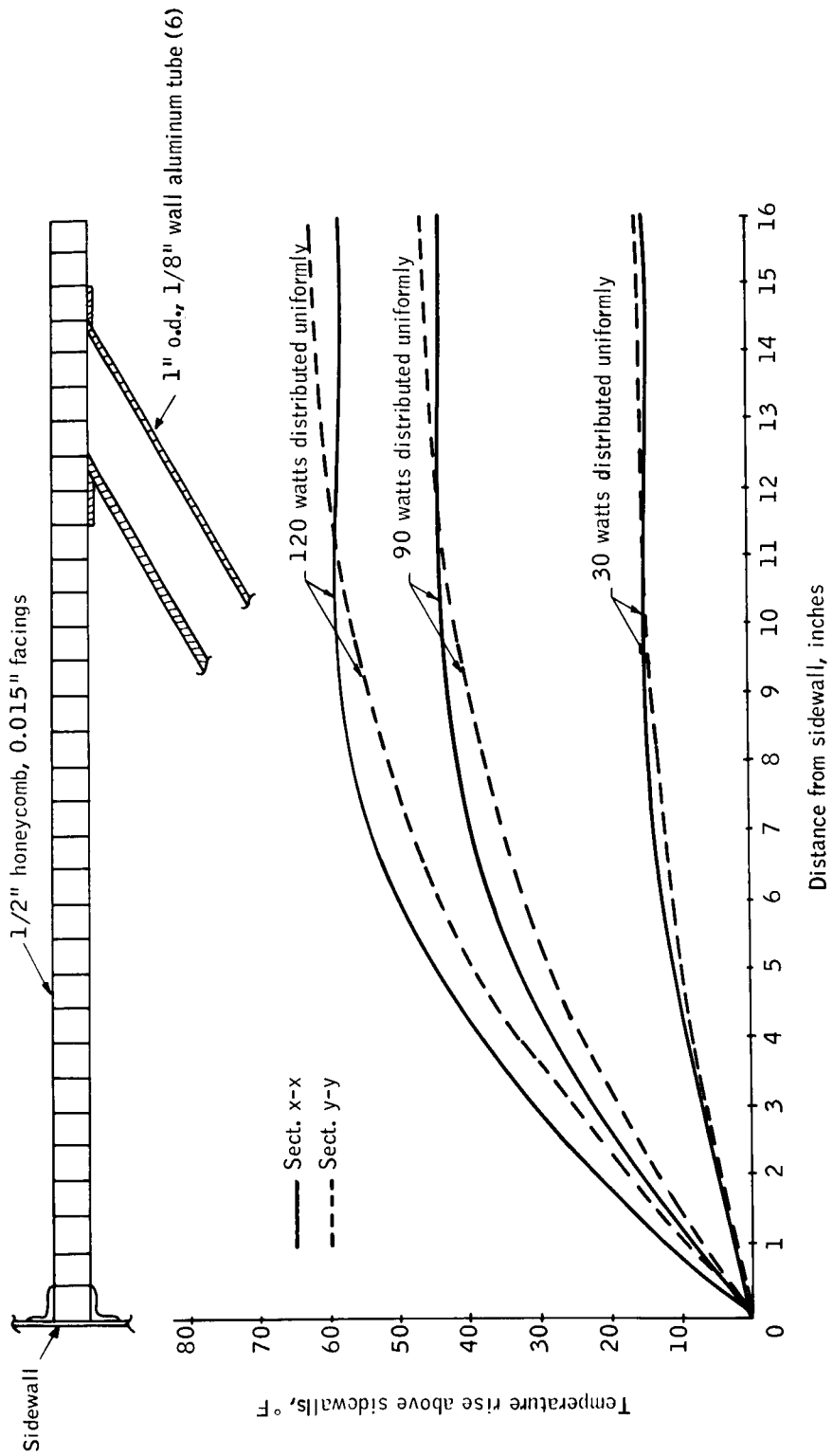


Figure 36. Temperature of Electronics Platform, Uniform Heat Dissipation

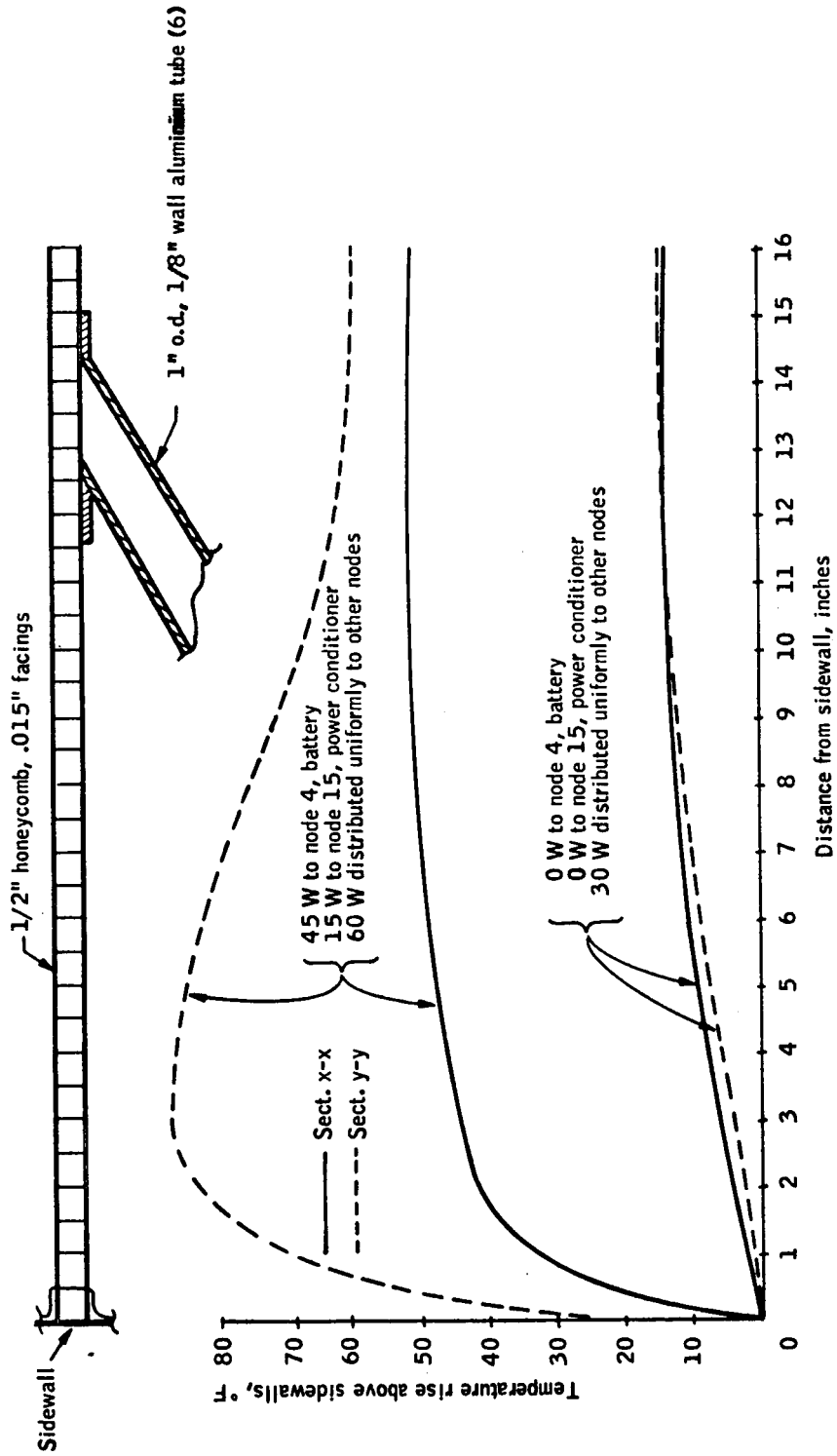


Figure 37. Temperature of Electronics Platform, Nonuniform Heat Dissipation

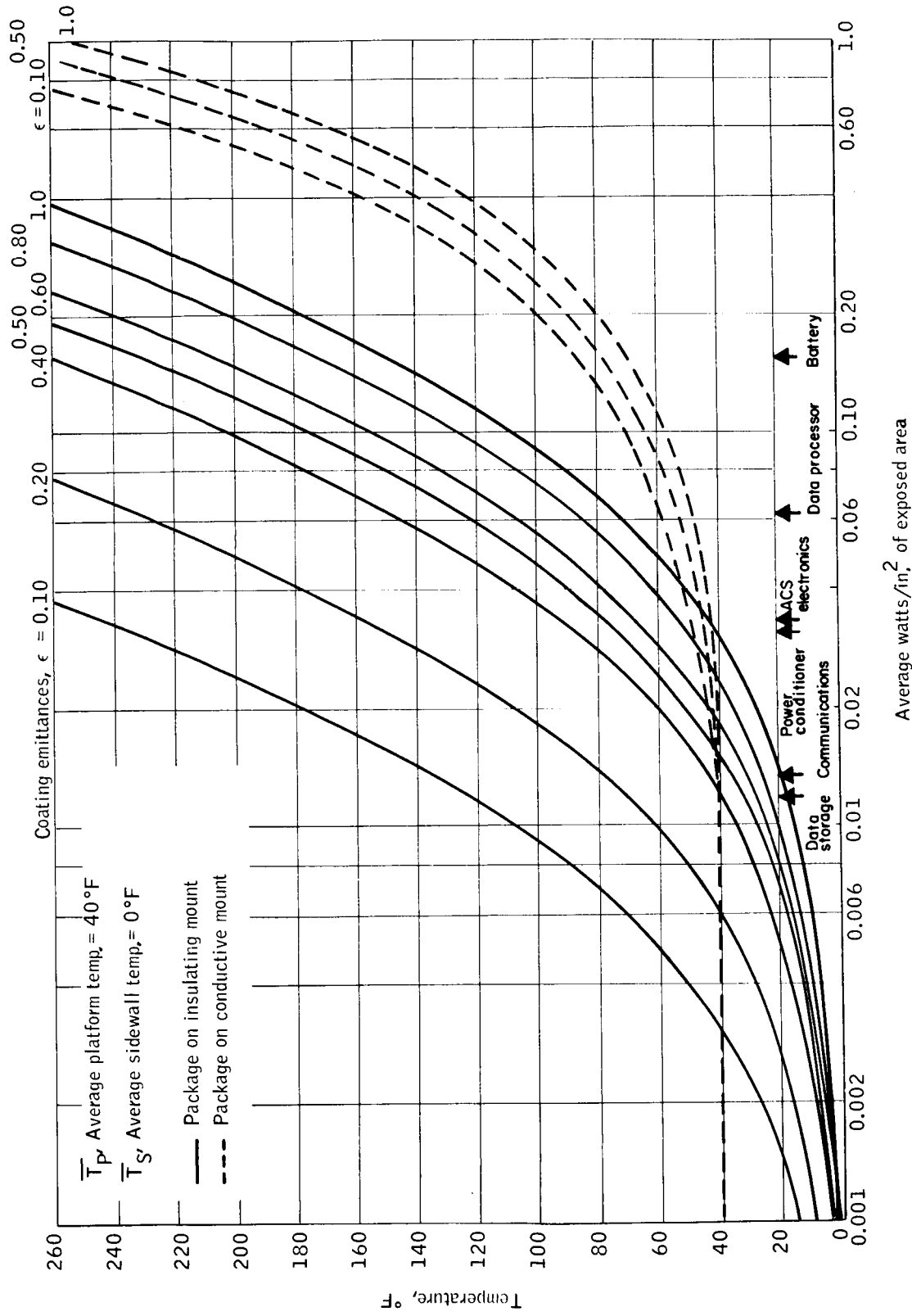


Figure 38. Component Temperature versus Heat Dissipated

The communications package, for example, would reach an equilibrium temperature of about 20°F if coated with a black emitter and about 130°F if coated with an emittance of 0.10. The battery on the other hand would heat up to about 140°F even with an emittance of 1.0. If the package is mounted with good thermal conduction between package and platform, the equilibrium package temperature is shown as dashed lines. In this case, both conduction and radiation from the package play a role in determining the temperature. Sparse packing of equipment was assumed, with an emission view factor of unity. In this case, the communications package would remain at essentially the platform temperature (40°F) with any coating. The battery temperature would range from 70°F to about 90°F depending on its coating.

The intent of the foregoing was to point out factors influencing the temperature levels of the electronic packages, and to do this, the simplifying assumptions that have been pointed out were necessary. In a detailed thermal analysis of a given electronics platform layout, many of these assumptions would not be required, and the actual package temperatures could be predicted quite accurately. This analysis would consider realistic insulation for each package, radiation interchange between packages, the finite thermal inertia of the platform and packages, orbital variations in sidewall temperatures, and temperature gradients within the platform by modeling with a multinode thermal network. Such detailed analysis was not warranted for the present program, since the above discussed modeling analyses were sufficient to determine feasibility of the proposed thermal control approach.

THERMAL CONTROL SUMMARY

On the basis of the above discussed Thermal Control Conceptual Design, it is suggested that the requirements of the HDS can be met with a highly reliable, passive approach. Key elements of this approach are

1. Low α_s/E coatings on all external surfaces (except the solar cell surfaces).
2. Thermal isolation of the cover and solar panels from the rest of the spacecraft (except by radiation).
3. Thermal connections as needed from the electronic support equipment to the sidewalls only by the way of the mounting bulkhead, thermal straps, and radiation.
4. A local sun shield around the radiometer view port to eliminate solar energy incident to the experiment package.
5. Very careful thermal isolation of the experiment package - radiometer, starmappers, sun sensors, cryogenic cooler - from all parts of the spacecraft except the highly radiative baseplate.

SPACECRAFT CONCEPTUAL DESIGN

The spacecraft system was conceptually configured to fulfill the integrated requirements of the experiment and the supporting subsystems. The principal goal of the individual subsystem study areas was a conceptual definition of that subsystem and its interfaces that would fulfill the defined system and mission requirements. The spacecraft design and integration effort was concerned with gathering these subsystems and experiment elements together in an integrated spacecraft system configured within the defined HDS requirements envelope. During this integration and configuration effort, various constraints (physical, environmental, etc.) evolved that affected both individual subsystems and the total system. These constraints were fed back to the affected areas, analyzed, and evaluated through pertinent tradeoff studies, and the subsequent changes - if any - were integrated into the various system levels. This same feedback loop served to incorporate and evaluate the continually changing concepts and design approaches that are an essential part of such a study program.

EVOLUTION

The initial spacecraft system concept was a 54-inch diameter, circular cylinder, 36 inches deep. Configured upon the first subsystem definitions, it served to estimate the volume that would be needed to contain the subsystems and to provide a basis for total system weight estimation. By incorporating a central bulkhead for mounting the subsystems, it appeared that the 36-inch depth would provide sufficient volume for the subsystems as they were then defined.

The second concept was a hexagonal cylinder as shown in Figure 39, 54 inches across the corners of the hexagon and 36-inches deep. This approach was especially compatible with fold out solar panels and provided flat panels around the perimeter for radiometer view ports. The experiment package, mounted at the geometric center of the spacecraft, was defined as two radiometers viewing outward in diametrically opposite directions, a cryogenic cooler, and two starmappers, which had to view out the rear face at about 20 degrees off the spin axis. An investigation of internal positioning of subsystems on a central bulkhead again showed that adequate volume was available for the subsystems.

A radioisotope thermoelectric generator (RTG) was given consideration as a possible, primary power source. From the spacecraft standpoint, it appears that the RTG would have caused serious problems in achieving the required degree of balance for a spin-stabilized system, but it was dropped from consideration for other reasons.

Several hexagonal spacecraft concepts were studied which incorporated the cold experiment package approach. The first concept had starmappers viewing out the baseplate at 45° off the spin axis. It also was the first to incorporate larger solar panels which allowed removal of body-mounted

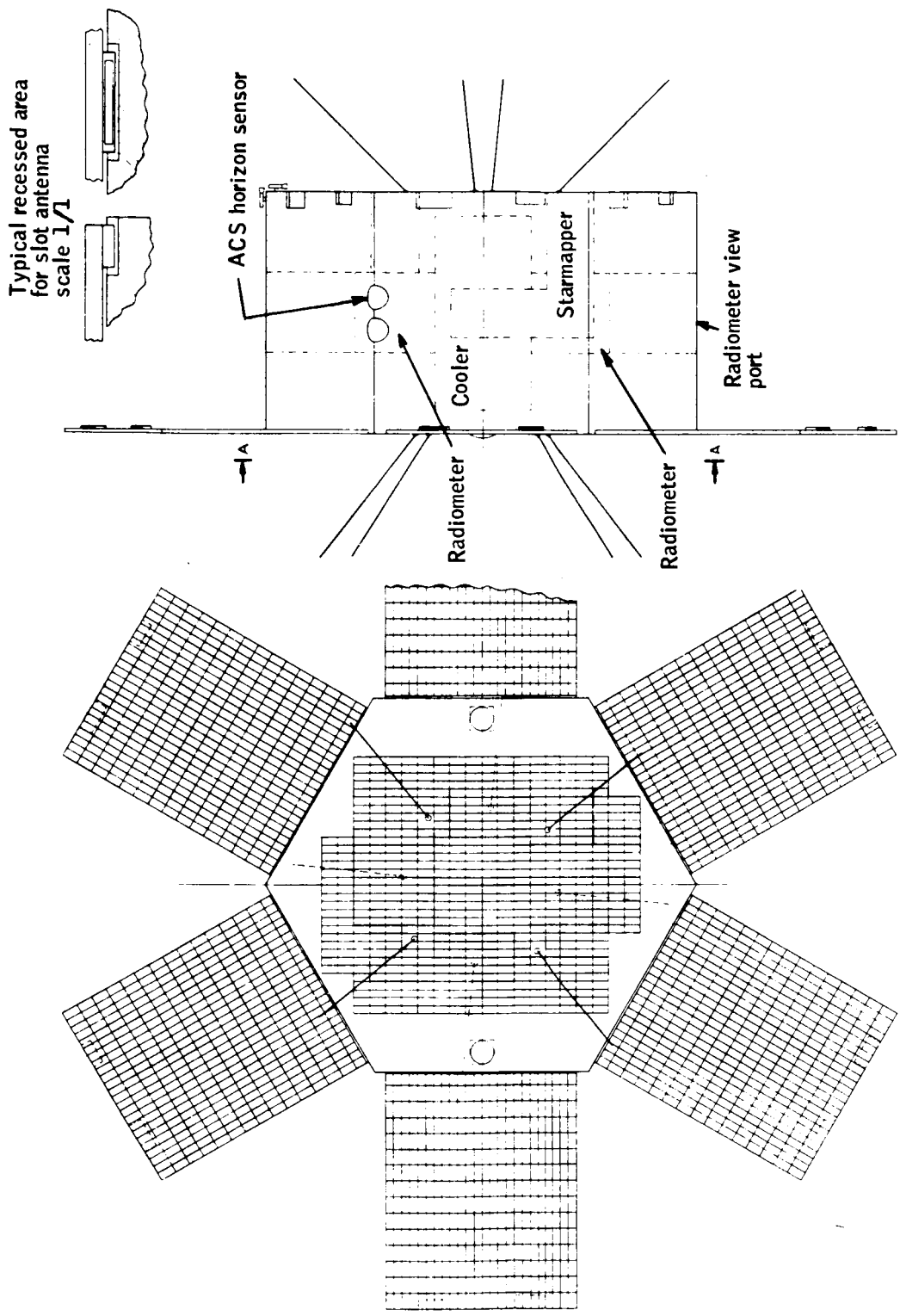


Figure 39. Preliminary Hexagonal Cylinder Spacecraft Concept

cells. Another similar concept incorporated a new version of the experiment package which was now defined to have considerably larger diameter radiometers and a 28-inch-long cryogenic cooler. The computer program discussed in Appendix A, whose use will be discussed in detail in a later section, was used to predict the balance characteristics of this concept. The moment of inertia was approximately the same about all axes, indicating that a shorter spacecraft would be necessary or that more judicious positioning of components would be required.

It appeared that radiation from the back side of the fold-out solar panels might be high enough to saturate the radiometer detector. Several spacecraft concepts, a hexagonal version with only four solar panels and a rectangular version with two solar panels, were suggested to eliminate the problem. The rectangular concept was studied in sufficient detail to show the feasibility of thermally controlling the experiment package and the internal components and to determine that there was sufficient volume for mounting the subsystem components.

An analysis was conducted to determine the change in moment of inertia that would occur upon folding out the very large solar panels associated with the rectangular spacecraft. The values given below resulted, where x is the spin axis and y and z are the transverse axes (in the directions with and perpendicular to the direction the panels fold out, respectively).

	<u>Panels in</u>	<u>Panels out</u>
I_x , lb-ft ²	1385	2160
I_y , lb-ft ²	1880	1800
I_z , lb-ft ²	1090	1800

These values indicate a high degree of instability (about the desired axis) when the panels are folded in.

An analysis was also conducted to determine the resonant frequency of these large panels. It was shown that, with a hinge stiffness equal to the stiffness of the 1/2-inch-deep honeycomb panel, the panel natural frequency would conservatively be 40 times the rotational frequency. Therefore, the panels should not cause any major disturbance to spacecraft control.

Attempts were made at one point during the study to configure a spacecraft which could accommodate redundant starmappers with 26-inch-diameter baffles, as shown earlier in Figure 10, and which viewed out the rear face at 45 degrees off the spin axis. Substituting conical, spherical, or segmented bases for the flat plate or extending a sun shading lip downward from the base plate provided only the capacity to incorporate approximately 18-inch baffles at 25 degrees off axis without making major spacecraft changes or abandoning the thermal control approach of radiative cooling from the base plate. Smaller

megaphone-type baffles for use in the dark portion of the orbit and sun sensors for use in the lit portion of the orbit were later substituted for the large multi-surface absorbing fables.

As the radiometer concept evolved, it became increasingly difficult to include the dual redundant units in the Improved Delta spacecraft concept. A study was conducted to suggest several methods of installing dual radiometers in a spacecraft compatible with the Improved Delta. Table 14 shows the related diameters and lengths.

As the horizon definition system study progressed, a radiometer concept incorporating a single optical system with redundancy in the critical areas was defined. This approach was integrated into the experiment package concept shown in Figure 40 and greatly enhanced the experiment package/spacecraft compatibility. A sun shield around the radiometer view port was also incorporated into the system at this time and served to eliminate radiation from the hot solar panels and the sun into the radiometer detector and to reduce the heat load into the experiment package.

Balance calculations were made for this concept with a basic mounting bulkhead and three revised versions of the bulkhead. The very promising results of $I_s/I_t = 1.2$ obtained indicated feasibility of balance for the rolling-wheel concept for use in this mission.

Another configuration of an integrated experiment package, as shown in Figure 41, allowed a reduction in spacecraft length to 40 inches. A study of this version was made relative to component positioning and balancing, and it was found to provide an attractive ratio of spin-axis to transverse-axis moments of inertia of about 1.25.



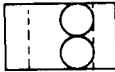



FINAL SPACECRAFT CONCEPT DESCRIPTION

General

The finally evolved concept of the total spacecraft, shown pictorially in Figures 42 and 43, was configured to meet the requirements of the six subsystems. Several important features of this final concept are

- A dual temperature environment is maintained within the spacecraft; the experiment package is kept at approximately - 100°F and the supporting equipment at about 75°F.
- The domed ends allow room for the long experiment package without upsetting the spacecraft balance.
- The solar panels and sun shade are folded along the body of the spacecraft in the launch configuration. Upon orbital orientation by the booster, the solar panels fold out to their final position. The spacecraft is then ready for spin-up.

TABLE 14. - DUAL RADIOMETER INSTALLATIONS
IN AN IMPROVED DELTA SPACECRAFT

Spacecraft	Diameter, in.	Length, in.	Remarks
Hexagonal	Under 12	45	 <p>Side by side between two opposite faces; fairly simple to sun shield.</p>
Hexagonal	Under 20	27-inch length for 20 inch diameter. Length increases for smaller diameter.	 <p>Installed at an angle approaching the angle of the face adjacent to the exit aperture.</p>
Hexagonal	Under 20	45	 <p>On top of each other between two opposite faces, hard to sun shield, thermal control and power subsystem seriously affected. Spacecraft balance affected because cooler is off-axis. Spacecraft becomes very long.</p>
Hexagonal	Under 20	45	 <p>Staggered above each other as in last case. Same remarks apply.</p>
Hexagonal	Under 20	23	 <p>Single tube, back-to-back radiometers pointing opposite directions.</p>
Square	Under 17	38	 <p>Side by side in a square spacecraft, thermal design and power design need revision. Balance may be difficult.</p>

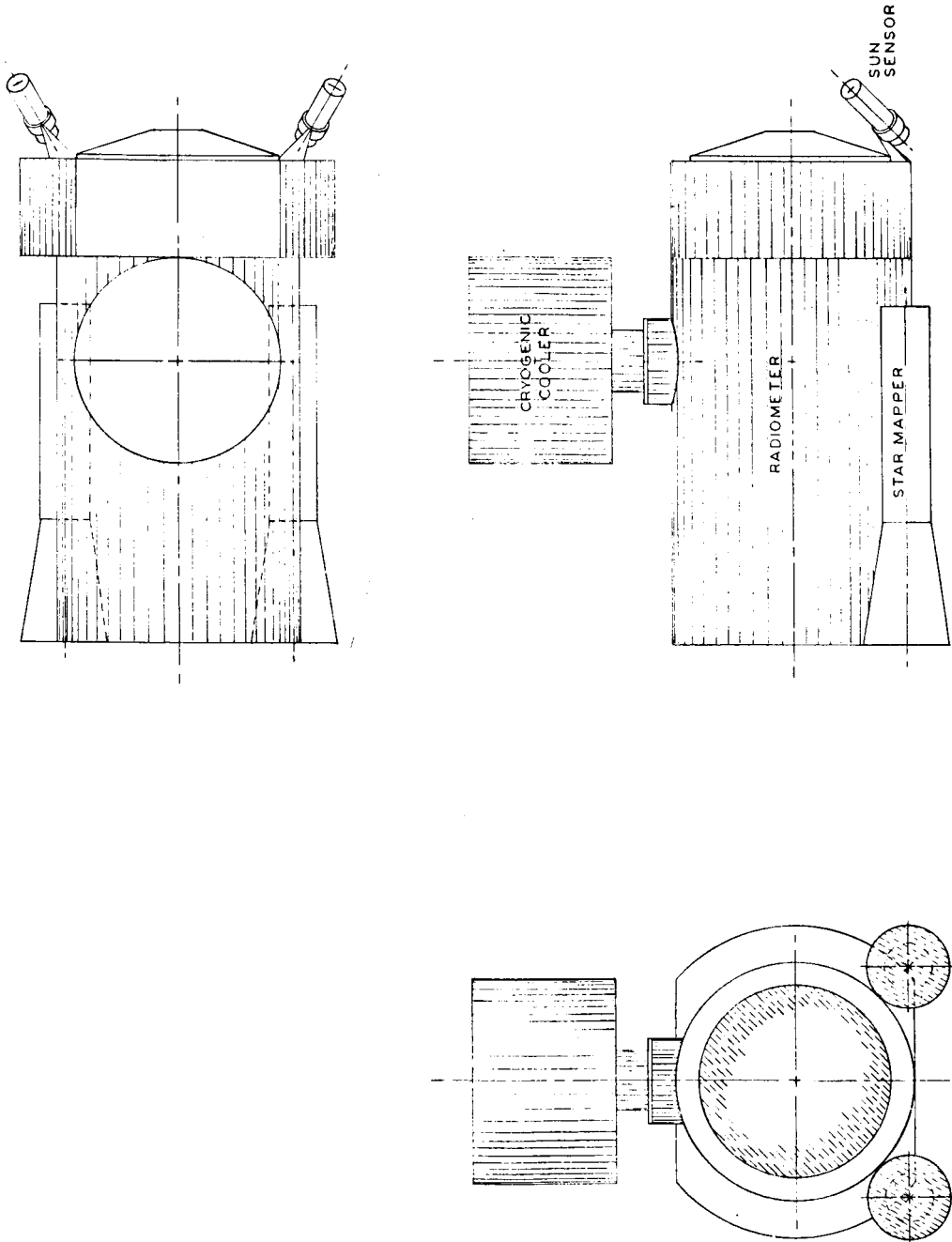


Figure 40. Experiment Package Concept - Starmappers Viewing Forward

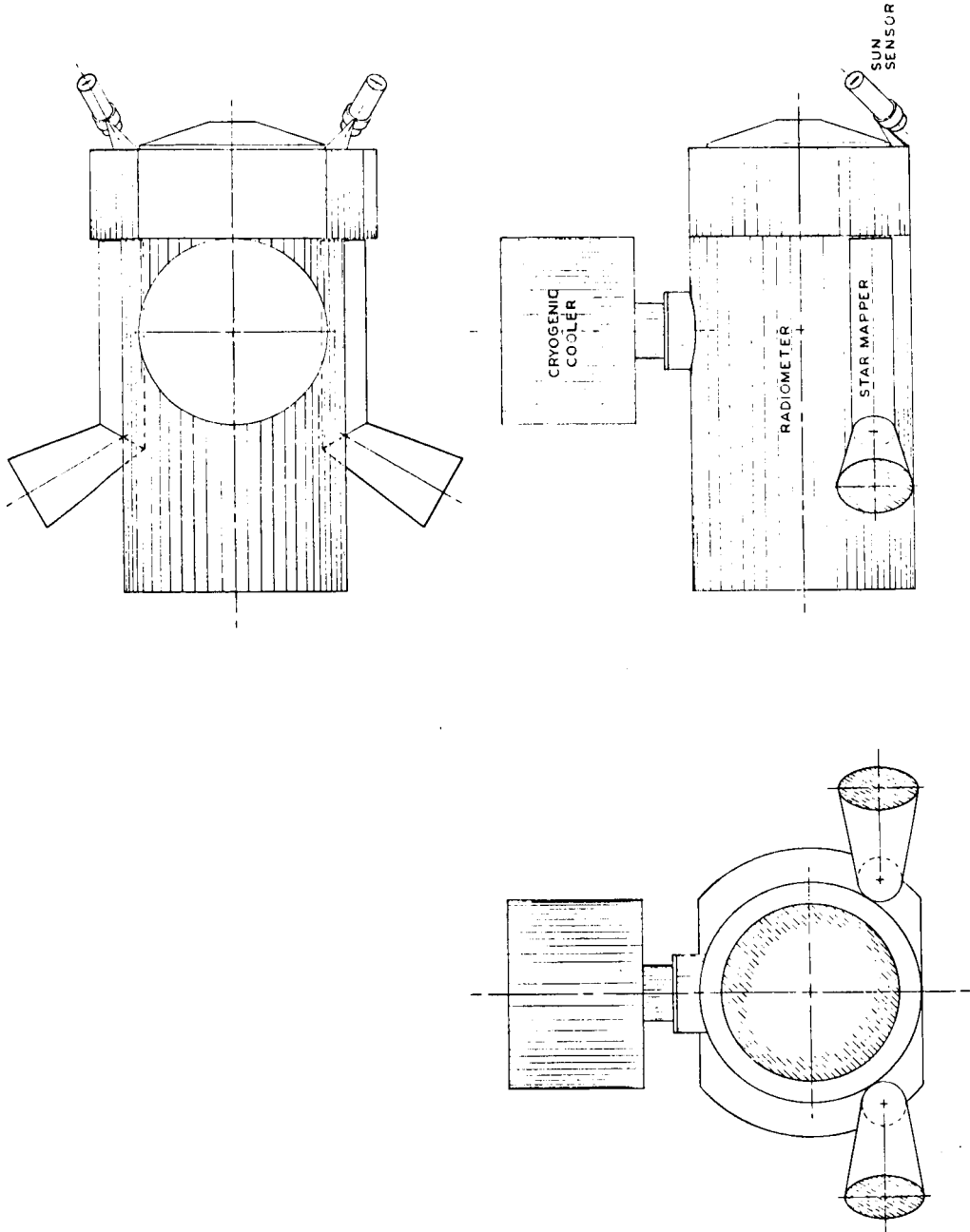


Figure 41. Experiment Package Concept - Starmappers
Viewing 60° Off Axis

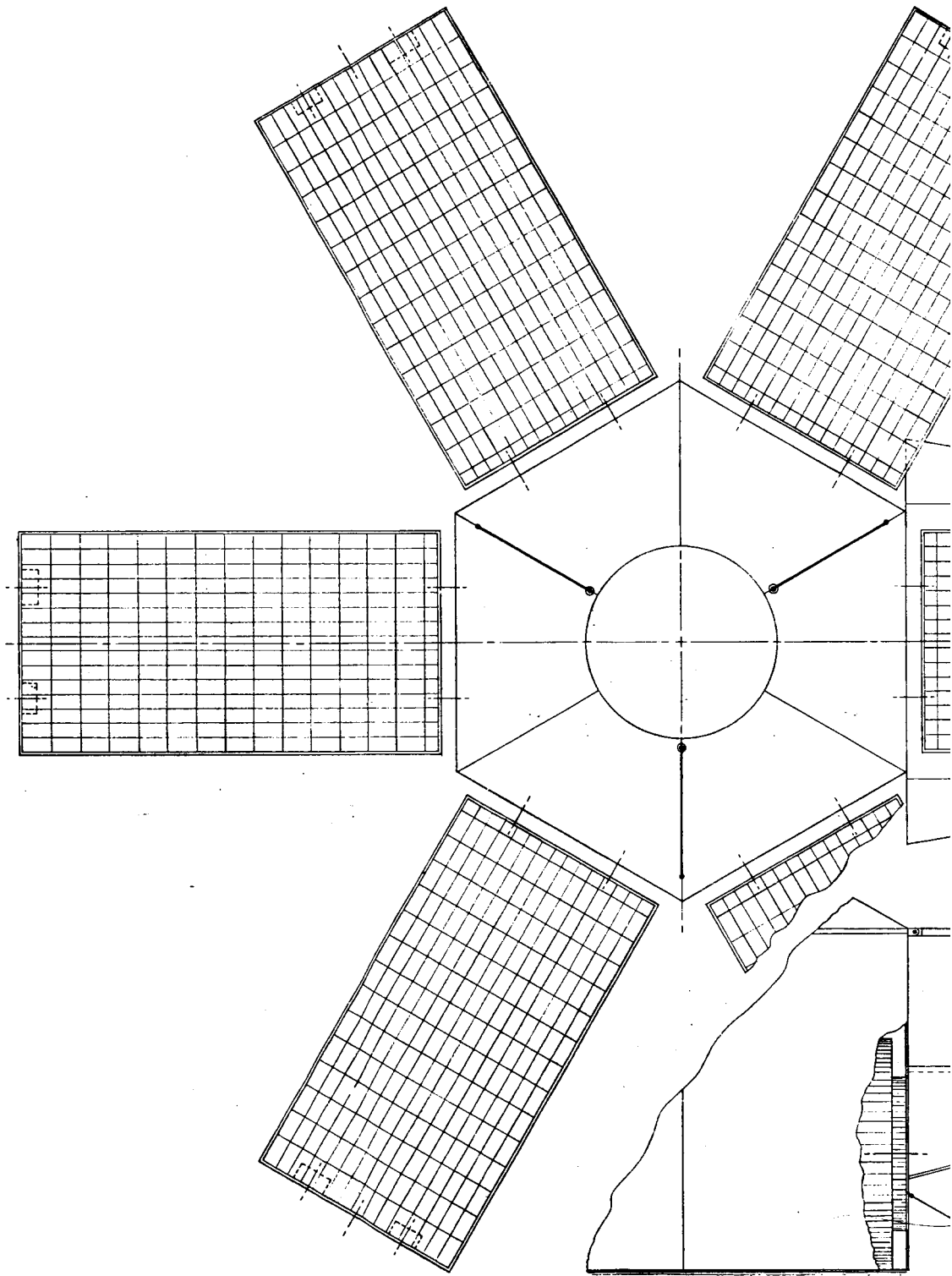
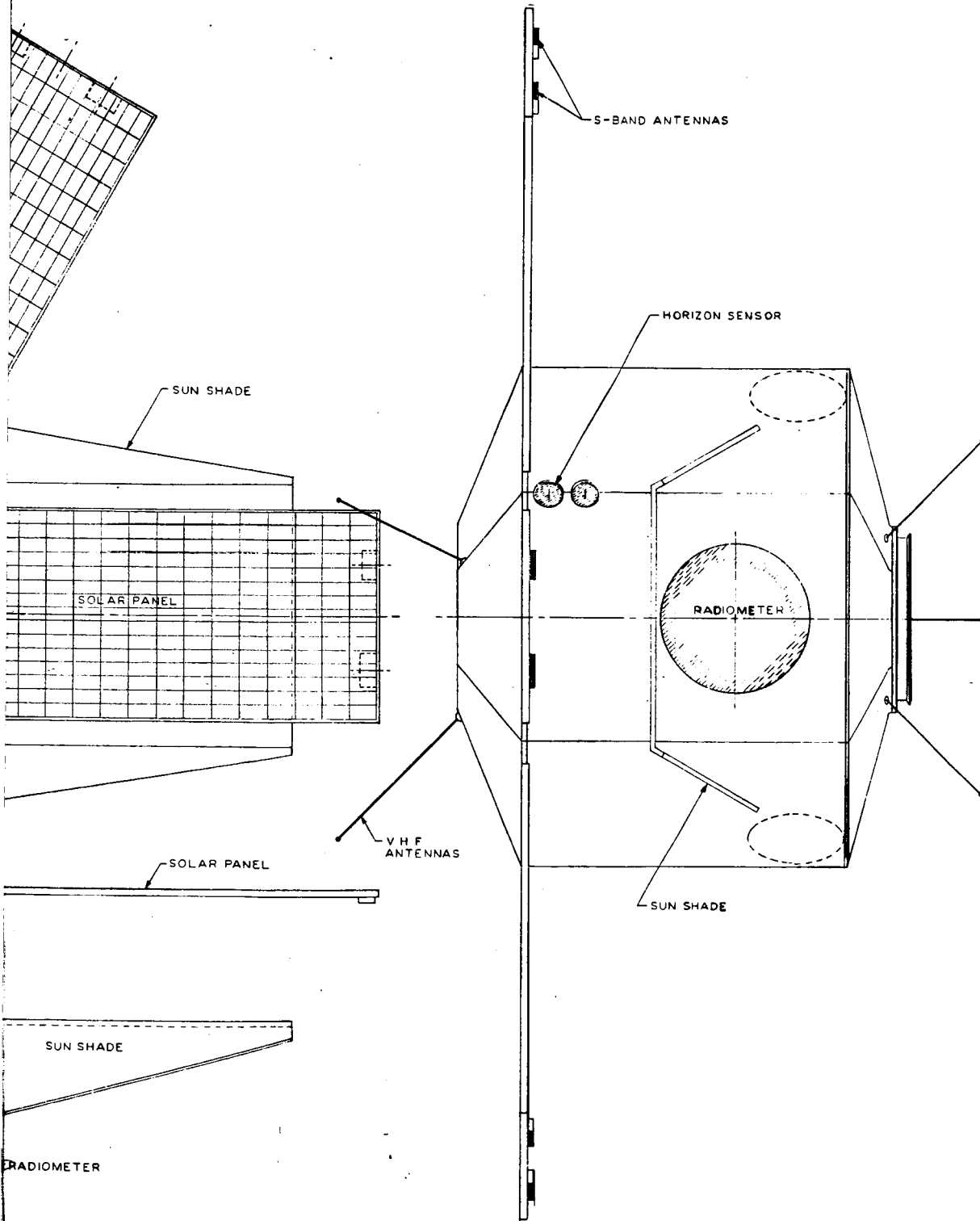


Figure 42. Conceptual



Spacecraft - External Layout

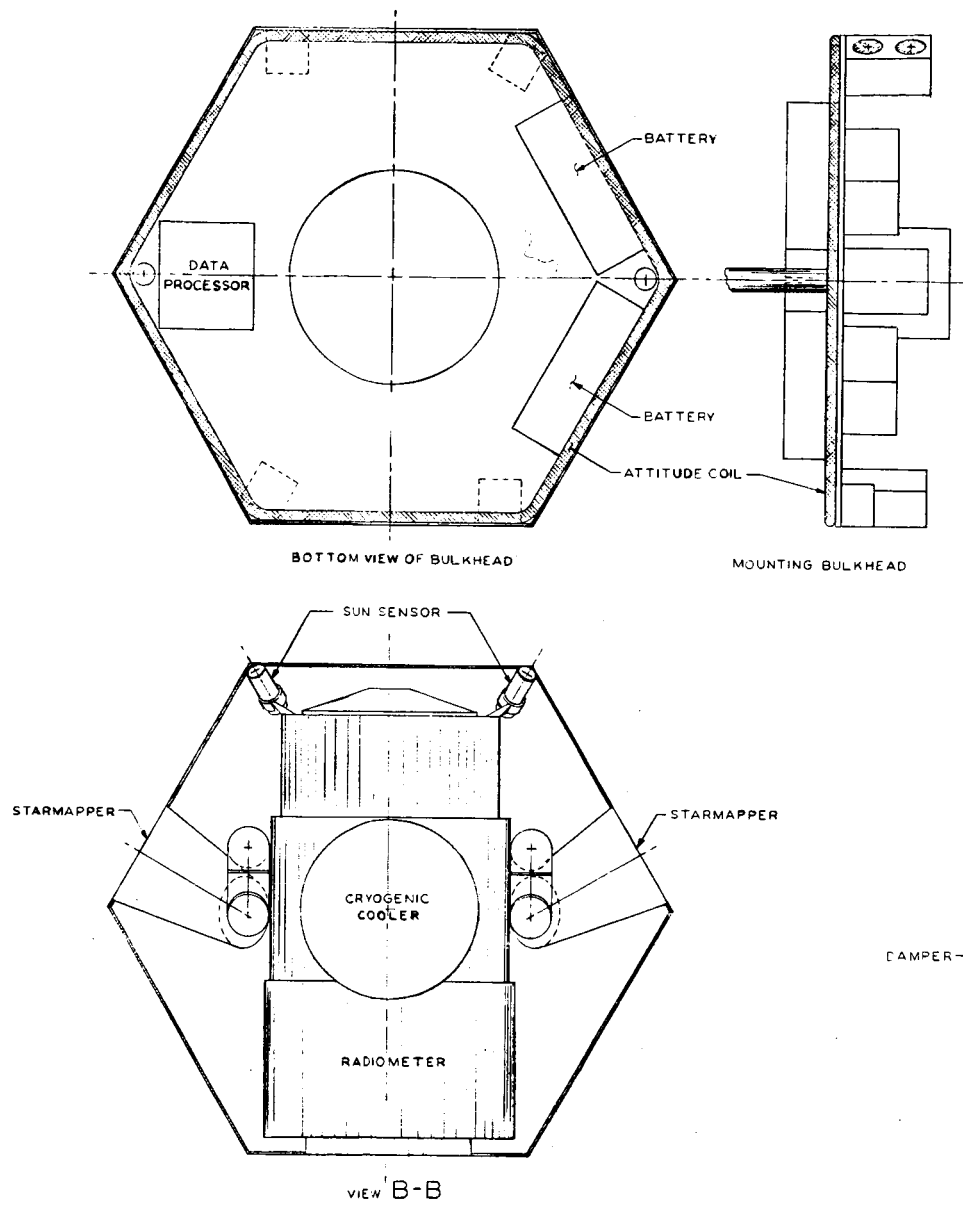
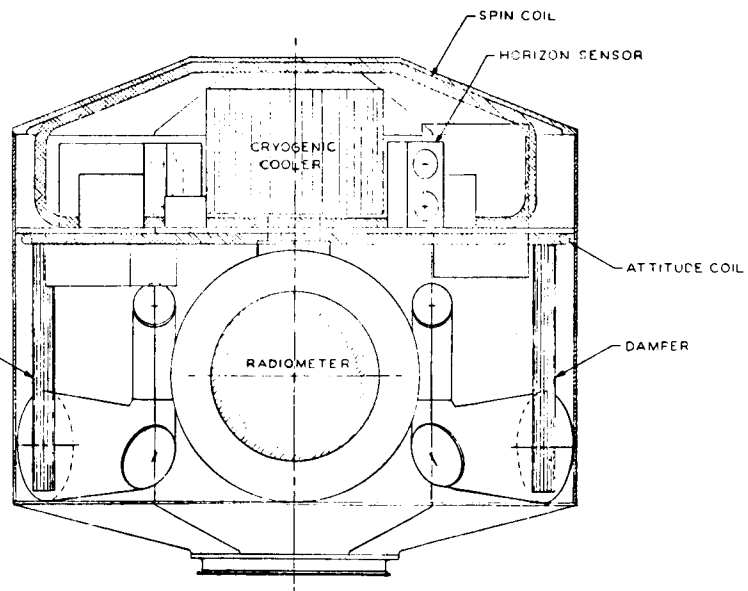
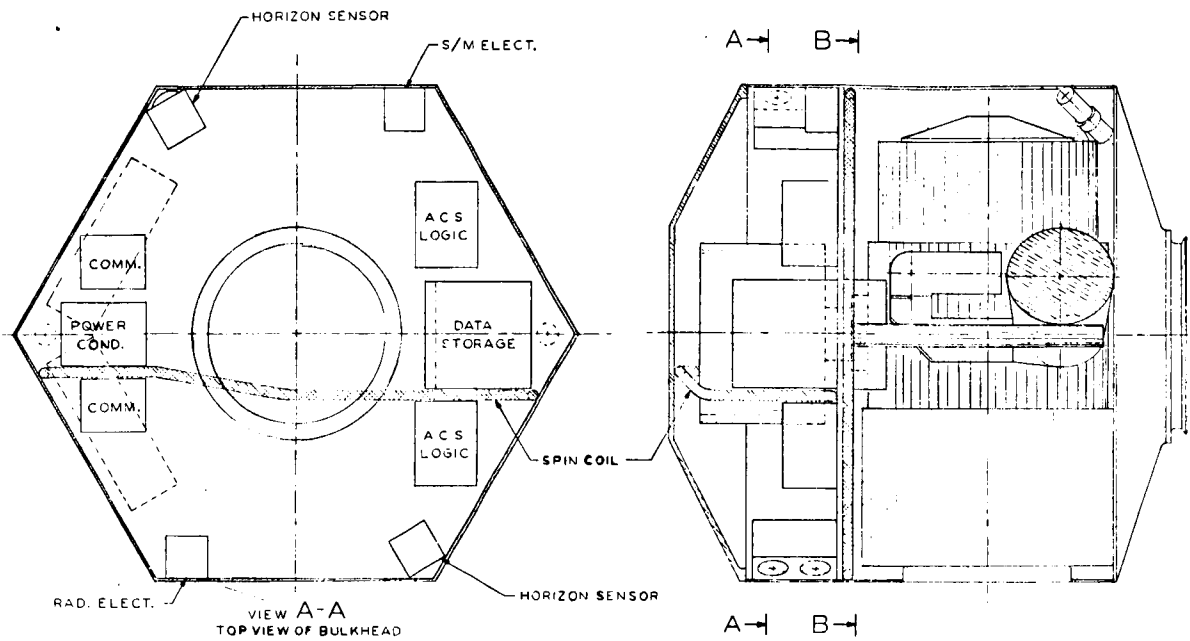


Figure 43. Conc



Conceptual Spacecraft - Internal Layout

- A very clean and simple external surface is available for complete use in spacecraft thermal control.

Structural Subsystem

The final configuration of the structural subsystem is shown in Figures 44 and 45. This configuration demonstrates compatibility with both the system requirements and the selected launch vehicle. The heavy, cast aluminum baseplate carries thrust from the booster out to the periphery of the spacecraft where the load from the upper portion of the spacecraft will be supported. Even more important, it serves as the mounting platform and cooling radiator for the experiment package. The casting assures good thermal conduction (minimum thermal gradients) and a minimum of internal stresses. The flat, external surfaces offer no cavities for higher heat absorption and can be covered with special coatings if needed. Mating surfaces, such as the booster interface bolt circle, the internal mounting platform, the periphery, and the spacecraft sidewall mounting surface will be machined surfaces. As was shown in Figure 16, the baseplate and experiment package are thermally isolated from the rest of the spacecraft.

The superinsulation, which was described in the earlier thermal control section, will enclose all parts of the experiment package except the megaphone baffles on the starmappers. It will require special attachment and support design to minimize heat transfer and will tie directly into the plastic supports between the baseplate and sidewall.

The plastic supports between the baseplate and the sidewall serve to reduce the heat transfer from the sidewall into the baseplate. They must also carry the thrust load, but these plastics are typically in the 20 000 psi compressive-yield strength class, so several square inches of plastic would yield a very high safety factor and reduce the heat conduction to an acceptable level. The plastic insulating ring at the top of the sidewall is a similar design; however, the thrust level is greatly reduced.

The white painted, aluminum sidewalls and the structural skeleton are fully described in Figure 44. Screw attachments between the wall panels and skeleton stringers will allow removal of each panel as needed for access to internal components.

The spacecraft cover serves to enclose the structure and reflect solar energy. It is envisioned as a plastic honeycomb core between two highly reflective sandwich faces. It should have high strength and good insulating properties.

The solar-panel substrate will be an aluminum-honeycomb material with very high strength-to-weight properties, high resonant frequencies, and satisfactory thermal conduction, an approach proven a number of times in space applications. They will be thermally insulated from the body of the spacecraft.

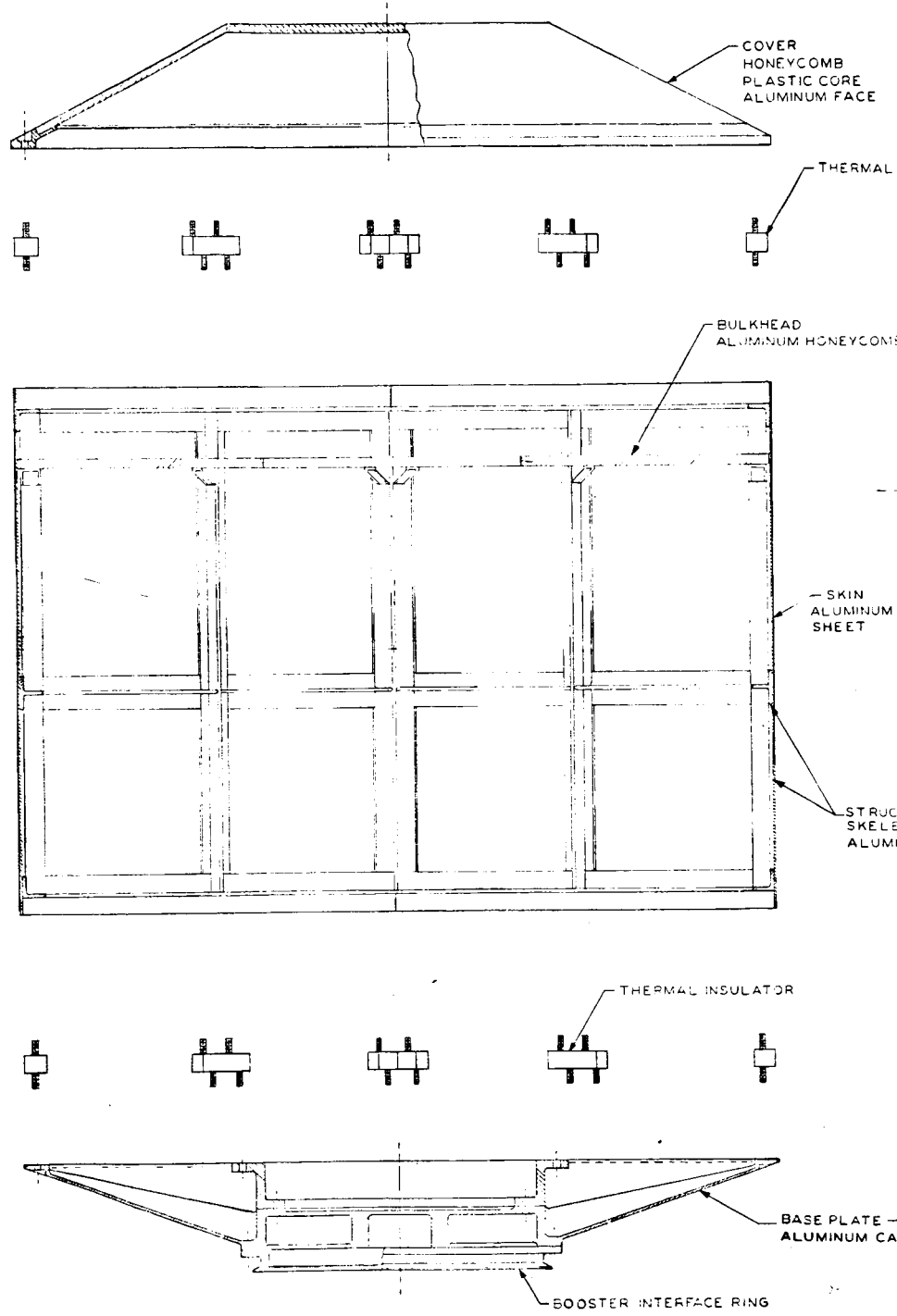
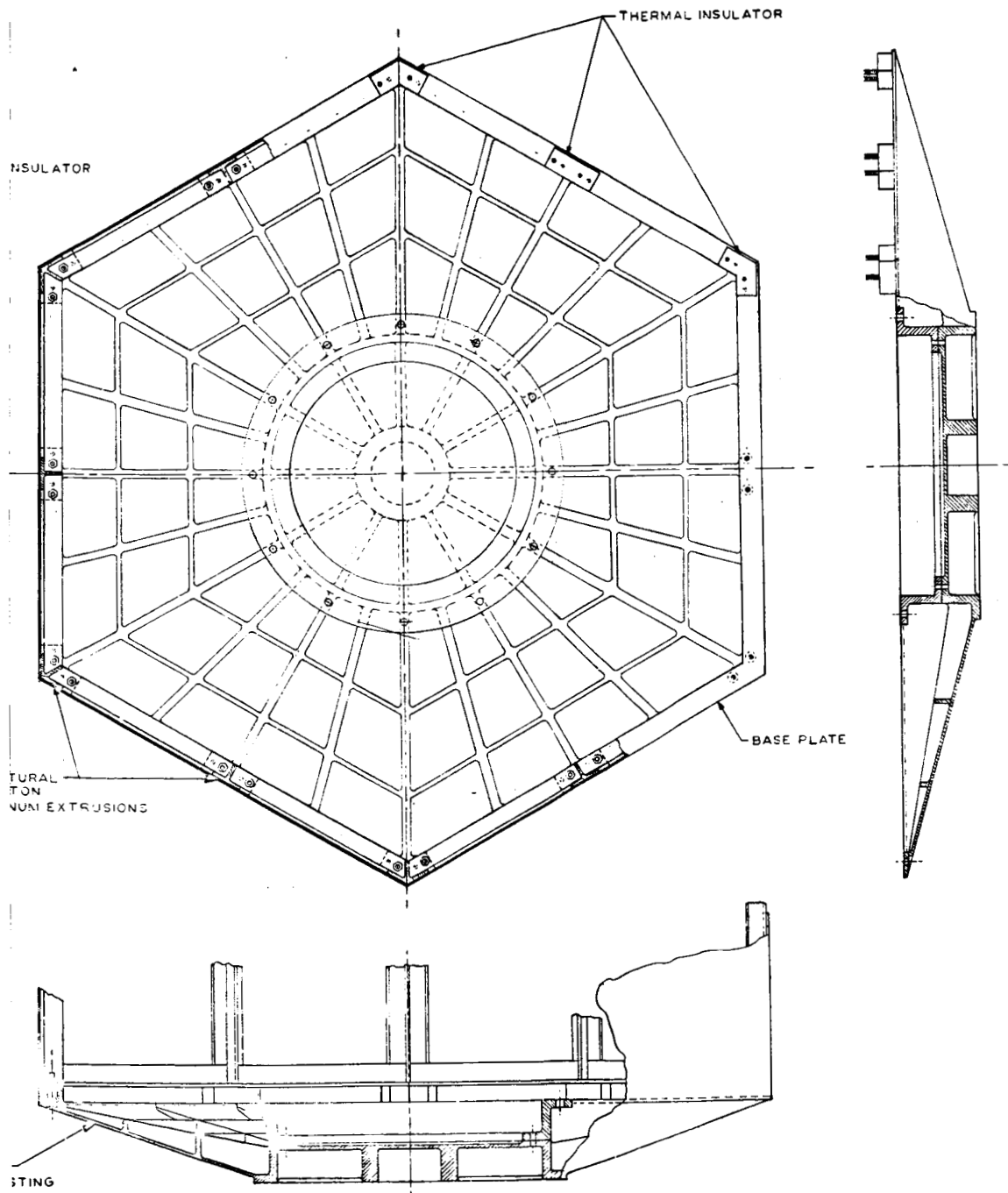


Figure 44. Space



craft Structural Subsystem

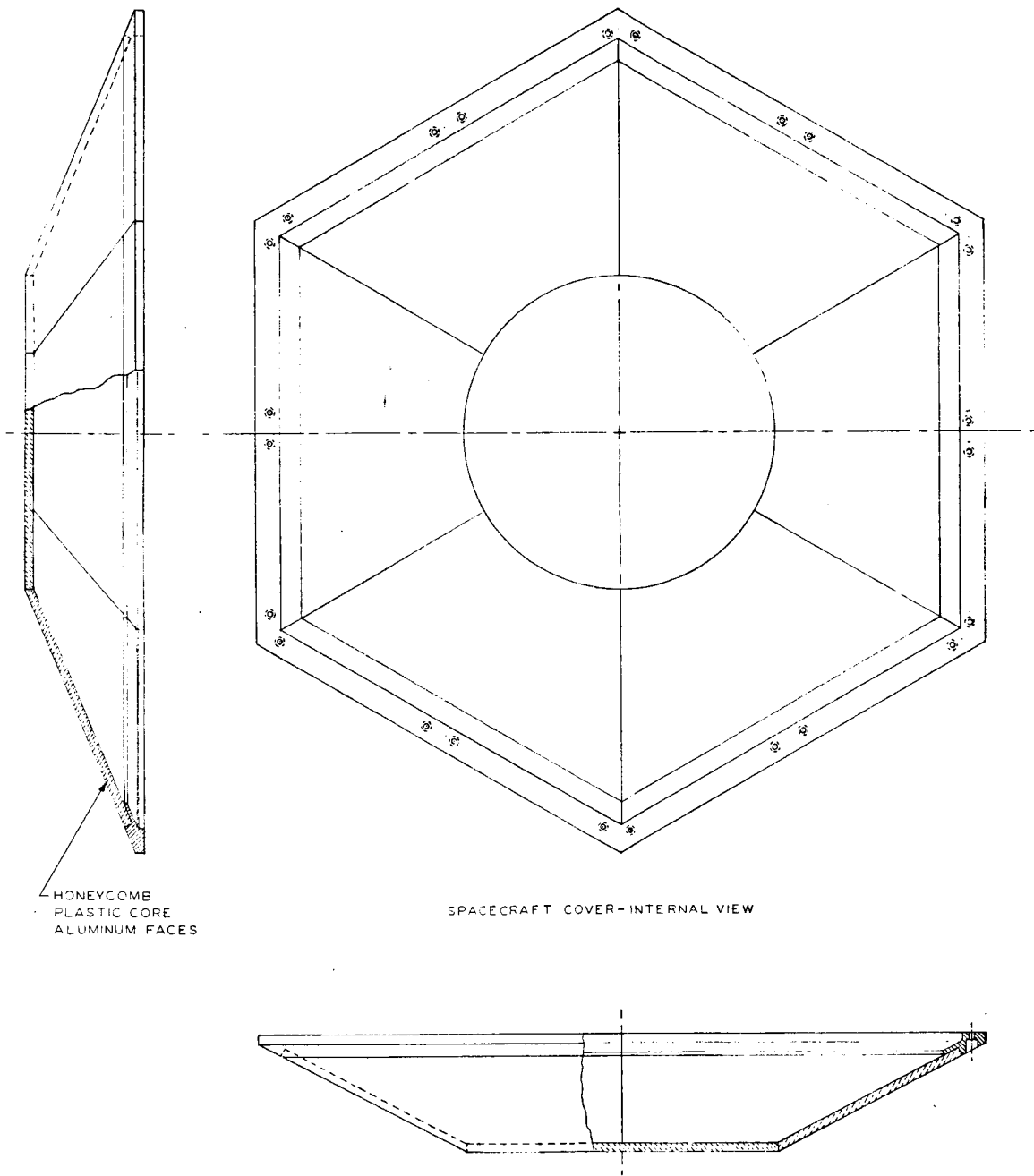


Figure 45. Conceptual Spacecraft Cover

The radiometer view port sun shade, which folds around the hexagonal corners of the spacecraft, will be constructed of a highly insulated sandwich material with a very radiative surface on the shaded side. The shape, shown in Figure 46, is such that the sun can never shine on any part of the radiometer port.

A restraining scheme, deploying mechanism, and hinges will be required for the solar panels and sun shade. These areas were only studied in a cursory manner since they are well within the state of the art and will not have an effect on the feasibility of the concept. Their reliability would be commensurate with the level of design effort expended.

The internal component mounting bulkhead, made of aluminum-honeycomb material, also serves as a heat conductor. Combined with the thermal control/thrust lines that were designed into the thermal control scheme, it is a path for heat to the sidewall where it can be radiated to space.

Subsystem Integration

Each subsystem has special mounting or integration requirements. Some of the major items that were met by the final spacecraft concept are discussed below.

Experiment package. -- This single unit, a precisely aligned optical instrument, is enclosed within a cooled and stable environment. The radiometer views out one panel of the spacecraft rim and its port is shaded from the sun and solar panels by a cool shade. The starmappers view radially outward, 120 degrees ahead of and behind the radiometer. Their megaphone-type baffles, thermally insulated from the rest of the experiment package, are tied into the sidewall for cooling. Axial mounting of the cryogenic cooler protects the "cold finger" which extends from the cryogen to the radiometer detector. Essentially all heat producing electronics associated with the experiment package have been installed on the bulkhead, with only a minimum number of well-insulated wire connections across the superinsulation.

Figure 47 depicts the conceptual approach of filling and servicing the cryogenic cooler after it is installed in the spacecraft (even after the spacecraft is mounted on the booster). Quick-connect fittings through the cover plate on the booster interface ring accept cryogen and refrigerant lines for refilling and freezing through the Mylar lines to the cooler as needed. Access to the quick-connects will be through a hole in the fairing which matches a hole in the booster adapter ring. The lines also serve as venting lines to remove sublimates during orbit operation. They will be oriented so that any thrust from sublimates venting will be through the spacecraft center of mass.

Attitude control. -- The horizon sensors view radially outward, but 30 degrees in the axial direction. They also are about 68 degrees behind the spin-coil plane, so they intersect the earth's horizon at the proper time for signal synchronization. The precession dampers on opposite sides of the spacecraft are oriented in the axial direction of the spacecraft.

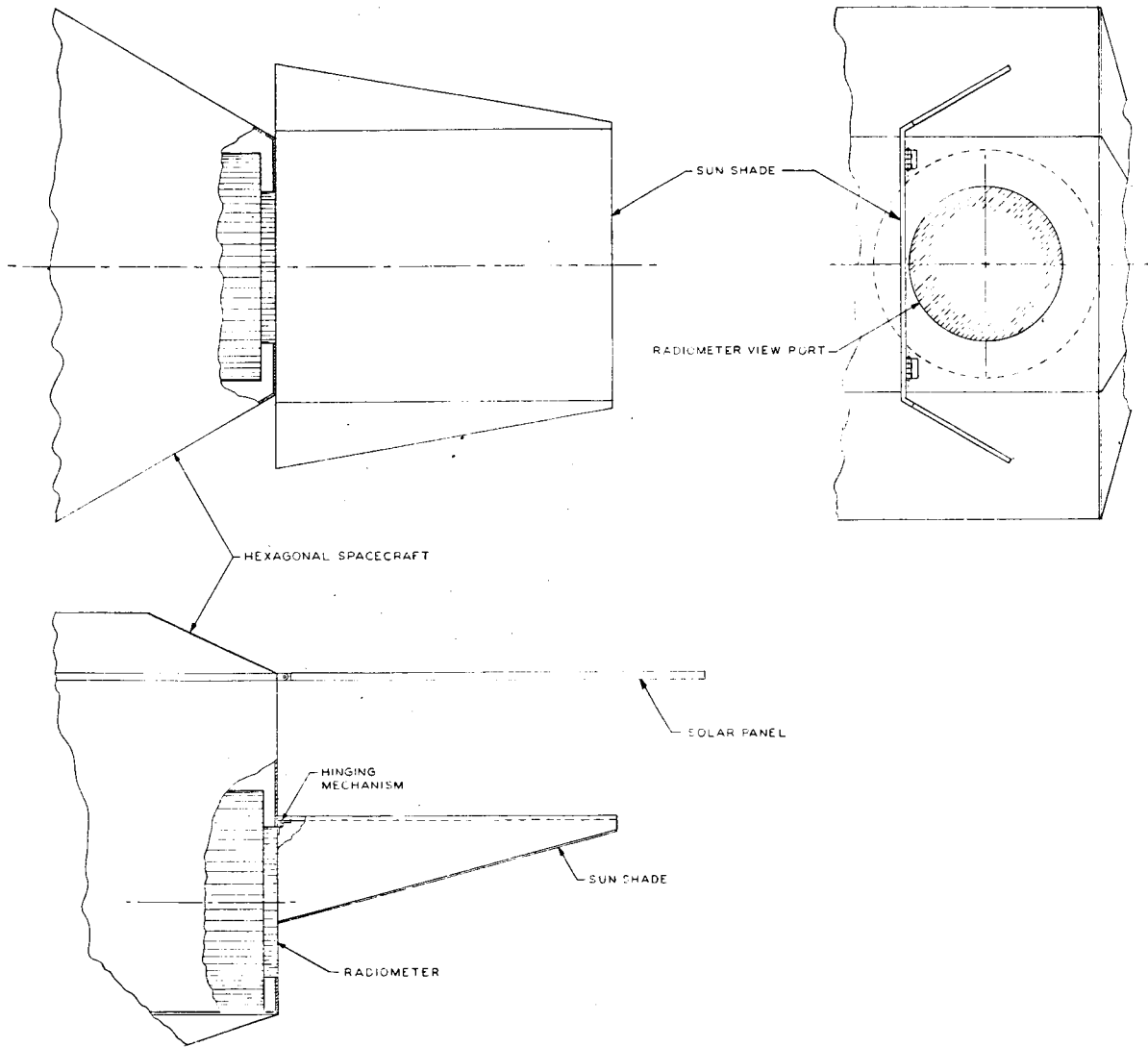


Figure 46. Radiometer View Port Sun Shade

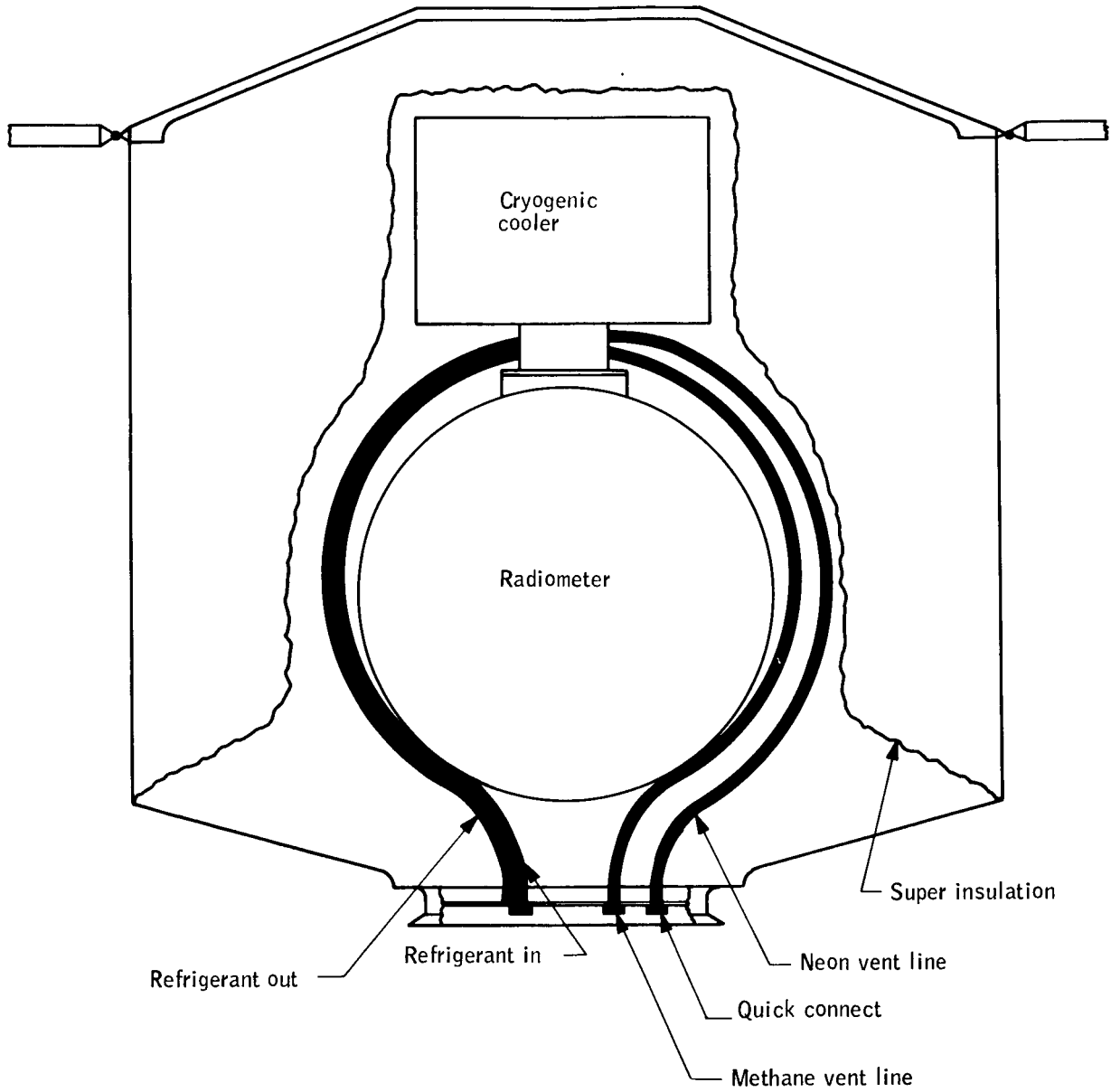


Figure 47. Cryogenic Cooler Venting and Refrigerant Lines

Data handling. -- The data processor and data storage boxes are on opposite sides of the bulkhead, meeting the requirement for short interconnecting lines.

Communications. -- The transmitting antennas are positioned so their energy will not affect readings made by the starmappers or radiometers. All sets of antennas are positioned so their transmitting pattern or receiving field of view will not be affected by other spacecraft protrusions, i. e., the stubs are on the ends of the spacecraft and the slots are on the ends of the solar panels.

Power. -- The fold-out solar panels are mounted so they will never be shaded from the sun if earth orientation and orbital limits are maintained.

Component mounting bulkhead. -- The assumption was made that each component could be built with EMI control and that the major interference requirement for mounting components on the bulkhead would be to use care in positioning the interconnecting wires. It was therefore possible to position components on the bulkhead to achieve spacecraft balance.

Spacecraft Balance

The computer program, which was discussed earlier in this report and is included in Appendix A, was used to analyze the balance of the final spacecraft concept. The details of the analyses are included in Appendix B.

The total spacecraft can be pictured as being made up of two types of components; those that must be in a certain place (such as the experiment package, walls, solar panels, etc.) and those which could be moved around somewhat if necessary to achieve balance (such as components on the mounting bulkhead). The moments of inertia of this concept due only to the fixed components showed a considerable unbalance, mainly because the heavy radiometer optics and sun shade are located far off axis.

A number of earlier moment of inertia calculations indicated what might be a desirable bulkhead arrangement. Using those results, the arrangement shown in Figure 43 was tried and resulted in

$$I_x = 2436 \text{ lb-ft}^2$$

$$I_y = 1873 \text{ lb-ft}^2$$

$$I_z = 1896 \text{ lb-ft}^2$$

Adding five pounds of weight on the baseplate in each corner opposite the radiometer optics yielded

$$I_x = 2476 \text{ lb-ft}^2$$

$$I_y = 1930 \text{ lb-ft}^2$$

$$I_z = 1934 \text{ lb-ft}^2$$

The principal spin axis was about 3.9 degrees off the geometric, preferred axis. These results indicate that the desired ratio of $I_x/I_y = 1.20$ was surpassed (1.29 without dead weight) and that the desirable ± 5 percent variation in the transverse moments of inertia was achievable (approximately zero), even with the large assemblies of subsystem components assumed here. Breaking these boxes into smaller portions would simplify the balance procedure. The fold-out solar panels provide a significant portion of the total spacecraft mass moments of inertia. It was determined that the values shown below were true for one case calculated.

	<u>Panels in</u>	<u>Panels out</u>
$I_x, \text{ lb-ft}^2$	1735	2210
$I_y, \text{ lb-ft}^2$	1565	1870
$I_z, \text{ lb-ft}^2$	1565	1870

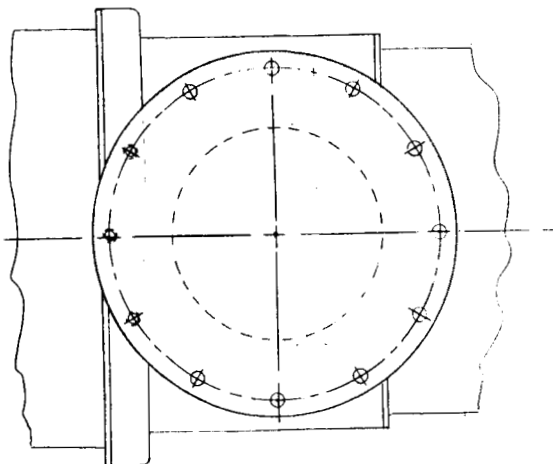
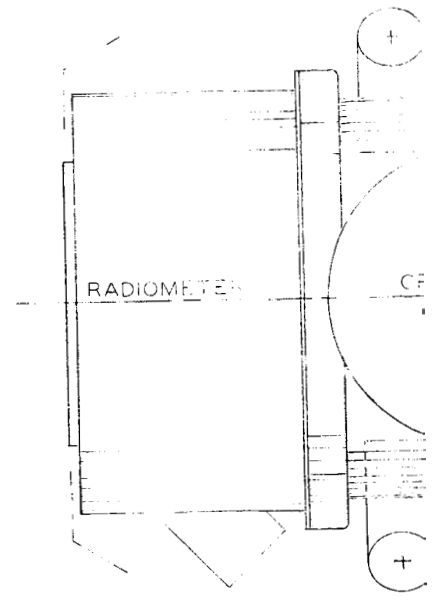
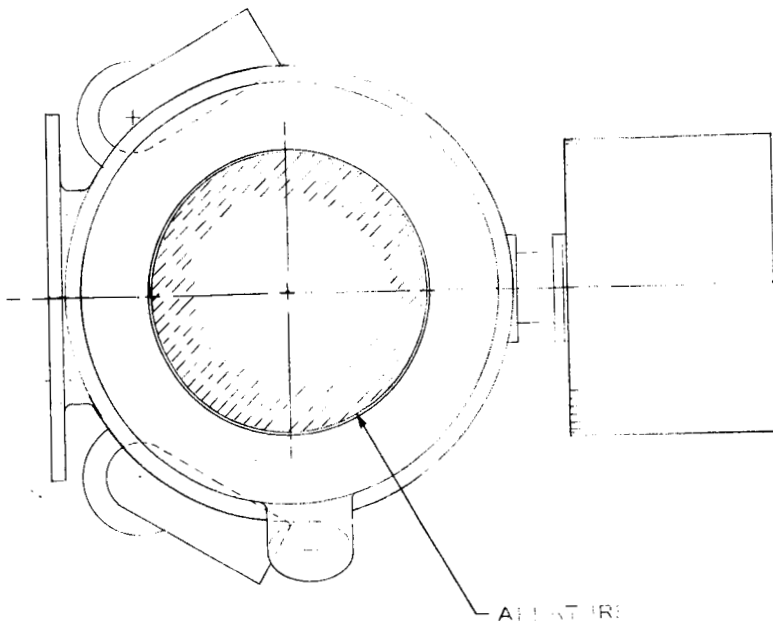
It can be seen that no significant unbalance occurs for this hexagonal concept when the panels are folded along the body of the spacecraft.

Spacecraft Thermal Control

The final spacecraft concept incorporates a local sun shield around the radiometer view port, a superinsulated experiment package compartment, a component mounting bulkhead thermally tied to the spacecraft sidewalls, and radiation from all spacecraft external surfaces. This approach is just as was discussed in Thermal Control Conceptual Design. Therefore, the experiment package will stay at about -100°F and the bulkhead temperature will be about 75°F .

Alternate Spacecraft Concept

An alternate conceptual spacecraft was configured to accommodate the experiment package shown in Figure 48. This somewhat revised experiment package is different from the final version described earlier in Figure 11 in that it has "straight through" starmappers viewing in the opposite direction from the radiometer. It also shows an approach at assembling all parts of the package into a single unit.



BOTTOM VIEW OF MOUNTING PLATE

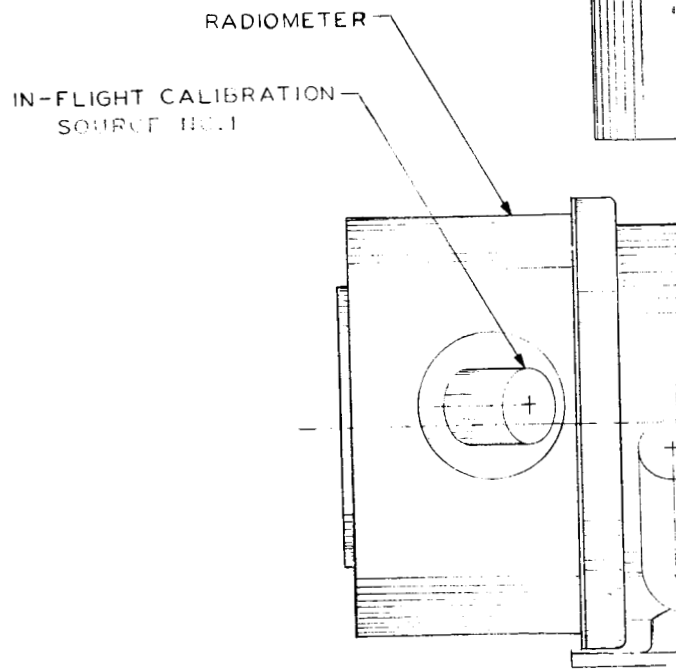
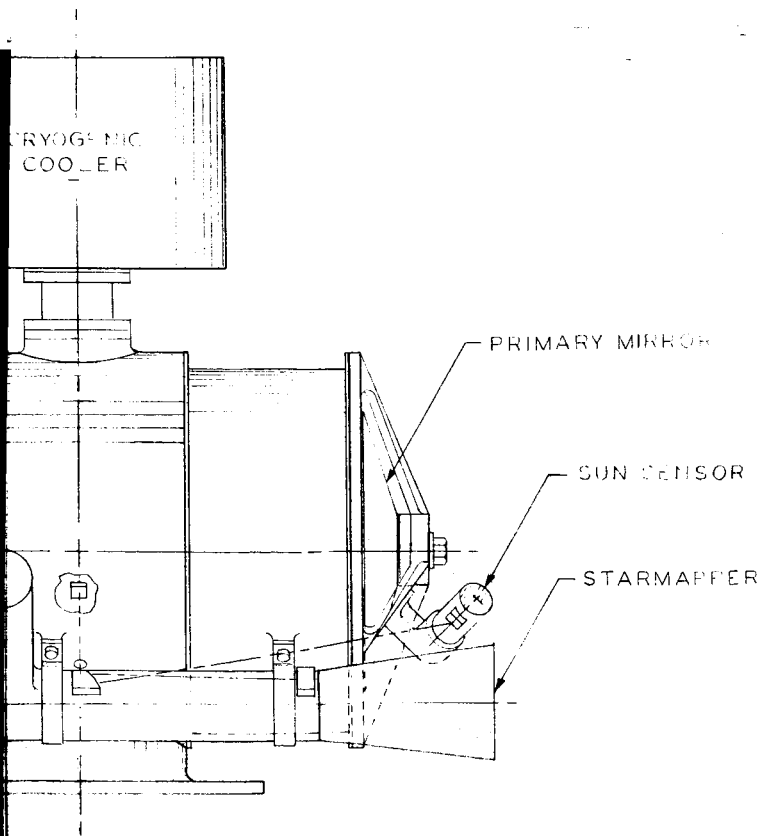
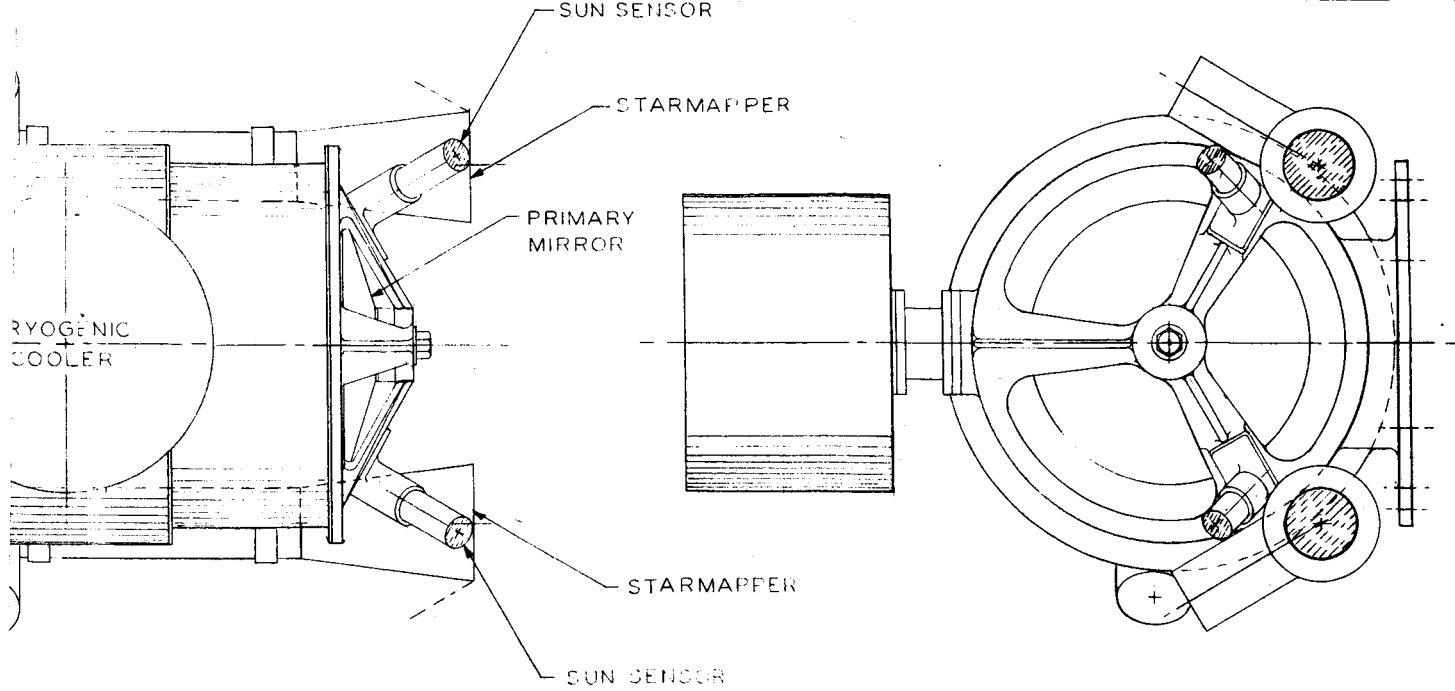


Figure 48. Experiment Pack



The most significant change necessary in the conceptual design was to lengthen the spacecraft two inches. This change affected the spacecraft balance since all components were repositioned with respect to the center of mass. Balance calculations showed

$$I_x = 2432 \text{ lb} - \text{ft}^2$$

$$I_y = 1950 \text{ lb} - \text{ft}^2$$

$$I_z = 1973 \text{ lb} - \text{ft}^2$$

The spin-axis to transverse-axis moment of inertia ratio is approximately 1.24, only slightly greater than the desired minimum of 1.20. The thermal control approach is unchanged from the previously discussed concept. This concept offers a very attractive method of assembling the experiment package and certainly merits further study.

Booster Interface

The final spacecraft concept would interface with the standard Delta and the long Agena fairing as shown in Figure 49. There is a considerable excess length and a small margin in diameter for some spacecraft protrusions or growth. Bumper pad mounting between the spacecraft and fairing could be provided if needed.

The standard 18-inch-diameter booster interface ring was selected because it mates nicely with the desired thrust line into the experiment package. The spacecraft side of the V-block clamping ring has been shown as a bolt-on, but could just as well be cast directly onto the baseplate.

Operational Changes

Only minor changes in the physical properties of the spacecraft will occur during the one-year operation. Assuming the cryogen in the cooler will all be used, there will be a decrease in mass moment of inertia about the spin axis of about 3 lb-ft^2 and a decrease about the transverse axis of about 18 lb-ft^2 . Neither value will have a significant effect on the body dynamics.

CONCLUSIONS

Several significant conclusions were drawn from this conceptual design study of an integrated system configuration and the structural and thermal control subsystems. They are summarized below:

- A hexagonal cylinder, 54 inches across the hexagonal corners with 35-inch side walls and 7-inch-deep domed ends, was configured within the basic requirements set forth in the Horizon Definition Study. Specific features of this concept are:

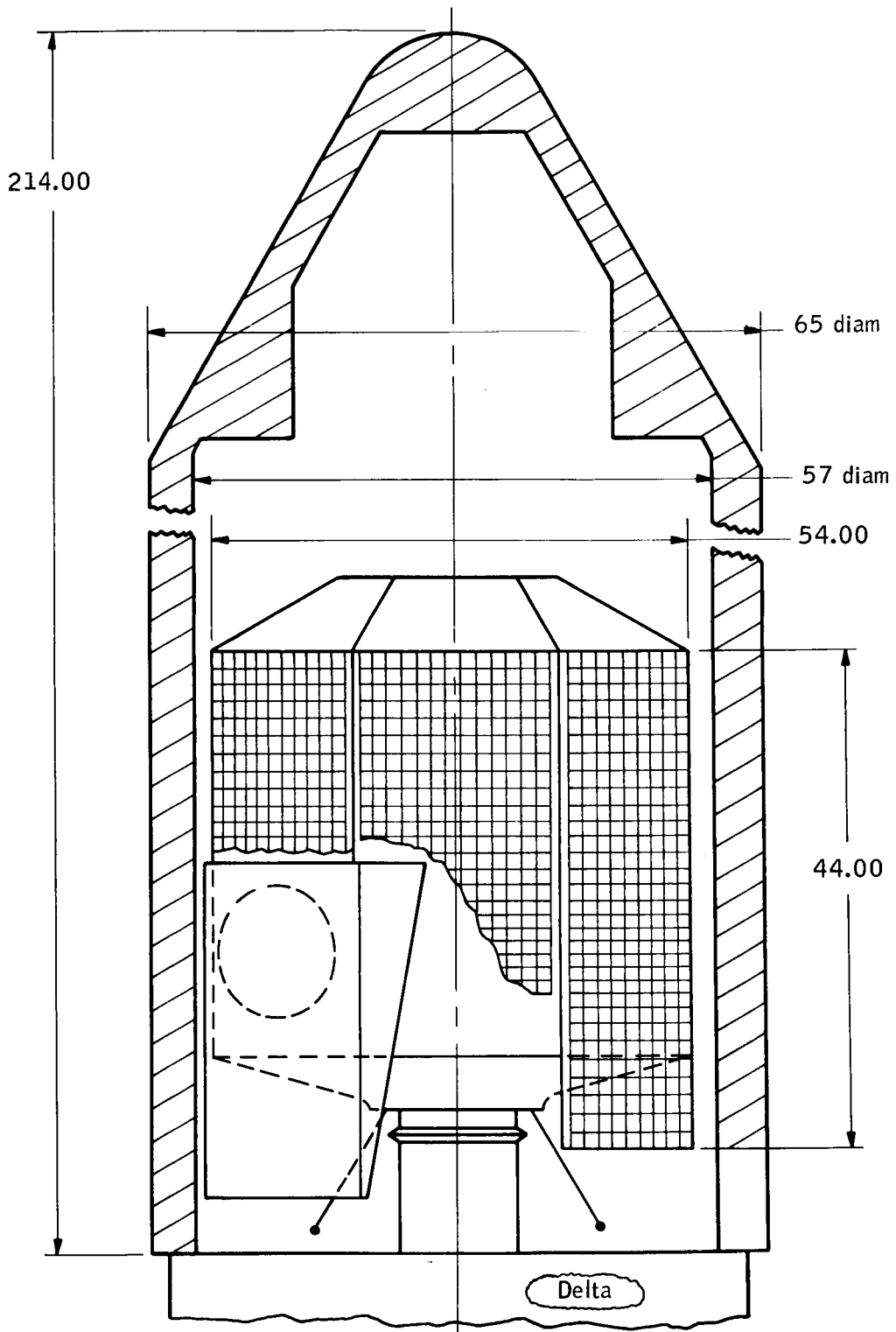


Figure 49. Spacecraft/Booster Interface

- ▶ Dimensions are well within the allowable 57-inch-diameter and 120-inch-length envelope of the Improved Delta nose cone.
 - ▶ A total spacecraft launch weight of 723 pounds, is also well within the capability of the Improved Delta.
 - ▶ High reliability is inherent in the simple, passive type of operation after initial erection of fold-out solar panels and sun shade.
 - ▶ All materials and procedures to be used are well within the state of the art.
 - ▶ The "clean" exterior of the spacecraft is completely available for thermal control.
 - ▶ A stable thermal environment for the experiment package, conducive to maintaining the necessary precise alignment.
 - ▶ Sufficient design flexibility to accommodate variations in experiment package configuration, subsystem supporting electronics, solar panel length versus power requirements, and heat input power and heat dissipation characteristics of the subsystem components.
- The spacecraft system discussed above exhibits physical and functional interface compatibility between all components and subsystems.
 - A spin-axis to transverse-axis moment of inertia ratio of 1.29 was achieved for the final concept, well in excess of the desired minimum of 1.20. The spin axis for the final concept was only about four degrees away from the geometric axis which could be corrected by repositioning components or adding other weight.
 - Thermal balance calculations, based on the subsystems as they are presently defined, showed that careful thermal control design would provide a compartment for the experiment package that could be maintained within five degrees of -100°F . Similarly, a section for electronic support equipment could be kept near 75°F .

PRECEDING PAGE BLANK NOT FILMED.

APPENDIX A

A TECHNIQUE FOR EVALUATING THE MOMENTS
OF INERTIA AND PRINCIPAL AXES OF
ASSEMBLY OF COMPONENTS (TEMPAC)

APPENDIX A

A TECHNIQUE FOR EVALUATING THE MOMENTS OF INERTIA AND PRINCIPAL AXES OF AN ASSEMBLY OF COMPONENTS (TEMPAC)

SUMMARY

A computer program has been written which uses a definition of the components comprising a total assembly, such as a spacecraft or missile, and calculates important dynamic properties of the assembly. Those properties are total mass, mass moments of inertia about some set of reference axes, center of mass location, mass moments of inertia about axes through the center of mass and coincident to the reference axes, principal mass moments of inertia, and the orientation of the corresponding principal axes. The program has been designed so a number of fixed components can be input and the calculated values stored. Many different combinations of variable components can then be added to the stored values, making the program a powerful design tool as well as a calculating tool.

TECHNICAL DEVELOPMENT

The mass moments of inertia of an assembly of individual components controls the dynamics of the assembly. It is made up of two parts: the moment of inertia of each component about its own axes and the transfer term to the total assembly axes.

By choosing a set of coordinates as shown in Figure A1, where P_x , P_y , and P_z are the component principal axes and P_{xx} , P_{yy} , and P_{zz} are axes coincident with the assembly geometric axes, it is possible to describe fully the location and orientation of a component relative to the central axes by giving x , y , and z and Euler angles θ , ϕ , and ψ . Furthermore, the component moments of inertia about P_{xx} , P_{yy} , and P_{zz} can be found from the double dot product of the appropriate unit vectors and the inertia dyadic formed from the component principal moments of inertia.

Table A1 shows the component shapes that have been incorporated into the computer program. The code and dimensions serve to instruct the computer to form the inertia dyadic for the particular shape chosen. These shapes were found to be sufficient for most cases.

Transferring of moments of inertia to the geometric axis of the assembly can then be accomplished, but is not yet sufficient because a spinning body will spin about its principal axis, always through the center of mass. The possible orientation and transfer needed is shown in Figure A2. A cubic equation

describing the momental ellipsoid can then be formed from the center of mass moments and products of inertia; its solution yields the three principal axes, and their orientation can be determined by substituting values back into the ellipsoid equations.

COMPUTER PROGRAM

The program, written in Fortran IV language, requires only a definition of the component in terms of code (from Table A1), mass, coordinates, orientation angles, and dimensions corresponding to the code, all on one input card for each component. A typical output is shown as Table A2, where explanations of the outputs are given.

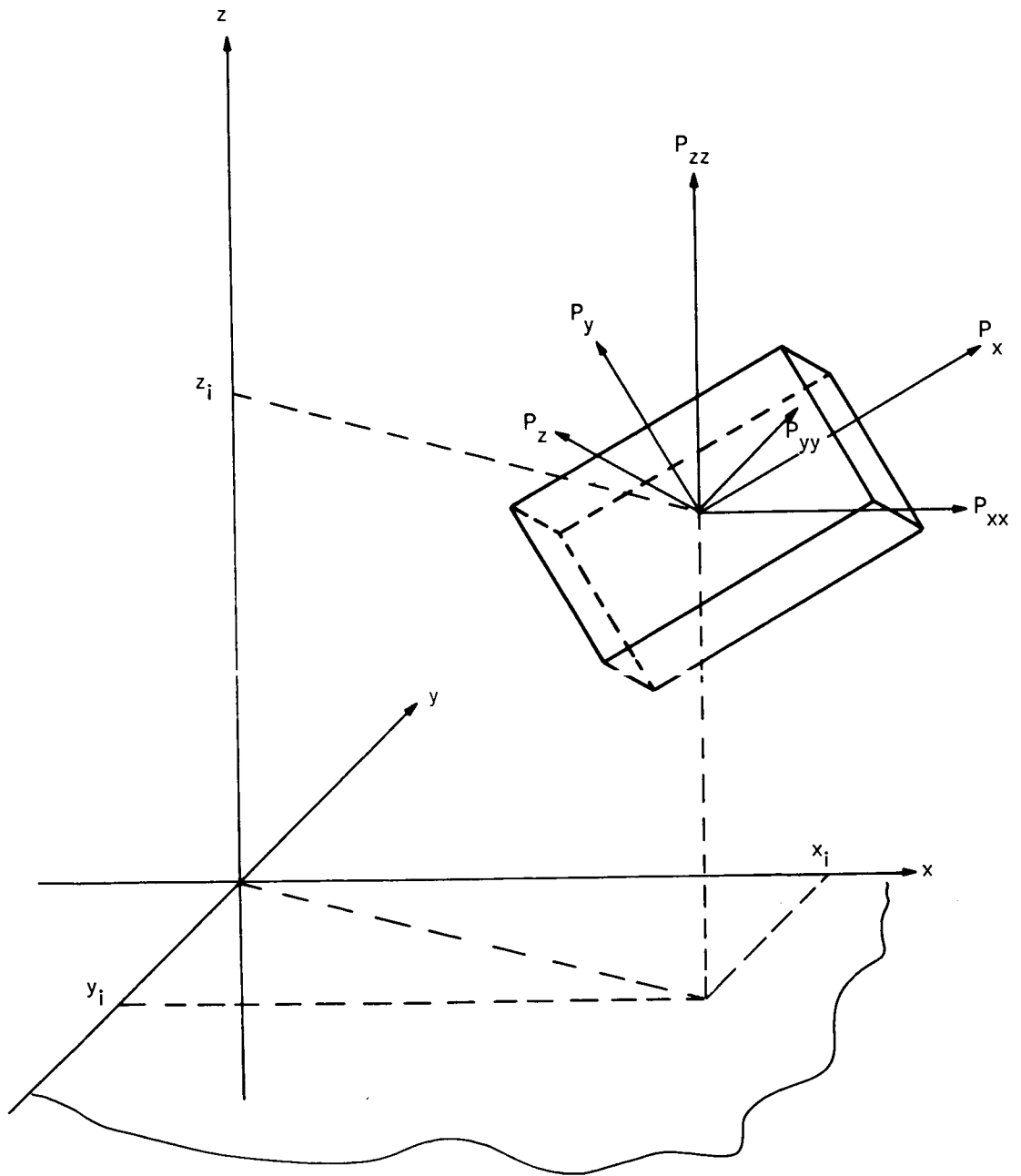


Figure A1. Component Orientation and Location

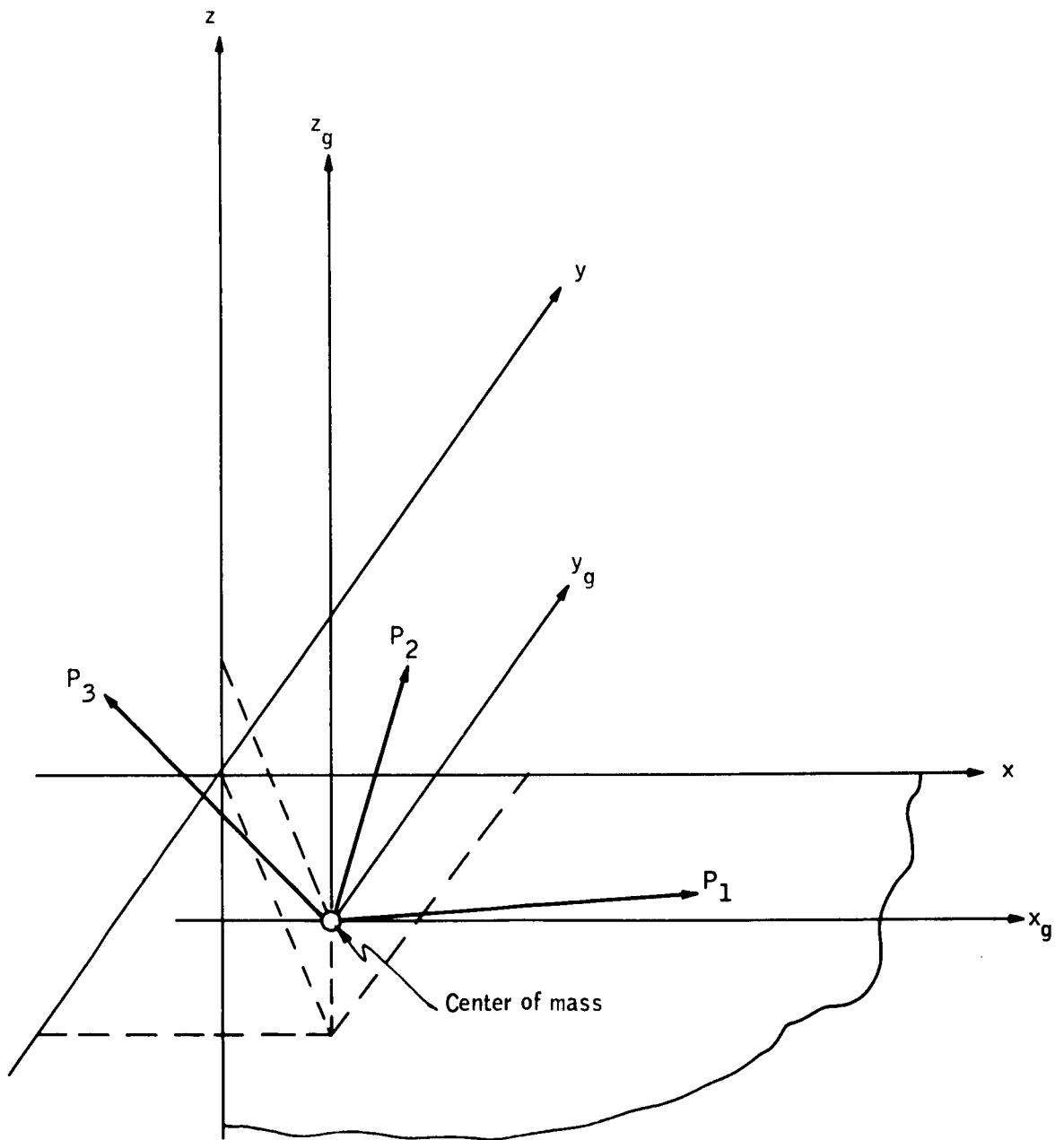


Figure A2. Total Assembly Coordinate Systems

TABLE A 1. - COMPONENT SHAPE AND MOMENT OF INERTIA EQUATIONS

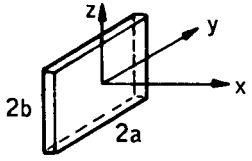
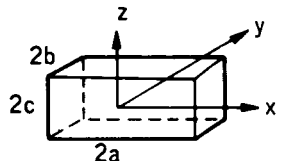
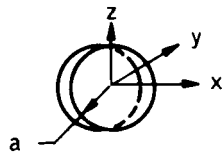
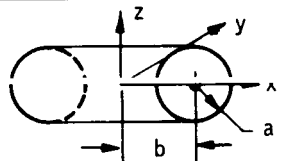
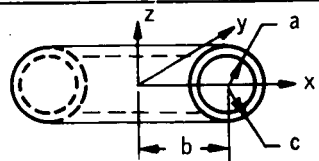
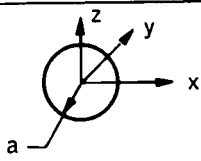
Computer code	Shape	I_{P_x}	I_{P_y}	I_{P_z}
0		0	0	0
1	Any shape	Given	Given	Given
2	Rectangular plate 	$\frac{1}{3}m(b^2 + a^2)$	$\frac{1}{3}m b^2$	$\frac{1}{3}m a^2$
3	Rectangular cuboid 	$\frac{1}{3}m(b^2 + c^2)$	$\frac{1}{3}m(c^2 + a^2)$	$\frac{1}{3}m(a^2 + b^2)$
4	Circular plate 	$\frac{1}{2}ma^2$	$\frac{1}{4}ma^2$	$\frac{1}{4}ma^2$
5	Solid cylinder 	$\frac{1}{2}ma^2$	$\frac{1}{12}m(3a^2 + 4b^2)$	$\frac{1}{12}m(3a^2 + 4b^2)$
6	Hollow cylinder 	$\frac{1}{2}m(a^2 + c^2)$	$m\left(\frac{a^2 + c^2}{4} + \frac{b^2}{3}\right)$	$m\left(\frac{a^2 + c^2}{4} + \frac{b^2}{3}\right)$
7	Sphere 	$\frac{2}{5}ma^2$	$\frac{2}{5}ma^2$	$\frac{2}{5}ma^2$

TABLE A2. - TYPICAL COMPUTER PRINTOUT

Case I

Number of input cards - 54

M - 676.000000 - Total mass

IX - 1972.5205999

IY - 2004.7548416

IZ - 1973.7242583

IXY - 1.1250000

IXZ - -38.6034000

IYZ - -12.9600000

Moments and products of inertia about chosen axes

X(BAR) - -0.0431953

Y(BAR) - 0.0161538

Z(BAR) - 0.1632840

Center of mass location relative to chosen origin

IXG - 1954.3209094

IYG - 1985.4702493

IZG - 1972.2865565

IXYG - 1.5966923

IYZG - -14.7430615

IXZG - -33.8355065

Moments and products of inertia about center of mass axes

P - 0.591208E 04

Q - 0.116493E 08

R - -0.765025E 10

Momental ellipsoid equation coefficients

K1 - 2004.72872

0.00000 - Principal moment of inertia

X/Y - 0.91140E 00

Y/Z - 0.71175E 00

X/Z - 0.64869E 00

Orientation of principal axis

K2 - 1926.46457

0.00000

X/Y - 0.43468E 01

Y/Z - -0.28317E 00

X/Z - -0.12309E 01

K3 - 1980.88442

0.00000

X/Y - -0.52934E 00

Y/Z - -0.27146E 01

X/Z - 0.14369E 01

APPENDIX B
FINAL SPACECRAFT BALANCE

APPENDIX B
FINAL SPACECRAFT BALANCE

In order to demonstrate the use of the computer program for spacecraft balance calculations, the total procedure is shown in this appendix using the final version of the conceptual design as shown in Figures B1 and B2. The encoding procedure for the computer is shown as Tables B1 and B2 with some explanation provided on the table. The origin of the axes was chosen to be the geometric center of the hexagon at the plane of intersection between the sidewall and the baseplate, with x along the spacecraft spin axis, z parallel to the radiometer view direction, and y completing the right-handed system.

Table B1 represents those components which are not movable. There are no variations from Figures B1 and B2 except that the bulkhead integration section has been grouped into a single unit. This portion of the table represents the Case 1 output, Table B3.

Table B2 represents those components which are free to be moved around on the bulkhead to achieve spacecraft balance. The arrangement shown resulted from earlier balance studies. Case 2, the combination of the movable and nonmovable parts of the spacecraft, is shown in Table B4. Adding a five-pound dead weight in each lower corner of the spacecraft opposite the radiometer mirror results in Case 3 shown as Table B5.

In all output cases the x , y , and z components of the principal axes can be determined by assigning a value to z and calculating x and y . For Case 2, the total spacecraft without the addition of dead weight, the values are:

$$x = 8.27$$

$$y = 0.13$$

$$z = -1.00$$

for the principal spin axis. This corresponds to about a seven-degree variation away from the geometric spin axis. The center of mass is 20 inches above the baseplate, about 1/2 inch off-axis toward the radiometer optics.

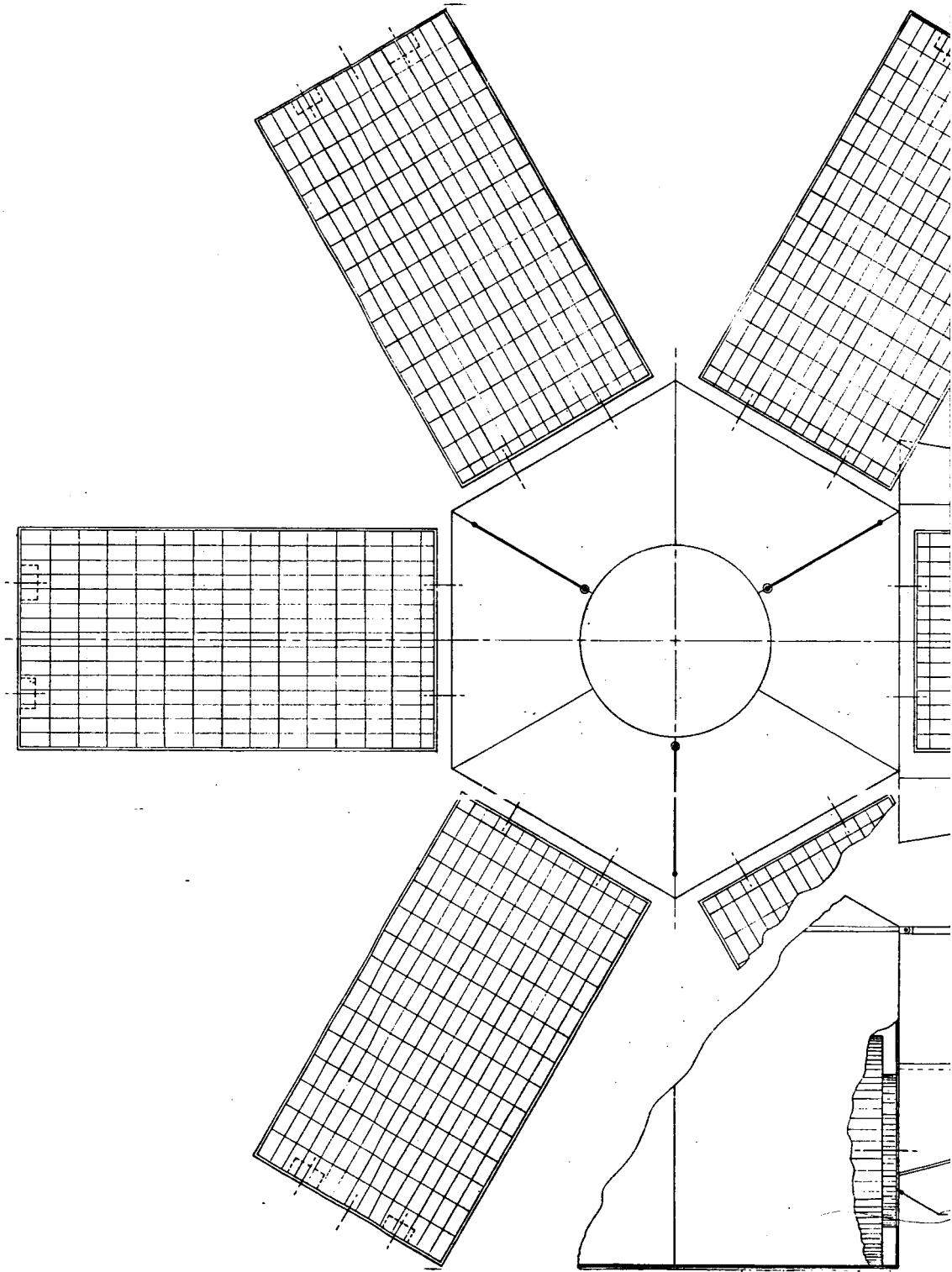
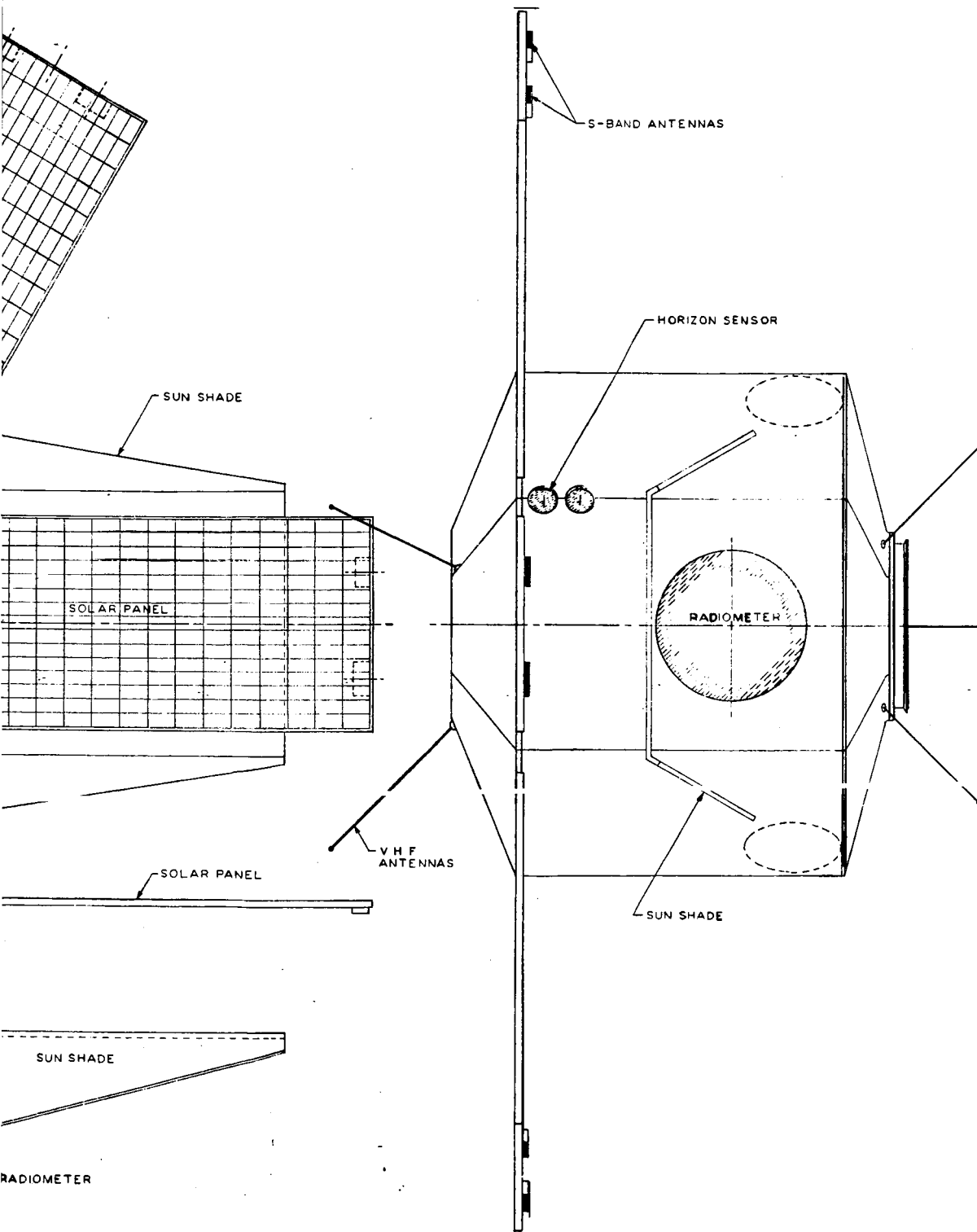


Figure B1. Conceptu



al Spacecraft - External View

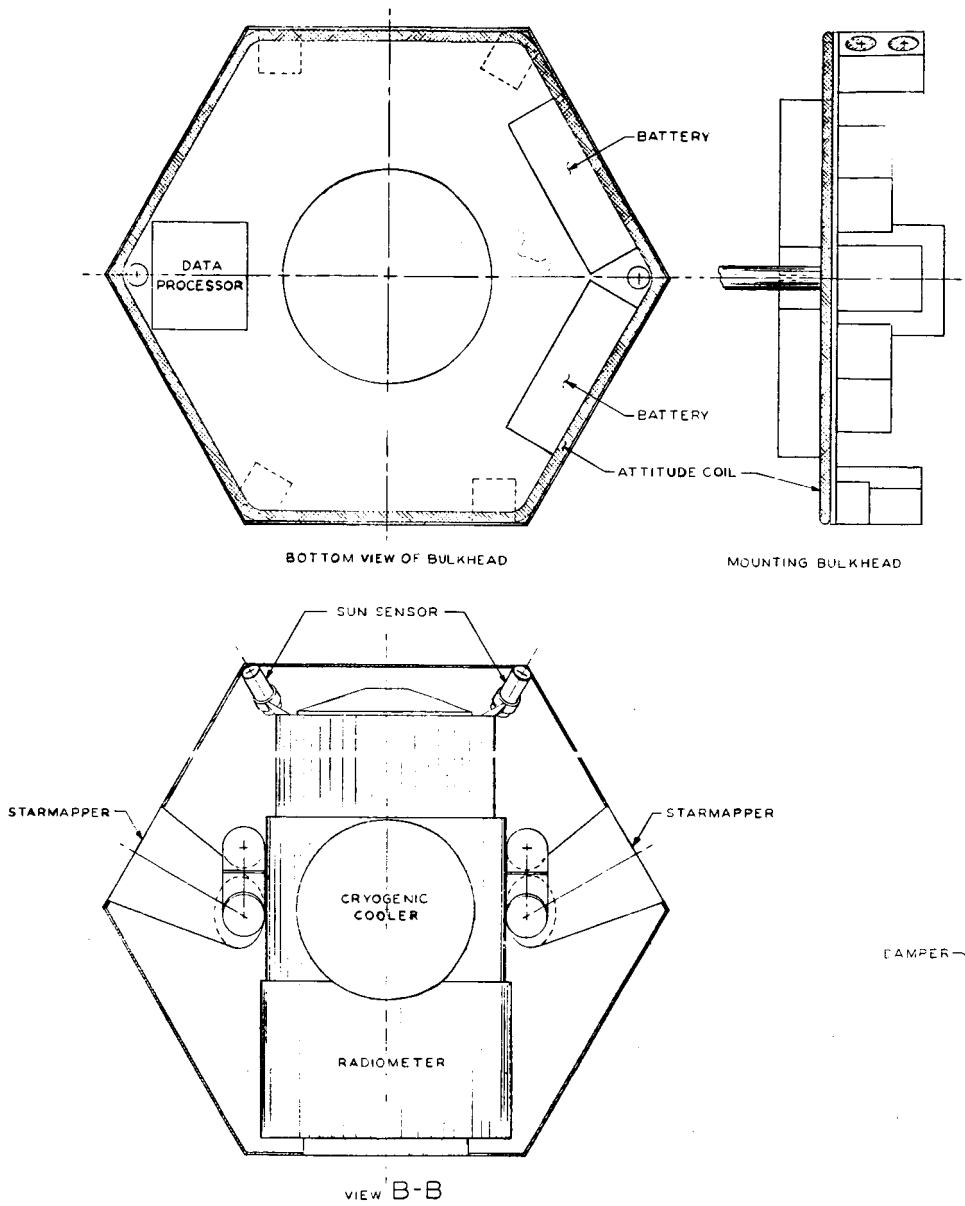
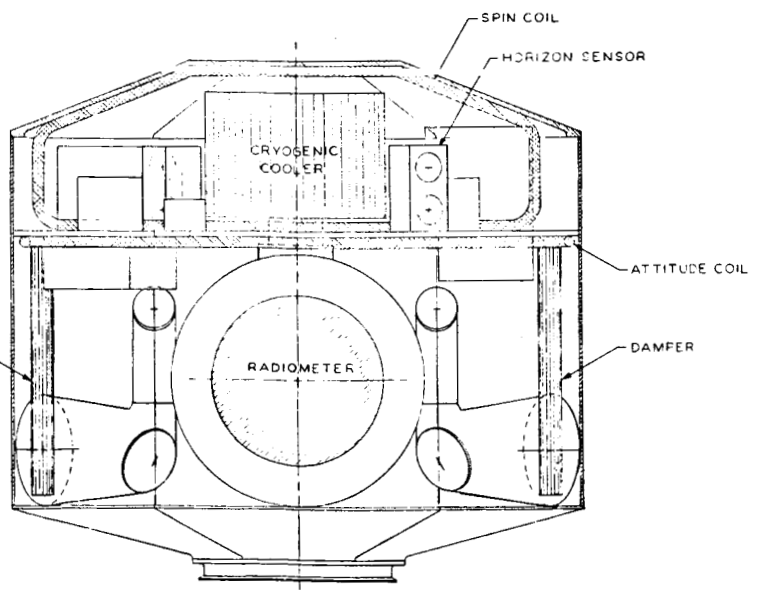
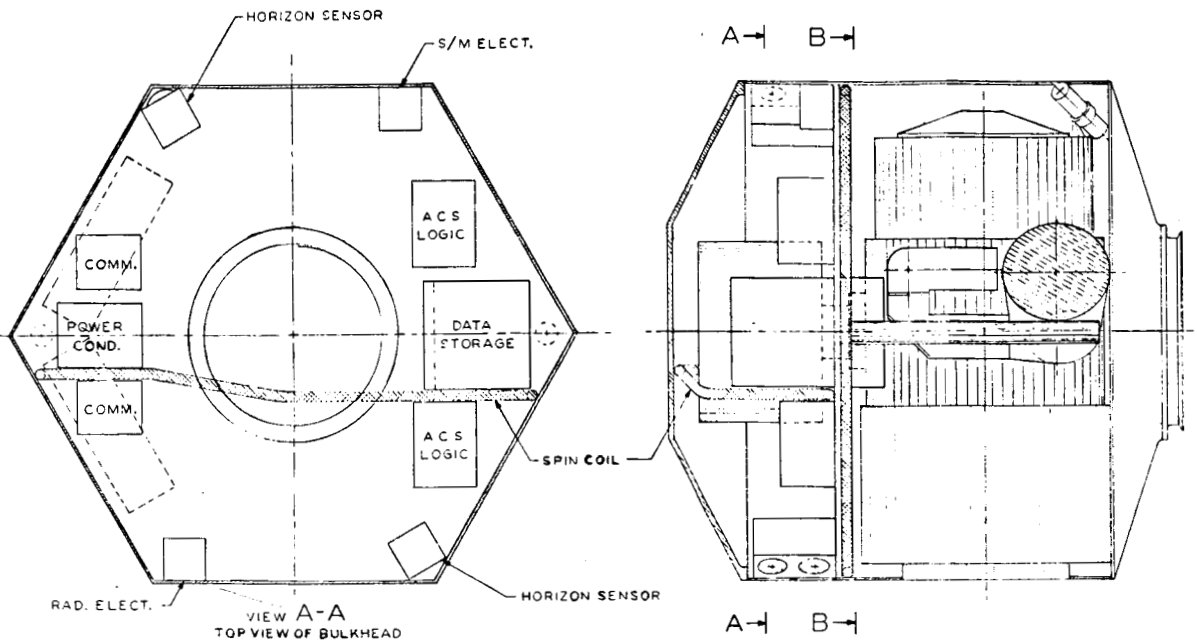


Figure B2. Con



ceptual Spacecraft - Internal View



TABLE B1. - TEMPAC
COMPONENT I ENCODING SHEET -
FIXED COMPONENT

Number	Component	Description	Cost	m ₁	v ₁	v ₂	v ₃	v ₄	v ₅	v ₆	z	ψ	α	l ₁	c
1	Experiment package	24 x 40 hollow cylinder	5	32.1	1.00	0.00	0.25			90	0	0	0.67	1.67	0.96
2	Baffle	4 x 20 cylinder	7	60.1	1.00	0.00	1.50			90	0	0	0.88	0.12	0.00
3	Mirror	12 x 17 cylinder	5	4.1	2.80	0.00	0.00			0	0	0	0.71	0.50	0.00
4	Cooler		6	8.3	1.25	0.00	0.00			0	0	0	1.00	1.40	1.33
5	Casting		5	10.1	0.32	-1.00	0.50			90	0	0	0.17	0.75	0.00
6	Starmapper	4 x 18 cylinder	5	10.1	0.42	1.00	0.50			90	0	0	0.17	0.75	0.00
7	Starmapper	4 x 18 cylinder	5	10.1	0.42	1.00	0.50			90	45	0	0.12	0.75	0.00
8	Sun sensor	2 x 6 cylinder	5	1.1	0.35	1.00	1.67			90	45	0	0.12	0.25	0.00
9	Sun sensor	2 x 6 cylinder	5	1.1	0.35	-1.00	-1.67			90	45	0	0.12	0.25	0.00
10	ACS														
11	Horizon sensor	4 x 4 x 8 box	3	5.1	2.50	1.00	1.62			0	0	30	0.33	0.17	0.17
12	Horizon sensor	4 x 4 x 8 box	3	5.1	2.50	1.00	1.62			0	0	30	0.33	0.17	0.17
13	Attitude coil	Bundle of wires	6	10.1	2.08	0.00	0.00			0	0	0	1.75	0.95	1.83
14	Spin coil		6	1.1	2.52	0.00	0.81			0	90	0	1.25	0.05	1.32
15	Damper	2 x 24 cylinder	5	2.1	1.04	2.08	0.00			0	0	0	0.08	1.00	0.90
16	Damper	2 x 24 cylinder	5	2.1	1.04	2.08	0.00			0	0	0	0.08	1.00	0.90
17	Communications														
18	VHF up antennas	3 Slots	1	5.1	0.32	0.00	0.00			0	0	0	0.60	0.35	0.35
19	S-band up antennas	6 Slots	1	1.1	2.52	0.00	0.00			0	0	0	36.00	18.00	17.00
20	VHF down antennas	3 Slots	1	1.1	4.25	0.00	0.00			0	0	0	0.60	0.35	0.35
21	S-band down antennas	6 Slots	1	1.1	2.52	0.00	0.00			0	0	0	36.00	18.00	17.00
22	Power														
23	Hinge	Metal on box, corner	1	2.1	2.52	0.00	0.00			0	0	0	8.00	4.00	1.70
24	Solar panel	26 x 44 plate	2	8.1	2.52	-3.14	1.91			0	0	-60	1.10	1.83	0.00
25	Solar panel	26 x 44 plate	2	8.1	2.52	0.00	3.86			0	0	0	1.10	1.83	0.00
26	Solar panel	26 x 44 plate	2	8.1	2.52	3.14	1.91			0	0	60	1.10	1.83	0.00
27	Solar panel	26 x 44 plate	2	8.1	2.52	-3.14	-1.91			0	0	-60	1.10	1.83	0.00
28	Solar panel	26 x 44 plate	2	8.1	2.52	0.00	-3.86			0	0	0	1.10	1.83	0.00
29	Solar panel	26 x 44 plate	2	8.1	2.52	-3.14	-1.91			0	0	60	1.10	1.83	0.00
30	Structure														
31	Baseplate	50-inch plate	4	30.1	-0.25	0.00	0.00			0	0	0	2.08	0.00	0.00
32	Skeleton and skin	50-inch hollow cylinder	6	24.1	1.36	0.00	0.00			0	0	0	2.00	1.46	2.16
33	Sun shade	30 x 16 plate	2	10.1	1.75	0.00	3.42			0	0	0	1.25	1.50	0.00
34	Cover	50-inch plate	4	8.1	3.20	0.00	0.00			0	0	0	2.08	1.00	0.00
35	Bulkhead integration														
36	Bulkhead	50-inch hollow cylinder	6	8.1	2.16	0	0			0	0	0	0.83	0.25	2.08
37	Component supports	50-inch hollow cylinder													
38	Power lines	50-inch hollow cylinder													
39	Heat paths	50-inch hollow cylinder													
40	Miscellaneous	50-inch hollow cylinder													

TABLE B3. - COMPUTER OUTPUT, FIXED COMPONENTS

CASE 1

NUMBER OF INPUT CARDS = 30

M = 572.000000
 IX = 1982.1935166
 IY = 3081.4019749
 IZ = 2787.0499413
 IXY = .0447735
 IXZ = -1.5958500
 IYZ = -16.2000000

X(BAR) = 1.5297902
 Y(BAR) = .0000000
 Z(BAR) = -.0677998

IXG = 1979.5761164
 IYG = 1740.1518497
 IZG = 1448.1223145
 IXYG = .0447735
 IXZG = 57.6629748
 IYZG = -16.2000000

P = .516815E 04 Q = .882891E 07 R = -.498317E 10

K1 = 1985.77684	.00000	X/Y = -.13747E 03
		Y/Z = .67649E-01
		X/Z = -.92999E 01
K2 = 1441.36655	.00000	X/Y = -.19765E 01
		Y/Z = -.54203E-01
		X/Z = .10713E 00
K3 = 1741.00688	.00000	X/Y = .12953E-01
		Y/Z = .18934E 02
		X/Z = .24526E 00

TABLE B4. - COMPUTER OUTPUT, FIXED AND MOVABLE COMPONENTS

CASE 2

NUMBER OF INPUT CAPDS = 11

M = 723.0000000
 IX = 2430.2602499
 IY = 3899.6351416
 IZ = 3028.6956749
 IXY = -.0412265
 IX7 = 2.2698000
 IY7 = .3596000

X(BAR) = 1.6735546
 Y(BAR) = .0074412
 Z(BAR) = -.0513278

IXG = 2428.3154415
 IYG = 1872.7627317
 IZG = 1903.6880060
 IXYG = -9.0444504
 IX7G = 64.3754124
 IY7G = .6357436

P = .620477E 04 Q = .127313E 00 R = -.864941E 10

K1 = 2436.24480 .00000

X/Y = .61773E 02
 Y/Z = -.13390E 00
 X/Z = -.82714E 01

K2 = 1872.60831 .00000

X/Y = -.18297E-01
 Y/Z = -.57329E 02
 X/Z = .10490E 01

K3 = 1895.91307 .00000

X/Y = .61348E 01
 Y/Z = .19651E-01
 X/Z = .12055E 00

TABLE B5. - COMPUTER OUTPUT, FIXED AND MOVABLE COMPONENTS WITH ADDED DEAD WEIGHTS

CASE 3

NUMBER OF INPUT CARDS = 13

M = 733.0000000
 IX = 2473.8648499
 IY = 3933.4957416
 IZ = 3939.0672749
 IXY = -.0412265
 IXZ = 5.1378000
 IYZ = .3596000

X(BAR) = 1.6529259
 Y(BAR) = .0073397
 Z(BAR) = -.0256617

IXG = 2473.3426664
 IYG = 1930.3853564
 IZG = 1936.4000980
 IXYG = -.0000000
 IXZG = 36.2889593
 IYZG = .4976598

P = .634013E 04 Q = .133005E 08 R = -.924265E 10

K1 = 2475.930A7 .00000

X/Y = .60837E 02
 Y/Z = -.24433E 00
 X/Z = -.14864E 02

K2 = 1930.23565 .00000

X/Y = -.18223E-01
 Y/Z = -.37715E 02
 X/Z = .68729E 00

K3 = 1933.96161 .00000

X/Y = .23777E 01
 Y/Z = .27796E-01
 X/Z = .66099E-01

REFERENCES

1. Thompson, William T.; and Reiter, Gordon S.; Attitude Drift for Space Vehicles. Journal of the Astronautical Sciences, vol. VII, no. 2, Summer 1960.
2. Anon.: Impinging Heat Loads and Temperatures of Oriented Spacecraft Orbiting Planets of Variable or Constant Surface Temperature. Contract No. NAS 9-1059, Midwest Research Institute Project No. 2669-E, modified by NASA Manned Space Flight Center, modified by Honeywell Radiation Center.
3. Anon.: T B Heat Transient Thermal Analyser. Honeywell-Aerospace Division Automath Language Computer Program.
4. Anon.: PXNSP, Matrix Inversion Program for Steady State Temperature Distributions. Honeywell-Aerospace Division, Automath Language Program.

May 1967

NASA CR-66380

CONCEPTUAL MECHANIZATION STUDIES FOR
A HORIZON DEFINITION SPACECRAFT
STRUCTURES AND THERMAL SUBSYSTEM

By: Ivan W. Russell
David C. Peterson
Richard M. Jansson
Clarence A. Jenson

ABSTRACT

The spacecraft conceptual configuration developed during the Horizon Definition Study is a spin-stabilized, hexagonal cylinder configured for launch on a two-stage Improved Delta (DSV-3N). This configuration utilizes extended solar panels for primary power and incorporates passive radiation cooling of the spacecraft body. Separate thermal environments are provided for the experimental package and the supporting subsystem components.

May 1967

NASA CR-66380

CONCEPTUAL MECHANIZATION STUDIES FOR
A HORIZON DEFINITION SPACECRAFT
STRUCTURES AND THERMAL SUBSYSTEM

By: Ivan W. Russell
David C. Peterson
Richard M. Jansson
Clarence A. Jenson

ABSTRACT

The spacecraft conceptual configuration developed during the Horizon Definition Study is a spin-stabilized, hexagonal cylinder configured for launch on a two-stage Improved Delta (DSV-3N). This configuration utilizes extended solar panels for primary power and incorporates passive radiation cooling of the spacecraft body. Separate thermal environments are provided for the experimental package and the supporting subsystem components.

May 1967

NASA CR-66380

CONCEPTUAL MECHANIZATION STUDIES FOR
A HORIZON DEFINITION SPACECRAFT
STRUCTURES AND THERMAL SUBSYSTEM

By: Ivan W. Russell
David C. Peterson
Richard M. Jansson
Clarence A. Jenson

ABSTRACT

The spacecraft conceptual configuration developed during the Horizon Definition Study is a spin-stabilized, hexagonal cylinder configured for launch on a two-stage Improved Delta (DSV-3N). This configuration utilizes extended solar panels for primary power and incorporates passive radiation cooling of the spacecraft body. Separate thermal environments are provided for the experimental package and the supporting subsystem components.

May 1967

NASA CR-66380

CONCEPTUAL MECHANIZATION STUDIES FOR
A HORIZON DEFINITION SPACECRAFT
STRUCTURES AND THERMAL SUBSYSTEM

By: Ivan W. Russell
David C. Peterson
Richard M. Jansson
Clarence A. Jenson

ABSTRACT

The spacecraft conceptual configuration developed during the Horizon Definition Study is a spin-stabilized, hexagonal cylinder configured for launch on a two-stage Improved Delta (DSV-3N). This configuration utilizes extended solar panels for primary power and incorporates passive radiation cooling of the spacecraft body. Separate thermal environments are provided for the experimental package and the supporting subsystem components.